

Electronic Thesis and Dissertation Repository

7-25-2012 12:00 AM

Calcium-calmodulin regulation of TRPM2 currents

Brian M. W. Lockhart
The University of Western Ontario

Supervisor

Dr. John F. MacDonald
The University of Western Ontario Joint Supervisor

Dr. Michael F. Jackson
The University of Western Ontario

Graduate Program in Anatomy and Cell Biology

A thesis submitted in partial fulfillment of the requirements for the degree in Master of Science

© Brian M. W. Lockhart 2012

Follow this and additional works at: <https://ir.lib.uwo.ca/etd>



Part of the [Neurosciences Commons](#)

Recommended Citation

Lockhart, Brian M. W., "Calcium-calmodulin regulation of TRPM2 currents" (2012). *Electronic Thesis and Dissertation Repository*. 663.

<https://ir.lib.uwo.ca/etd/663>

This Dissertation/Thesis is brought to you for free and open access by Scholarship@Western. It has been accepted for inclusion in Electronic Thesis and Dissertation Repository by an authorized administrator of Scholarship@Western. For more information, please contact wlsadmin@uwo.ca.

CALCIUM-CALMODULIN DEPENDENT REGULATION OF TRPM2 CURRENTS

(Spine title: CA²⁺-CAM REGULATION OF TRPM2)

(Thesis format: Monograph)

by

Brian Michael Walter Lockhart

Graduate Program in Anatomy and Cell Biology

A thesis submitted in partial fulfillment
of the requirements for the degree of
Master of Science

The School of Graduate and Postdoctoral Studies
Western University Canada
London, Ontario, Canada

© Brian Lockhart 2012

CERTIFICATE OF EXAMINATION

Supervisor

Dr. John MacDonald

Supervisory Committee

Dr. Vania Prado

Dr. Marco Prado

Dr. Jeff Dixon

Co-Supervisor

Dr. Michael Jackson

Examiners

Dr. Arthur Brown

Dr. Walter Rushlow

Dr. Stephen Pasternak

The thesis by

Brian Michael Walter Lockhart

entitled:

**Calcium-calmodulin dependent regulation of TRPM2
currents**

is accepted in partial fulfillment of the
requirements for the degree of
Master of Science

Date _____

Chair of the Thesis Examination Board

CALCIUM-CALMODULIN DEPENDENT REGULATION OF TRPM2 CURRENTS

By

Brian Lockhart

Master of Science

Department of Anatomy and Cell Biology

Western University Canada

2012

TRPM2 (1507 amino acids), a non-selective cation channel with substantial permeability for Ca^{2+} , is responsive to oxidative stress, and is a mediator of cell death in several cell types. Ca^{2+} -calmodulin has been shown to promote channel activation and inactivation, however the mechanisms are not fully understood. Identifying candidate CaM binding sites using *in silico* screening, I hypothesized that Ca^{2+} -dependent inactivation (CDI) of TRPM2 is mediated by an intracellular CaM binding domain unique from that of activation (406-415AA). I systematically determined the minimum binding domains for three CaM candidate sites on TRPM2's intracellular domains using truncated fragments and subsequent CaM-Sepharose pull-downs. TRPM2 with substitution mutations to candidate sites were transfected into HEK293 cells; currents were recorded using 2mM or 0.5mM Ca^{2+} extracellular fluid and adenosine diphosphate ribose (ADPR) in the patch pipette. Abolished and reduced currents respectively were observed as a result of amino acid substitution to CaM binding regions at 172-187AA and 1087-1101AA of TRPM2. The two identified CaM candidate sites may establish a potential molecular link to CDI of TRPM2.

Key Words: TRPM2, Calmodulin, Ca^{2+} -dependent inactivation, CDI, CaM-dependent inactivation, Ca^{2+} -CaM, Guamanian ALS

Acknowledgements

First of all, I would like to extend my thanks to my supervisor Dr. John MacDonald for providing me the opportunity to learn, develop and grow as his student over the past two years. I would also like to thank my co-supervisor Dr. Michael Jackson for his continued support, mentorship, and enthusiasm in all he contributes to this project and our laboratory. Thank you to all the past and present members of the MacDonald laboratory for their hard work and encouragement.

I would like to thank Oies Hussein for laying the groundwork for this project and Natalie Lavine for her persistence and leadership in overseeing the techniques required to carryout this study. Additionally I would like to thank *Jillipedia* “caffeine-buddy” Belrose, Matthew Johnston and Patrick “make me a gel” Langille for their hard work and company, which were invaluable to this thesis.

I would like to thank the members of my supervisory committee: Dr. Vania Prado, Dr. Marco Prado, and Dr. Jeff Dixon for their continued support, input and advice. I would like to acknowledge CIHR and Schulich School of graduate studies for the funding to support this project as well as members of the examining committee for their time and effort.

Finally, thank you to my family members (Randy [Dad], Diane [Mom], Scott, Candice, Keith and Matthew) and friends (Mark and Matt for putting up with me, Sabiha for the thesis companionship and Kristen for the meals) for their continued support of my educational aspirations, without whom none of this would be possible.

Cheers,

Brian Lockhart

Table of Contents

Certificate of Examination.....	ii
Abstract and Key Words.....	iii
Acknowledgements.....	iv
Table of Contents.....	v-vi
List of Figures.....	vii
List of Abbreviations.....	viii-x
Unique Constructs.....	x-xi
Section 1 – Introduction.....	1
1.1 General Introduction.....	2-3
1.2 TRP channels and TRPM2.....	3-7
1.3 Topography of TRPM2.....	7-11
1.4 Physiological roles of TRPM2.....	11-13
1.5 ADPR, H ₂ O ₂ and βNAD ⁺ mediated TRPM2 gating.....	14-17
1.6 Production of ADPR.....	17-19
1.7 Ca ²⁺ and TRPM2.....	19-21
1.8 Other TRPM2 regulation mechanisms.....	21-23
1.9 Antagonists of TRPM2.....	23-24
1.10 Guam hTRPM2 P1018L and CDI.....	24-25
1.11 Ca ²⁺ -dependent inactivation.....	25-28
1.12 Calmodulin, inactivation and VGCC binding.....	29-32
1.13 Rationale and hypothesis.....	33-34
Section 2 – Materials and Methods.....	35
2.1 Whole-cell patch clamp recording.....	36-38
2.2 JetPrime (polyplus) transfections of HEK293 cells.....	37
2.3 Generation of TRPM2 Intracellular Truncations.....	39-44
2.4 TNT Quick-Coupled Reticulocyte System (Promega).....	44
2.5 Calmodulin-Sepharose pull-down.....	44-45
2.6 TRPM2-CaM candidate site-directed Mutagenesis.....	45-46
2.7 Western Blotting.....	47
2.8 Drugs and Peptides.....	48
2.9 Statistical Analysis.....	48
Section 3 – Results.....	49
3.1 Extracellular Ca ²⁺ modulation of TRPM2 CDI.....	50-52
3.2 CaM-Sepharose pull-down of TRPM2 C-terminal truncation.....	53-54
3.3 A systematic analysis of TRPM2 C-term CaM candidate sites.....	55-62
3.4 A systematic analysis of TRPM2 N-term CaM candidate sites.....	63-67
3.5 6 Effects of substitution mutagenesis at TRPM2 candidate CaM sites....	64-67
3.6 Assessment of CaM site NT _{IQ} and flag-mTRPM2-CaM _{Mut} (NT _{IQ}).....	68-69
3.7 Assessment of CaM site CT ₁₋₁₄ and flag-mTRPM2-CaM _{Mut} (CT ₁₋₁₄).....	70-71
3.8 Assessment of CaM site CT _{IQ} and flag-mTRPM2-CaM _{Mut} (CT _{IQ}).....	72-73
3.9 Assessment of CaM site NT ₁₋₁₄ flag-mTRPM2-CaM _{Mut} (NT ₁₋₁₄).....	74-75

3.10 Analysis of the hTRPM2 P1018L substitution.....	76-77
3.11 TRPM2 CDI in hTRPM2 versus mTRPM2.....	78-79
Section 4 – Discussion.....	80
4.1 Summary of Key Findings.....	81-82
4.2 TRPM2 CDI is mediated by extracellular Ca ²⁺	82-83
4.3 Ca ²⁺ -CaM binding, Ca ²⁺ specificity and ApoCaM.....	83-85
4.4 NT _{IQ} and TRPM2 activation.....	86
4.5 CT ₁₋₁₄ and the TRPM2 NUDIX domain.....	86-87
4.6 CT _{IQ} and the TRPM2 CCR.....	87-88
4.7 NT ₁₋₁₄ and conserved NT regions.....	88-89
4.8 hTRPM2 P1018L CDI and peak amplitude.....	89-91
4.9 Implications of increased mTRPM2 CDI.....	91-92
4.10 Significance of Work.....	92-96
4.11 Future Directions.....	96-97
4.12 Overall Conclusions.....	97-98
Section 5 – References.....	99
Appendix.....	110
Curriculum Vitae.....	113

List of Figures

Section 1 – Introduction.....	1
1.1 Schematic of major TRPM2 topographical areas.....	8
1.2 Representative trace of TRPM2 Ca ²⁺ -dependent inactivation.....	28
Section 2 – Materials and Methods.....	35
2.1 Whole-cell patch-clamp recording setup.....	38
2.2 Schematic of TRPM2 truncations.....	42
2.3 Schematic of site directed substitution mutagenesis of TRPM2.....	46
Section 3 – Results.....	49
3.1 Effect of extracellular Ca ²⁺ and holding voltage on TRPM2 CDI.....	52
3.2 CaM-Sepharose pulldown of mTRPM2 C-terminal fragment.....	54
3.3 Summary schematic of TRPM2 candidate CaM sites identified with <i>in silico</i> screening.....	57
3.4 CaM-Sepharose pulldown of mTRPM2 C-terminal truncations.....	59
3.5 CaM-Sepharose pulldown of mTRPM2 CT3 truncations containing theoretical 1-8-14-consensus site at 1344-1373AA.....	60
3.6 CaM-Sepharose pulldown of mTRPM2 N-terminal truncations.....	62
3.7 CaM-Sepharose pulldown of mTRPM2 CT1 truncations containing theoretical 1-8-14-consensus site at 161-197AA.....	65
3.8 CaM-Sepharose pulldown of mTRPM2 CT1 truncations containing theoretical IQ-like consensus site at 1084-1105AA.....	66
3.9 CaM-Sepharose pulldown of mTRPM2 CaM candidate site mutated fragments.....	67
3.10 Analysis of flag-mTRPM2-CaM _{Mut} (NT _{IQ}).....	69
3.11 Analysis of flag-mTRPM2-CaM _{Mut} (CT ₁₋₁₄).....	71
3.12 Analysis of flag-mTRPM2CaM _{Mut} (CT _{IQ}).....	73
3.13 Analysis of flag-mTRPM2-CaM _{Mut} (NT ₁₋₁₄).....	75
3.14 Analysis of CDI for the hTRPM2 P1018L mutant.....	77
3.15 Analysis of CDI for mTRPM2 versus hTRPM2.....	79
Appendix.....	110
A1 TRPM2 recovery from Ca ²⁺ inactivation over time.....	110
A2 ADPR-dependent recovery from TRPM2 Ca ²⁺ -dependent inactivation.....	111
A3 Calmodulin-dependence of TRPM2 Ca ²⁺ -dependent inactivation.....	112

List of Abbreviations

0 Ca ²⁺ :	Ca ²⁺ -free extracellular solution
°C:	degrees Celsius
βNAD ⁺ :	beta-nicotinamide adenine dinucleotide
μg:	microgram
μl:	microliter
μm:	micro molar
[Ca ²⁺]:	calcium concentration
Aβ ₁₋₄₂ :	amyloid beta (1-42AA)
AA:	amino acids
AD:	Alzheimer's disease
ADPR:	adenosine diphosphate ribose
ALS:	amyotrophic lateral sclerosis
ANOVA:	analysis of variance
Apo-CaM:	calmodulin in the absence of Ca ²⁺
APS:	ammonium persulfate
Ascl:	Restriction enzyme from Ascl gene of <i>Arthrobacter</i>
BAPTA:	2-bis(o-aminophenoxy)ethane-N,N,N',N'-tetraacetic acid
BD:	bipolar disorder
BM:	2-mercaptoethanol
BCA:	bicinchoninic acid
BSA:	bovine serum albumin
Ca ²⁺ :	calcium
cADPR:	cyclic adenosine diphosphate ribose
CCR:	coiled-coil region
CDI:	Ca ²⁺ -dependent inactivation
cDNA:	complimentary-deoxyribonucleic acid
cip:	calf-intestinal phosphatase
CaM:	calmodulin
Chanzyme:	channel-enzymes
CO ₂ :	carbon-dioxide
C-term:	intracellular trail of TRPM2 (1060-1503AA)
DNA:	deoxyribonucleic acid
EC ₅₀ :	half maximal effective concentration
ECS:	extracellular solution
EGTA:	ethylene glycol tetraacetic acid
EF Hand:	helix-loop-helix structural domain that can bind a Ca ²⁺ ion
FFA:	flufenamic acid:
GFP:	green fluorescent protein
GST:	glutathione S-transferase
H ₂ O:	water
H ₂ O ₂ :	hydrogen peroxide
HEK 293:	human embryonic kidney cell line
HPLC:	high performance liquid chromatography

hTRPM2:	human- melastatin-related transient receptor potential 2
ICS:	intracellular solution
IQ-like:	calmodulin consensus binding site, IQXXRGXXXR
Iss/Ip:	steady state/peak ratio (Inactivation)
LTD:	long-term depression
K ⁺ :	potassium
KCl:	potassium chloride
kHz:	kilo Hertz
KOD:	<i>Thermococcus kodakarensis</i>
M'Ω:	mega Ohms
MEM:	Modified Eagle Medium
Mg ⁺ :	magnesium
Mg-ATP:	magnesium adenosine 5'-triphosphate
min:	minute
ml:	milliliter
mPTP:	mitochondrial transition pore opening
mM:	millimolar
mRNA:	messenger ribonucleic acid
mV:	millivolt
Na ⁺ :	sodium
nA:	nanoamp
ng:	nanogram
NotI:	Restriction Enzyme from NotI gene of <i>Nocardia otitidis-caviarum</i>
N-term:	intracellular trail of TRPM2 (1-750AA)
mm:	millimeter
nM:	nanomolar
mTRPM2:	mouse-melastatin-related transient receptor potential 2
NMDA:	N-Methyl-D-aspartic acid
NMDAR:	N-Methyl-D-aspartic acid receptor
NP-40:	nonyl phenoxypolyethoxyethanol
NUDIX:	nucleoside diphosphate coupled to a varying moiety X (NUDT9-H)
OSM:	osmolarity
pa:	picoamp
PARG:	polyADPR-glycohydrolase
PARP:	polyADPR-polymerase
PCR:	polymerase chain reaction
PD:	parkinson's disease
PTPL1:	protein tyrosine phosphatase L1
RNAi:	ribonucleic acid interference
ROS/RNS:	reactive oxygen/nitrogen species
RT-PCR:	real-time polymerase chain reaction
SIRT2:	NAD-dependent deacetylase sirtuin-2
SIRT3:	NAD-dependent deacetylase sirtuin-3
SNC:	substantia nigra pars compacta
SNP:	single nucleotide polymorphism
SSF-TRPM2:	TRPM2 missing first 214AA (striatum short-form TRPM2)

TEMED:	tetramethylethylenediamine
TNF α :	tumor necrosis factor
TRIS:	tris(hydroxymethyl)aminomethane
TRP:	transient receptor potential
TrpL:	TRP-like homolog
TRPM2:	melastatin-related transient receptor potential 2
TRPM2- Δ C:	splice variant resulting from a missing exon 27 (1292-1325AA)
TRPM2- Δ N:	splice variant resulting from a missing exon 11
TRPM2- Δ N Δ C:	splice variant missing both exon 11 and 27
TRPM2-AS:	TRPM2 antisense transcript caused by a promoter in intron 24
TRPM2-TE:	TRPM2 antisense transcript caused by a promoter in intron 24
TRPM2-S:	splice variant resulting from a stop codon between exons 16 and 17
UV:	ultraviolet
VGCC:	voltage-gated calcium channel
WP-ALS:	western Pacific amyotrophic lateral sclerosis
WT:	wildtype

Unique Constructs

pTNT-GST TRPM2 truncations generated for CaM-Sepharose pull down (figure 2.1)

CT1:	1047-1163AA
CT2:	1163-1278AA
CT3:	1278-1395AA
CT4:	1395-1507AA
CT5:	1047-1108AA
CT6:	1108-1163AA
CT7:	1047-1082AA
CT8:	1082-1163AA
CT10:	1277-1339AA
CT11:	1339-1396AA
CT12:	1277-1374AA
CT13:	1374-1396AA
NT1:	1-256AA
NT2:	250-505AA
NT3:	499-750AA
NT4:	1-150AA
NT5:	150-250AA
NT6:	1-201AA
NT7:	201-250AA
NT15:	395-423AA
MutCT5:	1047-1108AA substitutions (L1087Q/Q1088A/K1092A/K1097A)
MutCT11:	1339-1396AA substitutions (W1351S/A1358S/W1364S)
MutNT5:	150-250AA substitutions (V172S/A176S/F179S/L185S)
MutNT15:	395-423AA substitutions (I405A/Q406A/R410-412A/L415A)

Substitution mutagenesis to full-length TRPM2 CaM consensus binding sites

mTRPM2-CaM_{Mut}(CT₁₋₁₄): AA substitutions W1351S/A1358S/W1364S
mTRPM2-CaM_{Mut}(CT_{1Q}): AA substitutions L1087Q/Q1088A/K1092A/K1097A
mTRPM2-CaM_{Mut}(NT₁₋₁₄): AA substitutions V172S/A176S/F179S/L185S
mTRPM2-CaM_{Mut}(NT_{1Q}): AA substitutions I405A/Q406A/R410-412A/L415A

Section 1

INTRODUCTION

1.1 General Introduction

Ca^{2+} cellular rise is involved in many physiological processes and yet Ca^{2+} is toxic in high concentrations in the cytoplasm (Saimi and Kung, 2002). Ca^{2+} dysfunction is often associated with periods of oxidative stress, leading to cellular damage and degeneration (Hara et al., 2002). A protein channel named Transient receptor potential melastatin type-2 (TRPM2) has generated great interest due to its wide expression throughout the brain (Nagamine et al., 1998), involvement in important regulatory cells such as β pancreatic cells (Togashi et al., 2006) and several cell types of the immune system (Perraud et al., 2001). Furthermore, TRPM2 can alter the basal intracellular $[\text{Ca}^{2+}]$ under oxidative stress (Hara et al., 2002) and intracellular Ca^{2+} has been shown to be required for channel activation (Tong et al., 2006). This acts as a positive feedback mechanism whereby Ca^{2+} entry through TRPM2 further increases TRPM2 activation. Conversely published reports suggest a negative feedback mechanism involving Ca^{2+} , which limits TRPM2 activation (Perraud et al., 2003). However the mechanism responsible for TRPM2 Ca^{2+} -dependent inactivation have not been well characterized.

I will begin with an introduction to TRPM2, its topography and important physiological regulators. This will lead to a history of the discoveries that outline our current understanding of TRPM2 regulation. I will continue with a description of the future research frontiers, a current lack of specific antagonists for TRPM2 and the role TRPM2 plays in physiological cellular processes. Finally I will outline calmodulin (CaM), a ubiquitously expressed Ca^{2+} sensor and mediator of TRPM2, providing novel insight into TRPM2 Ca^{2+} -dependent inactivation (CDI). Results will

explore novel CaM consensus binding sites and their regulation of CDI. Measurements will occur through substitution mutagenesis of TRPM2 CaM candidate sites and whole-cell patch-clamp recordings. I also provide novel insight suggesting mutations within a TRPM2 variant found in a Guamanian genetic population results in a gain of function and will discuss the potential significance of this finding.

1.2 TRP channels and TRPM2

Transient receptor potential melastatin type-2 (TRPM2) is a Ca²⁺ permeable non-selective cation channel activated by oxidative stress (Hara et al., 2002), adenosine diphosphate ribose (ADPR) (Perraud et al., 2001) and intracellular Ca²⁺-Calmodulin (CaM) (Tong et al., 2006). First isolated from adult and fetal brains in 1998, it shares marked homology to the *Drosophila* TRP channel (Nagamine et al., 1998). The gene structure for TRPM2 consists of 32 exons spanning 90kb on human chromosome 21 mapping a 1503 amino acid long protein (Nagamine et al., 1998).

The transient receptor potential family of ion channels derives their name from a homologous protein studied in *Drosophila* and involved in the photo transduction cascade (Montell and Rubin, 1989). A mutation to this channel resulted in a transient response to bright light conditions (Montell and Rubin, 1989). *Drosophila* acted as though blind during continuous light exposure, but quickly returned to a baseline response when the stimulus was removed (Montell and Rubin, 1989). The transient response nomenclature has been maintained even though most TRP channels have no role in the photo transduction cascade (Montell and Rubin, 1989).

Unlike many families of proteins grouped by ligand selectivity or function, the TRP superfamily is grouped according to homology since very little was known about each channel when first discovered (Clapham, 2003). The TRP superfamily are expressed throughout the nervous system and differ widely in their ion selectivity, activation mechanics and physiological functions, which range from sensory transduction to cell death (Montell, 2005; Clapham, 2003). Despite the disparity within the superfamily they share several common characteristics including 6 transmembrane domains, tetrameric channel structure, a minimum of 20% sequence homology and permeability to cations (Montell, 2005; Clapham, 2003). All TRP channels share a similar pore structure, are structurally similar to other cation channels but lack a positively charged residue required for voltage sensing (Yu and Catterall, 2004). Most TRP channels have splice variants including several identified in TRPM2 (Clapham, 2003; Zhang et al., 2003a; Kuhn and Luckhoff, 2004; Uemura et al., 2005). Finally, TRP channels are of great scientific interest because many remain active at resting membrane potentials where cells spend most of their time (Clapham, 2003).

When first isolated TRPM2 was given the designation TRPC7 despite it not belonging to the so-called “short” subfamily of human TRP channels (Nagamine et al., 1998). Nomenclature proceeded from TRPC7 (Nagamine et al., 1998) to LTRPC2 grouped into the “long” TRP channel subfamily based on open reading frames of roughly 1600 amino acids (Harteneck et al., 2000). Finally it was assigned to the melastatin subfamily of TRP channels as TRPM2, designating it the second member of a family derived purely from homology (Montell et al., 2002). Currently 28 TRP

family members have been identified and separated into six subfamilies: TRPC (canonical), TRPV (vanilloid), TRPM (melastatin), TRPA (ankyrin), TRPP (polycystin) and TRPL (mucolipin), based on homology (Jiang et al., 2010).

The melastatin sub-family of TRP channels arose from TRPM1 (originally named melastatin) because of the different expression levels observed between metastatic and non-metastatic melanoma cells (Duncan et al., 1998). Aberrant melanoma cells lacking TRPM1 were unable to apoptose resulting in aggressive melanoma tumors (Duncan et al., 1998). 8 members of the TRPM sub-family have been classified and are expressed in a variety of tissues and cell types including both excitable and non-excitable (Montell, 2005; Fleig and Penner, 2004). Many of the sub-family members have several alternative splice variants, which are assumed to act in conjunction with unspliced members to alter channel function in the tetrameric subunit (Fleig and Penner, 2004). Most of the variability exists in the C-terminal of the channel, with three members being classified as highly unusual “chanzymes” (channel-enzymes); TRPM2 (NUDT9-H) is unique from TRPM6/7 (α kinase) in its purported enzymatic site (Montell, 2005). Many members are grouped into pairs with TRPM2 and TRPM8 being the nearest evolutionary break, each sharing 42% homology and similar Ca^{2+} permeability (Kuhn et al., 2007; Montell, 2005).

Early TRPM2 research focused on a wide variety of tissues including neutrophil granulocytes (Heiner et al., 2003), U937 monocyte cells (Perraud et al., 2001) microglia (Kraft et al., 2004), CRI-G1 insulinoma cells (Inamura et al., 2003). TRPM2 has been well defined in heterologous expression systems such as CHO-K1 cells and

HEK293 cells (McHugh et al., 2003; Kuhn and Luckhoff, 2004). More recently great interest has been derived from TRPM2 expression in cell types involved in important physiological functions such as cardiomyocytes (Yang et al., 2006), pancreatic β -cells (Togashi et al., 2006), endothelial cells (Hecquet et al., 2008), hippocampal neurons (Olah et al., 2009), and immune cells such as lymphocytes, macrophages and monocytes (Perraud et al., 2001; Sano et al., 2001; Beck et al., 2006; Yamamoto et al., 2008). Here, TRPM2 has been shown to regulate a host of important physiological functions including: insulin secretion (Inamura et al., 2002; Uchida et al., 2011), cytokine production (Yamamoto et al., 2009; Knowles et al., 2011), endothelial permeability (Hecquet et al., 2008; Dietrich and Gudermann, 2008), hippocampal LTD (Xie et al., 2011) microglia activation (Fonfria et al., 2006), and neuronal/pancreatic cell death in response to oxidative stress (Jiang et al., 2010). Interestingly TRPM2 is not limited to the plasma membrane and has been identified in the lysosomal organelle involved in release of Ca^{2+} from intracellular stores during oxidative stress or insulin release (Lange et al., 2009).

The diverse cellular tissues in which TRPM2 has been identified, and activation of TRPM2 by ROS, has made TRPM2 an attractive candidate for extensive study (Perraud et al., 2001). TRPM2 is currently a target for diabetes (Scharenberg, 2009; Romero et al., 2010; Zhang et al., 2012), stroke (Fonfria et al., 2006; Jia et al., 2011), bipolar disorder (Xu et al., 2009; Roedding et al., 2012), prostate cancer (Zhang et al., 2010) and inflammation (Yamamoto et al., 2009; Haraguchi et al., 2012), cardiovascular (Takahasi et al., 2012) and neurodegenerative diseases (Jiang et al.,

2010; Fonfria et al., 2004; Kanata et al., 2012; Hermosura and Garruto, 2007; Hermosura et al., 2008).

1.3 Topography of TRPM2

TRPM2 (figure 1.1) consists of intracellular N- and C-terminal tails separated by 6 transmembrane domains and a pore-forming loop (Perraud et al., 2003). The N-terminal is approximately 700 amino acids in length, thought to be required for channel expression/trafficking and consists of 4 highly conserved regions amongst TRPM family members (Perraud et al., 2003). Coiled-coil regions (CCR) are common protein-protein interaction sites and have been well defined in many protein families (Lupas et al., 1991); one such (CCR), on the N-term at 654-684AA, was mutated and found to inhibit channel expression and trafficking, but not subunit interactions in the tetramer (Mei and Jiang, 2009). A calmodulin (CaM) IQ-like consensus motif is located at 406-416AA of hTRPM2 and is responsible for the Ca²⁺-CaM dependent gating of TRPM2 (Tong et al., 2006).

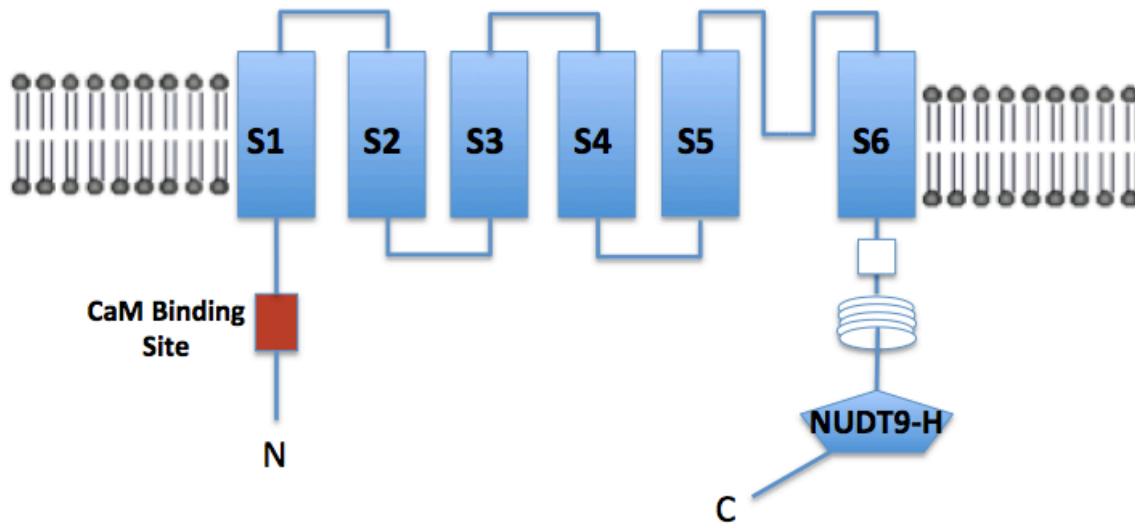


Figure 1.1 – Schematic of TRPM2 transmembrane topology and key structural domains (not to scale). The channel consists of a cytosolic 700AA N-term (left) highly conserved region including a Ca^{2+} -CaM binding site required for channel gating. 6 transmembrane segments and a pore forming loop account for a 300AA span of TRPM2 followed by 500AA for the intracellular C-terminal end (right). A highly conserved TRP box follows the S6 transmembrane domain; a C-term coiled-coil region (CCR) has been implicated in channel trafficking, expression, subunit formation of the tetrameric structure and protein-protein interaction. Finally the nucleoside diphosphate coupled to a varying moiety X (NUDIX) domain, consisting of the homologous NUDT9 enzymatic region, gives TRPM2 the unique distinction of being a chanzyme (although adenosine diphosphate ribose-ase activity is highly suppressed). Adenosine diphosphate ribose (ADPR) binding is required for TRPM2 channel gating at this site in addition to Ca^{2+} -CaM at the N-term.

The transmembrane sequence spans roughly 300 amino acids, consisting of 6 transmembrane sequences and a pore forming hydrophobic loop (between segments 5 and 6) that is thought to form the channel pore in tetrameric TRPM2 (Perraud et al., 2003). It has been suggested that the highly conserved nature of the S5 and S6 domain amongst TRPM family members is critical for the cationic current (Perraud et al., 2003). Highly conserved cysteine residues at 996 and 1008AA are both required within the pore for channel functioning (Mei et al., 2006a). Mutants to these TRPM2 sites showed normal expression and trafficking but gating was abolished (Mei et al., 2006a). Furthermore a substitution mutation targeting I1045K on the distal end of the S6 domain was responsible for discriminating charge, switching the channel from cation to anion currents (Kuhn et al., 2007). An area dubbed the TRP box, overlapping the S6 domain of TRPM2 at the C-term distal end, is highly conserved amongst all members of the TRP family. The role of the area is unknown but presumed to be required for the assembly and function of the TRPM2 pore region (Montell et al., 2005).

The C-terminal of TRPM2 spans the remaining roughly 500 amino acids, consisting of a 100 amino acid CCR, a spacer and finally the nucleoside diphosphate coupled to a varying moiety X (NUDIX) domain. The NUDIX contains the NUDT9-H enzymatic adenosine diphosphate ribose (ADPR) hydrolase binding region, which gave TRPM2 the unique chanzyme designation (Perraud et al. 2003; Montell, 2005). The CCR region is hypothesized to serve several important functions: trafficking, gating and tetrameric assembly (Jiang, 2007a). The CCR is also a predicted site for an unknown protein-protein interaction possibly responsible for TRPM2 gating

(Perraud et al., 2003). Site-directed mutagenesis of the CCR substantially reduced subunit interaction and currents. This was not due to altered expression, but instead due to reduced trafficking of the subunit and thereby proper localization at the membrane (Mei et al., 2006b). It was hypothesized the CCR functions by changing the energy and conformation of the linker region upon activation (Mei et al., 2006b). The linker region between CCR and NUDT9 domain is unlikely to serve an important physiological role, when removed no difference between WT and mutants were found; furthermore the sequence is not highly conserved between human and mouse TRPM2 (Perraud et al., 2003).

The NUDT9-H region (1236-1503AA), named after its homologous enzymatic domain responsible for ADPRase activity in mitochondria, has proven to be of significant early interest and vital to gating TRPM2 via ADPR binding (Perraud et al., 2003). The NUDIX region consists of 2 domains: the C-term core contains the structures necessary for ADPRase activity and the N-term acts as a CAP domain by enhancing the ADPR affinity of binding (Perraud et al., 2003). The domain shares 39% sequence homology to human NUDT9 ADPR pyrophosphatase. Importantly, a glutamate residue at position 320 has been replaced by isoleucine (E320I), which greatly diminishes (~1%) the enzymatic activity of the domain, when compared to the activity of NUDT9 (Shen et al., 2003). TRPM2 function was greatly reduced by reestablishing full enzymatic activity through substitution mutagenesis at sites 1405 and 1406 (Kuhn and Luckhoff, 2004); this suggests hydrolysis of ADPR is not required for channel gating, instead the domain has been adapted as an ADPR binding site only (Perraud et al., 2005).

Several splice variants of TRPM2 have been discovered. The first splice variant TRPM2-S (“short”) is missing everything beyond transmembrane segment 2 (4 transmembrane segments and the C-terminal). It is commonly found in hemapoetic cells, cloned from bone marrow and is a result of a stop codon between exons 16 and 17. Interestingly it shows similar membrane localization and is immunoprecipitated along with full length TRPM2 (Zhang, 2003a). Another set of splice variants missing either exon 11 (TRPM2- Δ N), exon 27 (TRPM2- Δ C) or both (TRPM2- Δ N Δ C) was identified in neutrophil granulocytes; intriguingly the TRPM2- Δ C variant is missing 1292-1325AA, which overlaps with the ADPR NUDIX domain (Wehage et al., 2002; Kuhn and Luckhoff, 2004). Finally, a short form of hTRPM2 found in the striatum (caudate nucleus and putamen) and nicknamed SSF-TRPM2 (striatum short-form TRPM2) may be expressed on the plasma membrane. It is transcribed from intron 4 onwards and is missing 214AA of the N-terminal, therefore being 1289AA long (Uemura et al., 2005). The TRPM2-S variant has been shown to traffic and express on the cell membrane forming tetramers with full-length TRPM2. As subunits lack an ADPR binding domain the subunits interrupt functional TRPM2 tetrameres; transfection of TRPM2-S was a method successfully employed in early TRPM2 research to reduce the functional expression of the channel on the membrane (Wehage et al., 2002; Zhang, 2003a; Kuhn and Luckhoff, 2004; Uemera et al., 2005;).

1.4 Physiological roles of TRPM2

Expression of TRPM2 throughout the body/CNS and role in oxidative mediated Ca^{2+} influx makes it a strong candidate to mediate many physiological processes. In addition, a role for TRPM2 in cellular death and apoptosis was suggested (Nadler et al., 2001). Furthermore TRPM2 knockouts or knockdown with RNAi strategies protects cells from oxidative-stress mediated cellular death (Miller, 2004; Grubisha et al., 2006). TRPM2 is localized in mouse dendritic cells and is required for dendritic cell maturation via chemokine production and thereby cell migration (Toledo et al., 2011). However, TRPM2 holds roles beyond cellular death mediating important physiological processes and maintaining cellular homeostasis.

Ca^{2+} influx is required for insulin release in pancreatic beta cells endogenously expressing TRPM2 (Inamura et al., 2002). TRPM2 is not limited to the plasma membrane and may release Ca^{2+} from intracellular lysosomal stores during insulin release (Lange et al., 2009). TRPM2 is not inherently required for functional insulin release, but instead seems to be involved when Beta cells are stressed (Scharenberg, 2009). TRPM2 activation may instead lead to apoptosis of Beta cells when damaged from oxidative stress, or to mediate cytokines to attract inflammatory agents (Scharenberg, 2009).

Much attention has been dedicated to the role of TRPM2 in the inflammatory process due its expression in monocytes, neutrophils and lymphocytes (Yamamoto et al., 2009). The role of inflammation in the system is to taxi fluids containing the necessary cellular proteins and nutrients to eliminate injuring agents and trigger the repairing process (Yamamoto et al., 2009). Increased intracellular calcium via

TRPM2 is essential for function of activated microglia that release cytokines and nitrous oxide, suggesting a role for the channel in macrophage function (Kraft et al., 2004). TRPM2 Ca^{2+} influx is also thought to directly mediate cytokine release, which has a role in mediating recruitment of inflammatory cells to the site of injury (Yamatoto et al., 2009). Finally, during inflammation phagocytes produce ROS to promote host defense, however if left unchecked, ROS can be damaging to healthy tissue (Die et al., 2012). TRPM2 activated by ROS acts as a negative feedback loop by depolarizing phagocytes and restricting ROS production (Di et al., 2012). Mice deficient in TRPM2 given an endotoxin had a larger inflammatory response, more damage to lungs and reduced survival versus wild-type mice (Die et al., 2012).

Several less often discussed physiological roles of TRPM2 have been identified. Knock out of TRPM2 abolishes sweet and sour tastes, but has no effect on acidic or bitter transduction (Zhang et al., 2003b). The channel also participates in immune response, which is triggered by Ca^{2+} (Sano et al., 2001) requiring chemotaxis from sites of infection to lymphoid organs (Toledo et al., 2011). Reduced activity of cytokines in TRPM2 KO mice resulted in uncontrolled *Listeriosis* infection, suggesting a role in innate immunity (Knowles et al., 2011). TRPM2 is expressed in cardiac fibroblasts and its expression is induced by hypoxic stress (Takahashi et al., 2012). TRPM2 is also critical for N-Methyl-D-aspartic acid (NMDA) mediated long term depression (LTD) through regulation of GSK3 β and the scaffolding protein PSD95 (Xie et al., 2011). TRPM2 knockout results in decreased activation of GSK3 β (Xie et al., 2011). GSK3 β internalizes AMPA receptors, which has been shown to reduce hippocampal LTD (Xie et al., 2011). Finally TRPM2 may contribute to neuropathic

pain by aggravating inflammatory response and sensitizing the pain-signaling pathway (Haraguchi et al., 2012). The modification of TRPM2 regulation may be used to treat and identify a variety of diseases.

1.5 ADPR, H₂O₂ and βNAD⁺ mediated TRPM2 gating

TRPM2 was studied for its novel gating mechanisms induced by three seemingly unique signaling pathways: ADPR (Perraud et al., 2001), H₂O₂ (Hara et al., 2002) and βNAD⁺ (Sano et al., 2001). Before the characterization of TRPM2, ADPR had no defined role in vertebrates, although it had been found to be produced in many contexts including apoptosis, the pyridine nucleotide cycle and cADPR breakdown in the mitochondria (Perraud et al., 2001). Research focused around the NUDT9-H domain of TRPM2, which is homologous to the mitochondrial pyrophosphatase of ADPR (Perraud et al., 2001). The identification of NUDT9H as a specific ADPR hydrolyase led directly to the finding that TRPM2 is gated through intracellular ADPR (Perraud et al., 2001).

TRPM2 mediated cell death and metabolism of ADPR drew more interest to the field (Sano et al., 2001). This led to the finding that 10mM of H₂O₂ evoked currents in 92% of TRPM2 expressing cells providing a direct link to oxidative stress mediated cell death (Hara et al., 2002). Importantly, suppressing endogenous TRPM2 expression using an antisense oligonucleotide significantly protected against H₂O₂ mediated cell death in Rat RIN-5F cells and monocyte U937 cell line (Hara et al., 2002). The findings were replicated using TRPM2-S (a splice variant of TRPM2) co-expression to reduce H₂O₂ mediated currents and subsequent

susceptibility to cell death and apoptosis (Zhang, 2003a). Additionally, H₂O₂-mediated currents were isolated in the tetracycline induced HEK293 TRPM2 expression cell line; current-voltage relationship was linear and reversed at 0mV consistent with a non-selective cation channel (McHugh et al., 2003). These early findings, especially by the groups supporting βNAD⁺ and H₂O₂ mediated TRPM2 currents, would soon be explained by a unifying theory with ADPR as the mediator of TRPM2 activation (Scharenberg, 2005).

Conflicting evidence of the precise mechanism through which TRPM2 was pharmacologically activated was common. H₂O₂ mediated gating of TRPM2 was believed to be independent from ADPR as the TRPM2-ΔC splice variant (missing 1292-1325AA and accordingly part of the NUDT9H region) prevented gating by ADPR but curiously not in response to H₂O₂ (Wehage et al., 2002). Furthermore cells co-expressing SSF-TRPM2 still maintained an H₂O₂-mediated current despite the complete lack of a NUDT9-H binding domain (Uemera et al., 2005). However H₂O₂ activation without ADPR binding was not reproduced by another group (Kuhn and Luckhoff., 2004). Characteristic H₂O₂-mediated currents were slow to develop (3-6min delay), defined by a second Ca²⁺ rise not seen in cells without TRPM2 and could be abolished by mannitol, a radical species scavenger, suggesting H₂O₂ action was via intracellular free radicals (Wehage et al., 2002).

Meanwhile βNAD⁺ was also implicated as an activator of TRPM2 channels and at the time was believed to interact directly with the NUDT9-H domain in a manner similar to ADPR (Sano et al., 2001). TRPM2 mRNA was isolated from neutrophil granulocytes and characteristic TRPM2 currents evoked by both ADPR

and β NAD⁺ (Heiner et al., 2003). The slow β NAD⁺ evoked inward currents were thought to be a result of weaker binding affinity than ADPR alone, although β NAD⁺ worked synergistically with ADPR (Sano et al., 2001). It has been suggested that ADPR contamination is common amongst NAD commercial samples (Scharenberg, 2005). Another explanation of slow currents was slow wash out of ATP, which can suppress β NAD⁺ (Sano et al., 2001).

β NAD⁺-mediated TRPM2 currents were inconsistent in their reproduction by several groups (Kuhn and Luckhoff, 2004; Wehage et al., 2002), this may have been a result of ADPR contamination in earlier studies (Scharenberg, 2005). β NAD⁺ gating of TRPM2 was also abolished with any ADPR-insensitive splice variants (Kuhn and Luckhoff, 2004; Perraud et al., 2005). However it was quickly speculated the structure of β NAD⁺ seemed unlikely to bind to the NUDIX region (Kolisek et al., 2005), indeed crystal structure analysis revealed the NUDT9-H is unable to accommodate the additional nicotinamide group required for β NAD⁺ binding (Perraud et al., 2005). Radiolabeled β NAD⁺ failed to efficiently compete for the ADPR binding domain (less than 20-fold) suggesting it does not bind directly with TRPM2 as previously speculated (Grubisha et al., 2006). Furthermore, the physiological relevance of very high 1mM β NAD⁺ was called into question; perhaps ADPR contamination during recordings was to blame (Kolisek et al., 2005; Perraud et al., 2005).

Research refocused on ADPR as the main pharmacological gating agent of TRPM2. TRPM2 currents were inhibited using an enzyme to prevent accumulation of ADPR in the cytosol by hydrolyzing ADPR; this eliminated the effects of ADPR

contamination via β NAD⁺ hydrolysis to ADPR (Perraud et al., 2005). Interestingly enzymatic activity at the NUDT9-H domain of ADPR is not required for TRPM2 gating as previously speculated (Perraud et al., 2001).

1.6 Production of ADPR

Since oxidative and nitrosative stress do not appear to gate TRPM2 directly, the processes must be linked to ADPR-mediated activation. This is further evidenced by a mutant preventing ADPR binding, which also prevented channel gating via ROS (Perraud et al., 2005). Two pathways have been proposed for ADPR release into the cytosol. The first: mitochondria are induced to produce ADPR and release it to the cytosol under stress gating of TRPM2 (Perraud et al., 2005).

Mitochondrial permeability transition pores (mPTP) are often recruited during oxidative stress or neuronal stress resulting from traumatic brain injury or stroke. Proteins underlying the mPTP are recruited to form a pore in the inner membrane of mitochondria allowing molecules less than 1500 Daltons to pass through the membrane such as ADPR (Perraud et al., 2005). ADPR is derived from its precursor NAD and the mitochondria are a major cellular store for NAD (Perraud et al., 2005). Accumulation of cytosolic ADPR release from the mitochondria is critical to nitrosative and oxidative stress-gating of TRPM2, providing evidence that H₂O₂ is an upstream releasing agent of ADPR from the mitochondria (Perraud et al., 2005).

The second pathway involves polyADPR-polymerase(PARP) and polyADPR-glycohydrolase (PARG). PARP-1 is a 113kDa nuclear enzyme which is recruited following DNA damage and hydrolyses β NAD⁺ to ADPR (Davidovic et al., 2001).

Following DNA breakage resulting from oxidants, alkylating agents or ionizing radiation (Virag and Szabo, 2002), the zinc fingers of the DNA binding domain of PARP-1 recognize the damaged area (Davidovic et al., 2001). Binding allosterically activates the catalytic domain of PARP-1 allowing posttranslational modification of the substrate β NAD⁺. PARP occurs late in the process catabolizing histone bound pADPR, allowing histones to bind DNA and form nucleosomes once more (Davidovic et al., 2001). PARP catalyzes the hydrolysis of branched polymers producing ADP-ribose (Soldani et al., 2001) and degrades PARP-1 (Soldani and Scovassi, 2002).

It has been proposed that H₂O₂ results in DNA damage possibly through peroxide, resulting in increased production of ADPR via PARP-1 and thereby feeding back on TRPM2 activation (Miller, 2004). TRPM2 activation leads to Ca²⁺ influx and PARP cleavage, thereby creating a negative feedback loop (Zhang et al., 2006). The role of PARP-1 on H₂O₂-mediated TRPM2 activation was examined in HEK293 cells (Fonfria et al., 2004). A series of structurally distinct PARP inhibitors were used with varying potency that inhibited H₂O₂-induced TRPM2 currents (Fonfria et al., 2004). PARP inhibitors did not influence ADPR mediated currents therefore they are not directly interacting with the NUDT9-H domain (Fonfria et al., 2004). It was found that over-activation of PARP-1 catabolizes all β NAD⁺, a precursor for ATP, causing cellular dysfunction (Fonfria et al., 2004).

One question remained unanswered: whether generation of ADPR in intracellular stores is sufficient to gate TRPM2. Basal ADPR levels are close to or above modulatory requirements as determined by a novel reverse-phase HPLC technique used to quantify ADPR (Gasser et al., 2005). This lends strong evidence to

a quick burst of ADPR as a modulatory mechanism of TRPM2, which is maintained by additional hydrolysis of NAD to ADPR (Gasser et al., 2005). ADPR alone has been shown to reach sufficient cytosolic concentrations to gate TRPM2 channels (Buelow et al., 2008). The H₂O₂ direct gating of TRPM2 has been ruled out in favour of downstream regulation by ADPR binding (Scharenberg, 2005). Nevertheless, while H₂O₂ does not bind directly with TRPM2, ROS are the most likely beginning to a chain of events that evokes Ca²⁺ influx through TRPM2 channels.

1.7 Ca²⁺ and TRPM2

Early TRPM2 research implicated a Ca²⁺-dependent gating of the channel in addition to ADPR requirement (Perraud et al., 2001). It was initially unclear whether Ca²⁺-dependence of gating occurs at the intra- or extra-cellular environment. When intracellular Ca²⁺ stores were depleted ADPR alone was no longer sufficient to evoke TRPM2 currents (Perraud et al., 2001). However intracellular buffering of Ca²⁺ greatly attenuates H₂O₂ mediated currents despite extracellular Ca²⁺ concentrations (McHugh et al., 2003). Other divalent cations (such as Mg²⁺) could not substitute for Ca²⁺ in promoting TRPM2 channel activation (McHugh et al., 2003). It is now thought that TRPM2 activation is dependent on intracellular Ca²⁺ and then maintained by influx of Ca²⁺ from the extracellular environment (Csanady and Torocsik, 2009). When intracellular Ca²⁺ falls below 100nM, TRPM2 inactivates (Starkus et al., 2007).

Extremely high ADPR in the absence of Ca²⁺ is sufficient to evoke TRPM2 currents (Starkus et al., 2007). On the other end of the spectrum 100μM

intracellular Ca^{2+} alone is also sufficient to gate TRPM2 and several splice variants lacking an ADPR binding domain (Du et al., 2009a). Of course, the physiological relevance of these two studies can be called into question since the concentration of ADPR and Ca^{2+} used are not at all physiological. For example, an analytical HPLC method (Gasser et al., 2005) was employed to measure ADPR concentrations (Heiner et al., 2006). These studies estimated that the physiological concentration of ADPR is in the range of $5\mu\text{M}$. Similarly, resting levels of intracellular Ca^{2+} are $1\mu\text{M}$. Importantly, within their respective physiological range neither Ca^{2+} nor ADPR can promote TRPM2 channel alone. Accordingly, given physiological levels of ADPR and Ca^{2+} it is more likely both work in concert to regulate TRPM2 (Heiner et al., 2006; Casanady and Torocsik, 2009). Indeed ADPR and Ca^{2+} show a synergistic effect; even in the presence of 100nM Ca^{2+} , ADPR was further able to increase currents 2.5-fold (Due et al., 2009a).

Single channel TRPM2 analysis identified four sites, likely one per channel subunit, which was required to initially gate and maintain TRPM2 current (Csanady and Torocsik, 2009). Calmodulin (CaM) a ubiquitously expressed Ca^{2+} sensor (see section 1.11 for a thorough review of CaM) appears to be responsible for the Ca^{2+} -dependent activation of TRPM2 (Tong et al., 2006). Additional 100nM CaM added to the patch pipette significantly increased ADPR mediated TRPM2 currents (Starkus et al., 2007). $2\mu\text{M}$ Calmidazolium, a CaM inhibitor, prevented ADPR mediated TRPM2 currents (Starkus et al., 2007). A dominant negative mutated form of CaM was able to compete with endogenous CaM and restrict TRPM2 mediated current, hinting at an intracellular binding domain (Tong et al., 2006). Immunoprecipitation

implicates a direct interaction between CaM and TRPM2; strong binding was identified in the N-terminal (1-730AA) and weak binding in the C-terminal (1060-1503AA) in the presence of 100uM free Ca²⁺ buffered with 5mM EGTA (Tong et al., 2006). This was taken as evidence that CaM was associating with the N-term only to activate TRPM2 (Tong et al., 2006). An IQ-like consensus binding motif on the 406-416AA N-terminal of the channel received substitution mutations to key residues (TRPM2-CaM_{Mut}(NT_{IQ})) which produced a mutant incapable of activation (Tong et al., 2006). Currents can not be elicited from TRPM2-CaM_{Mut}(NT_{IQ}) regardless of intracellular Ca²⁺ or ADPR (Du et al., 2009a). It is now fairly agreed upon, TRPM2 is gated by both ADPR binding to a C-term NUDT9-H domain concurrent with Ca²⁺-CaM binding to an intracellular N-term IQ-like motif (Perraud et al., 2005; Tong et al., 2006).

1.8 Other TRPM2 regulation mechanisms

Several other pharmacological modulators of TRPM2 gating have been uncovered recently that alter ADPR mediated currents. Heat alone has been found to potentiate hTRPM2 and works synergistically with βNAD⁺ and ADPR activation of TRPM2 (Togashi et al., 2006). cADPR is an intermediary cyclase converted from βNAD⁺ by CD-38 and can then be converted to ADPR (Togashi et al., 2006; Kolisek et al., 2005). Cyclic-ADPR was originally thought not to mediate TRPM2 (Perraud et al., 2001), however under body temperatures it can successfully gate the channel (Togashi et al., 2006). Heat maximizes TRPM2 current at a 35°C threshold, importantly EC₅₀ of βNAD⁺ was not altered (Togashi et al., 2006). The

concentrations of cADPR required to gate TRPM2 channel directly (100 μ M) are not physiologically relevant, but with small amounts cADPR can greatly potentiate ADPR and β NAD⁺ evoked TRPM2 currents (Kolisek et al., 2005).

Tyrosine phosphorylation status of TRPM2 is thought to be an important regulator because of research with PTPL1, a tyrosine phosphatase with a role in cell survival and tumorigenesis (Zhang et al., 2007). PTPL-1 promotes TRPM2 dephosphorylation, decreased intracellular calcium currents and increased cell survival from H₂O₂ mediated cell death (Zhang et al., 2007). PTPL-1 was immunoprecipitated with TRPM2, the mechanism remains unknown but PTPL-1 may be dephosphorylating tyrosine at the CaM, ADPR or pore region thereby altering binding affinity or channel gating kinetics (Zhang et al., 2007). Other proteins dephosphorylated by PTPL-1 are often phosphorylated by Src family kinases (Zhang et al., 2007). Our lab has preliminary evidence to suggest Fyn but not Src is the kinase responsible for TRPM2 tyrosine phosphorylation (MacDonald Lab, Unpublished).

Glutathione (a naturally occurring antioxidant) inhibits TRPM2 gating, shifting the dose response curve of ADPR 3.5-fold. The modification occurs independent of any cysteine residues (thiol-independent), currently the mechanism glutathione uses to modulate TRPM2 is unknown (Belrose et al., 2012).

Acidic pH may block TRPM2 channels at IC₅₀ 5.3pH extracellular and IC₅₀ 6.7 pH intracellular (Du et al., 2009b). Low extracellular pH may also irreversibly block TRPM2; likely due to different preparations this has been argued to occur at 4.0 pH (Du et al., 2009b), 5.0 pH (Starkus et al., 2010) or 6.0 pH (Yang et al., 2010). Several

conflicting hypothesis of pH regulation of TRPM2 have been proposed: intracellular permeation of ions through the pore interrupts Ca^{2+} binding at channel regulation sites (Starkus et al., 2010; Csanady, 2010). However Du et al., 2009b and Yang et al., 2010 argue protons bind at amino acid sites near the pore. Changing channel conformation or bound protons could decrease local Ca^{2+} concentrations and thereby Ca^{2+} influx required to promote TRPM2 activation (Du et al., 2009b; Yang et al., 2010).

1.9 Antagonists of TRPM2

The development of pharmacological agents capable of selectively inhibiting TRPM2 has lagged the significant advances made in understanding TRPM2 function. However, several non-specific inhibitors have been discovered that can be used in series with other inhibitors. Flufenamic acid (FFA) is an antagonist that inhibits TRPM2 with minimal recovery (~10-15%) observed after washout (Hill et al., 2004a). FFA can only block TRPM2 extracellularly and is potentiated by low pH (Hill et al., 2004a). Similarly antagonists (antifungal imidazoles) clotrimazole and econazole both inhibit TRPM2 in extracellular solutions at concentrations ranging from $3\mu\text{M}$ to $20\mu\text{M}$ (Hill et al., 2004b). Interestingly FFA and antifungal imidazoles block TRPM2 in RAT CRI-G1 cells but currents are fully recovered on washout, suggesting a cell specific effect of these antagonists (Hill et al., 2004a; Hill et al., 2004b). Problematically, FFA destabilizes cellular membranes (Hill et al., 2004a) and antifungal imidazoles are far from specific (Hill et al., 2004a). FFA blocks CaM, which is necessary Ca^{2+} sensor for many cellular processes and TRPM2 activation

(Hill et al., 2004b; Tong et al., 2006). It has been suggested FFA acts as a weak acid irreversibly blocking TRPM2 channels through the same mechanism outlined in pH sensitivity of TRPM2 (Naziroglu et al., 2007). N-(*p*-amycinnamoyl)anthranilic acid (ACA) also acts as a weak acid blocking TRPM2, however inactivation was found to be pH dependent (Kraft et al., 2006). Antagonism was fast and unable to recover at pH 6.0, but was slow and fully recovered at pH 7.4 (Kraft et al., 2006).

TRPM2 antagonists FFA and ACA have been used to partially block H₂O₂ mediated cell death in transfected HEK203 cells (Wilkinson et al., 2008). Current antagonists remain limited by their slow inhibition or irreversible inhibition of TRPM2 (Togashi et al., 2008). Other antagonists such as 2-APB provide a reversible block of TRPM2 upon wash-out (Togashi et al., 2008). However 2-APB has been shown to block other TRP channels and GAP junctions, and no specific TRPM2 blocker has yet been identified (Togashi et al., 2008).

1.10 *Guam hTRPM2 P1018L and CDI*

TRPM2 has been associated with Western Pacific amyotrophic lateral sclerosis (ALS) and Parkinsonism Dementia (PD). ALS type symptoms associated with muscle weakness are defined by neurodegeneration of the motor neurons and is eventually fatal (Rowland, 2001). Parkinsonism dementia is also highly correlated in this population, a disease defined by symptoms of both Parkinson's and dementia in the same individual (Hermosura and Garruto, 2007).

Epidemiological studies were interested in Guamanian diseases due to clustering amongst families, but little progress was made to identify candidate genes

(Hermosura and Garruto, 2007). Three factors are thought to contribute to the disease: the environmental conditions in Guam (low Mg^{2+} and Ca^{2+}), high incidence of ALS and PD and altered Ca^{2+} metabolism amongst patients fed a similar diet, and a genetic mutation to TRPM2 observed in this population (Hermosura and Garruto, 2007; Hermosura et al., 2008). A missense mutation was identified in hTRPM2 Guam genetic populations substituting a Proline for a Leucine at 1018AA (Hermosura et al., 2008). Computer modeling suggests the substitution relaxes the structural integrity of the pore-forming loop of hTRPM2, the Proline identified is highly conserved amongst species and other TRPM channels (Hermosura et al., 2008). Intriguingly Ca^{2+} rise was significantly inhibited in P1018L hTRPM2 transfected cells versus WT activated by H_2O_2 (Hermosura et al., 2008). Finally P1018L hTRPM2 showed inactivation over-time, a phenomenon they claimed was not seen in wild-type channels and was only increased by raised ADPR and extracellular but not intracellular Ca^{2+} concentrations (Hermosura et al., 2008). Considerable evidence has led to a focus of the role of TRPM2 in neurodegeneration. Furthermore, knowledge of TRPM2 inactivation over time is limited and rarely discussed in the literature. Our lab has grown interested in the mechanism behind TRPM2 inactivation, which has not been well defined.

1.11 Ca^{2+} -dependent inactivation

When TRPM2 ADPR dependence was initially characterized, some inactivation was observed in whole-cell recordings that could be abolished when intracellular Ca^{2+} concentrations were buffered to 100nM with 2-bis(o-aminophenoxy)ethane-

N,N,N',N'-tetraacetic acid (BAPTA) a Ca^{2+} chelator (Perraud et al., 2001). What has been defined as a rundown of current was observed in both human (Sano et al., 2001) and rat (Hill et al., 2006) TRPM2 channel recordings. Rundown was not successfully reduced by additional CaM, protein kinases and ATP or lowering intracellular Mg^{2+} (Csanady and Torocsik, 2009). Additionally 25uM dioctanoyl phosphatidylinositol 4,5-biphosphate, which has been shown to rescue other TRP channels from desensitization had no effect (Zhang et al., 2004; Csanady and Torocsik, 2009).

Preliminary evidence of TRPM2 inactivation from our laboratory has given us a clearer understanding of the kinetic and mechanistic process. HEK293 cells stably expressing doxycycline inducible TRPM2 were utilized in whole-cell patch-clamp recordings. $0.3\mu\text{M}$ ADPR, 1mM Ca^{2+} buffered with 10mM EGTA in the patch pipette and 2mM Ca^{2+} in the extracellular fluid (ECF) were utilized to evoke TRPM2 currents. What we observe (figure 1.2) is a slow increase in current reaching peak amplitude (I_p), followed by a marked decrease reaching a steady state (I_{ss}). When measuring and referring to inactivation we define it as the ratio between the I_{ss}/I_p .

It was originally speculated that hydrolysis of ADPR at the NUDT9-H domain may reduce ADPR intracellular concentrations and inactivate TRPM2 over-time (Minke and Cook, 2002). However, we now know enzymatic activity at the NUDT9H site is not required for ADPR mediated TRPM2 gating (Perraud et al., 2005; Kuhn and Luckhoff, 2004). An alternative explanation of TRPM2 inactivation involves the internalization of the channel in response to Ca^{2+} , seen in other cation permeable channels (Dargent et al., 1994). Preliminary evidence from our lab (Appendix –

Figure A1) indicates TRPM2 inactivation recovers over time when exposed to 0mM Ca^{2+} ECF. A time course of recovery was performed and peak recovery was observed at 3 minutes. Furthermore, increased concentrations of ADPR from 0.3mM to 1mM (Appendix -Figure A2) increased the recovery time from inactivation, the opposite effect if we expect inactivation to be a result of depleted ADPR. This indicates activation is neither regulated by hydrolysis of ADPR cytosolic stores nor the internalization of TRPM2 channels in response to Ca^{2+} currents, but rather some unknown mechanism.

A critical finding by Perraud et al, 2001 has identified inactivation as an intracellular Ca^{2+} -dependent process that can be abolished by buffering Ca^{2+} with BAPTA. Interestingly, inactivation in TRPM2 is also a CaM-dependent process: when intracellular CaM is increased beyond endogenous concentrations using 100 μM in the patch pipette there was a significant increase in inactivation (Appendix - Figure A3). Recall CaM is also responsible for the activation of TRPM2 by interacting with an IQ-like CaM binding site on the intracellular N-terminal of the channel (Tong et al., 2006). How CaM could be regulating TRPM2 inactivation remains to be discovered.

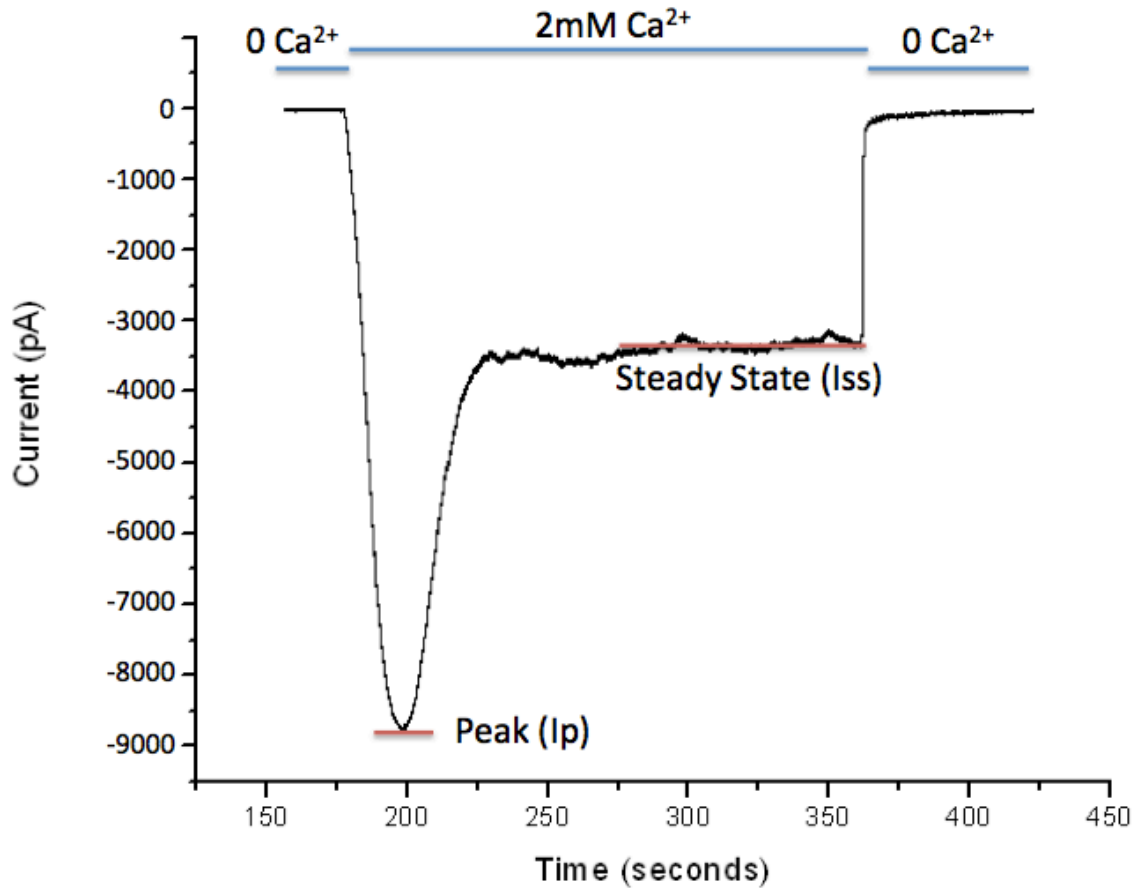


Figure 1.2 – Representative trace of a whole-cell voltage-clamp recording at -60mV using HEK293 cells stably expressing TRPM2 channels. Currents were elicited with 0.3mM ADPR and alternating applications of 0mM Ca^{2+} and 2mM Ca^{2+} ECF via a multi-barreled fast perfusion system. Notable inactivation was observed over time in response to Ca^{2+} containing ECF and measured as the ratio of the Steady state (I_{ss}) over the Peak (I_p), (I_{ss}/I_p). Marked inactivation of currents was easily reproducible using our recording protocol.

1.12 Calmodulin, inactivation and VGCC binding

Calmodulin is a ubiquitously expressed protein involved in a wide variety of regulatory functions in nearly every eukaryotic cell (Crivici and Ikura, 1995). It is known to activate more than 40 classes of proteins such as Ca²⁺ channels, TRP channels and Ca²⁺ release channels from internal organelle stores (Saimi and Kung, 2002). CaM has been essentially rediscovered multiple times throughout the literature due to its ubiquitous involvement in many physiological processes (Jurado et al., 1999). The nomenclature Calmodulin was finally assigned in 1979 and has been widely used ever since (Lynch and Cheung, 1979). CaM is a small soluble protein (17kDa) reaching concentrations of 1-10uM in the brain, nearly half of which is associated with the membrane (Saimi and Kung, 2002). CaM has a 100% conserved identity in vertebrates and its repeated expression found over several different genes; homology is essential for the diverse interactions of CaM amongst many different vertebrate proteins (Friedberg, 1990).

CaM consists of 4EF hands, two on each terminal, forming globular lobes connected by an alpha helix giving the three dimensional representation of a dumbbell (Babu et al., 1985). The alpha-helix is a hydrophobic region involved in protein interaction (Babu et al., 1985). CaM functions through its different conformational affinities for Ca²⁺ (Klevit et al., 194). Ca²⁺ binding changes the conformation of CaM, promoting opening the EF hands to expose the hydrophobic binding region (Saimi and Kung, 2002). Ca²⁺ bound to CaM EF hands 3 and 4 on the C-term does exist naturally in solution; this is due to a much stronger affinity for Ca²⁺ at EF hands 1 and 2 on the N-term (Klevit et al., 1984). While up to 16 different

conformational states of CaM may exist, most interactions of CaM can be summed up as 3-4 Ca²⁺ occupied EF hands or CaM in absence of Ca²⁺ (ApoCaM) (Jurado et al., 1999).

CaM complexes are varied; much of the structural information gained is from model peptides of target binding domains and mutated CaM (Crivici and Ikura, 1995). Binding sites are then mapped by deletions, truncations and site directed substitution mutations (Crivici and Ikura, 1995). Several types of CaM consensus binding sites have been identified (Hoeflich and Ikura, 2002). Three types of motifs are defined by aromatic amino acids bridged by bulky hydrophobic and basic amino acids and are named according to the relative position of these key amino acids (i.e. the so-called 1-10, 1-14 and 1-16 CaM binding motifs) (Hoeflick and Ikura, 2002). IQ-like motifs are defined by amino acid consensus site IQXXXRGXXXR, but substitutions are common (Jurado et al., 1999). ApoCaM has been shown to bind to IQ-like motifs, interaction with these sites increases CaM affinity to Ca²⁺ up to 1000-fold which is thought to hasten the responsiveness to Ca²⁺ (Jurado et al., 1999). ApoCaM shows much greater homology amongst binding sites than Ca²⁺-CaM diversity (Jurado et al., 1999). Interestingly, IQ-like motifs often overlap with phosphorylation sites of protein kinase C and are dephosphorylated by calcineurin, phosphorylation is thought to inhibit CaM binding (Apel et al., 1990). Several CaM inhibitors are commonly used for experimentation: W7, Calmidazolium and mastoparan (Saimi and Kung, 2002).

Research into CaM-mediated regulation of TRP channels can be traced back to the photo transduction cascade of TRP in *Drosophila* (Phillips et al., 1992). CaM has

been shown to regulate activation of TRPM2 on an N-term IQ-like consensus-binding site (Tong et al., 2006). Results were determined using Ca^{2+} imaging of single transfected cells (Tong et al., 2006). Immunoprecipitation of CaM and TRPM2 terminal fragments revealed strong binding to the N-terminal (1-760AA) and weak binding to the C-terminal (1060-1503AA) (Tong et al., 2006). Substitution mutagenesis was carried out to an IQ-like motif site on the N-term that reduced but did not eliminate CaM binding, suggesting a second CaM binding site may exist (Tong et al. 2006). CaM binding to the N-term IQ-like motif is essential for Ca^{2+} -dependent activation of TRPM2 and can no longer be activated with ADPR (Tong et al., 2006; Starkus et al., 2007; Du et al., 2009a).

Intriguingly, preliminary evidence exists for CaM-dependent regulation of TRPM2 Ca^{2+} -dependent inactivation (CDI) from our own unpublished laboratory findings (Appendix – Figure A3). Supplementing the patch pipette solution with 100 μM CaM increased the CDI observed from TRPM2 transfected HEK293 cells. The CaM-dependence of TRPM2 CDI cannot be elucidated by traditional means. CaM is required for channel activation and CaM inhibitors make it impossible to measure inactivation from an inactivated channel. A substitution mutagenesis strategy has been adopted for CDI linked to CaM consensus sites in other TRP homologs (Singh et al., 2002), however the efficacy may be limited for our use if CaM mutants interfere with channel activation.

Ca^{2+} -CaM regulation of inactivation is common within other ion channels and most commonly associated with L-type Ca^{2+} channels (Zhu and Reuter, 1998) and NMDA (Zhang et al., 1998). CaM is constitutively bound to an IQ-like consensus

site of L-type channels (Zhulke and Reuter, 1998; Peterson et al., 1999). The group carried out a series of truncation mutations to determine the minimum-binding domain (Zhulke and Reuter, 1998). Two strategies were then employed; a dominant negative expression of a CaM mutant with alanine substitutions in 3 of the 4 EF hands was shown to abolish CDI in L-type channels (Peterson et al., 1999). Furthermore amino acid substitutions replacing the IQ-like consensus sites with Alanine also abolished CDI (Zuhlke et al., 1999). Ultimately Apo-CaM bound to L-type channels was determined to both facilitate channel activity and later inhibit the channel in a Ca^{2+} -dependent manner (Zuhlke et al., 1999; Peterson et al., 1999). A similar substitution mutagenesis strategy for a CaM consensus site on the NR1 subunit of NMDA abolished CDI (Zhang et al., 1998).

It is unclear whether constitutively bound endogenous ApoCaM prevented a dominant negative effect of CaM mutants transfected into our HEK293 TRPM2 expression system. Nevertheless we hypothesize TRPM2 CDI might be occurring through an additional CaM binding site. This is further evidenced by TRPM2-CaM_{Mut}(NT_{IQ}) generated by Tong et al., 2006, which reduced but did not eliminate CaM immunoprecipitation. Furthermore multiple CaM sites are found in TrpL (TRP-like homolog) channels seen in *Drosophila* photo transduction cascade, each with a different regulatory role (Scott et al., 1997). In fact other proteins have been identified with multiple CaM binding sites, one responsible for activation and another CDI such as Caldesmon (Wang et al., 1989) and Phosphofructokinase (Buschmeier et al., 1987).

1.13 Rationale and Hypothesis

Given: 1) Ca^{2+} -dependence of TRPM2 inactivation, 2) differing sensitivities of Ca^{2+} for activation and inactivation, 3) undiscovered CaM consensus binding sites 4) the precedence of CaM-mediated CDI with a number of Ca^{2+} permeable channels and 5) ineffectiveness of dominant negative CaM mutants; I hypothesize that the CDI of TRPM2 involves Ca^{2+} -CaM binding to an undefined CaM consensus motif distinct from that of activation (NT_{10}).

We adopted a strategy similar to those previously outlined to determine the site of CaM-dependent TRPM2 CDI. CDI was further characterized by varying extracellular Ca^{2+} and voltage steps. Using an *in silico* TRPM2 CaM consensus search to identify candidate sites, we developed a series of overlapping TRPM2 truncations to elucidate minimum binding domains. CaM-Sepharose pull-downs of stably expressed TRPM2 intracellular truncations measured CaM binding to each fragment. A series of substitution mutations to key amino acids was used to abolish CaM binding in each region, truncated fragments were then generated and compared to WT for CaM-Sepharose binding. Full length TRPM2 incorporating CaM consensus site substitution mutations was transfected into HEK293 cells and currents measured with whole-cell patch-clamp recordings. We predicted abolished CaM binding at an unknown TRPM2 CaM consensus domain via substitution mutations lead to sustained TRPM2 currents and no CDI developing over time.

Research by Hermosura et al., 2008 that identifies a proline to leucine substitution in hTRPM2 causing inactivation over time, we are interested if this increased activation is the same as our novel observation of TRPM2 CDI. Given the

location of the substitution near the pore-forming loop, we hypothesized an increased Ca^{2+} mediated current causes an increase in CDI. We predicted hTRPM2 P1018L transfected into HEK293 will display be altered kinetics leading to greater Ca^{2+} influx and therefore increased CDI.

Section 2

MATERIALS AND METHODS

2.1 Whole-cell patch clamp recording

Dr. A.M. Sharenberg (University of Washington and Children's Hospital and Medical Center, Seattle, Washington) provided the TREX-293, cells stably expressing TRPM2, utilized for electrophysiological recordings. Tetracycline-controlled transcriptional activation prevents transcription of TRPM2 unless reversibly induced by the antibiotic tetracycline. TRPM2 was flag-tagged for Western blotting analysis. Cells were maintained in culture at 37°C with 5% CO₂ in Dulbecco's Modified Eagle Medium (Sigma). Media contained 10% fetal bovine serum. TRPM2 cells were plated on 35mm dishes 24-48 hours prior to TRPM2 induction with Doxycycline (1µg ml⁻¹), a stable derivative of tetracycline 12-24 hours prior to recordings.

The extracellular recording solution contained the following: 140mM NaCl, 25mM Hepes, 5.4mM KCl, 33mM Glucose and 1mM MgCl₂. The pH of the solution was adjusted to 7.4 using NaOH, and an osmolarity of 310-315 was reached using millipore H₂O. Three working solutions were generated with varying concentrations of Ca²⁺ (2mM CaCl₂, 0.5mM CaCl₂) and a calcium free solution using 2mM BaCl₂ to maintain total divalent cation concentrations. ICF was made no more than 5 days prior to recordings, aliquoted to 500µl and frozen. The ICF contained: 135mM CsGluc, 10mM Hepes, 10mM EGTA, 4mM Mg-ATP, 2mM MgCl₂, and 1mM CaCl₂.

T-Rex293 cells stably expressing TRPM2 were voltage-clamped at -60mV during whole-cell recordings (unless indicated) using Axopatch-1B amplifier (Molecular Devices, Sunnyvale, CA). Currents were evoked through the addition of 0.3mM ADPR

(unless indicated) to the ICF on the day of recording via the patch pipette with a resistance between 3 and 5 M Ω . Utilizing a multi-barreled fast perfusion system (figure 2.1), cells were exposed to either the calcium free or calcium containing solutions. TRPM2 was primed with 2mM Ca²⁺ solution until it reached a 1nA current followed by a minimum of 3 minutes in 0mM Ca²⁺ solution prior to data collection. Data was recorded by 3-minute applications of Ca²⁺ solution, followed by a 5-minute 0mM Ca²⁺ TRPM2 recovery phase. Membrane-holding voltage was raised by 20mV increments between Ca²⁺ sweeps. All data collected was filtered at 2kHz, digitized and acquired using pClamp (Molecular Devices).

2.2 JetPrime (Polyplus) transfections of Hek293 Cells

Less than 24 hours prior, Hek293 cells were plated on a 6 cm dishes resulting in approximately 60% cell confluence at time of transfections. 200 μ l of JetPrime buffer solution, 3 μ g of DNA (flag-hTRPM2, flag-mTRPM2, mTRPM2-CaM_{Mut}(CT₁₋₁₄), mTRPM2-CaM_{Mut}(CT_{1Q}), mTRPM2-CaM_{Mut}(NT₁₋₁₄) or mTRPM2-CaM_{Mut}(NT_{1Q})) and 1 μ g of green fluorescent protein (PLB-GFP) were combined in a sterile microtube and vortexed. 6 μ l of JetPrime enzyme was added to the mixture and vortexed for 10 seconds. Following a ten minute incubation at room temperature the mixture was added drop wise to Hek293 cells, shaken, and incubated for 4 hours at 37°C with 5% CO₂. Following the incubation cells were washed using PBS and the media was replaced. 24 hours after transfection cells were plated at 1/36 ratio and used for electrophysiological whole-cell recordings the following day (section 2.1). UV exposure was used to visualize successfully transfected cells having been co-transfected with GFP.

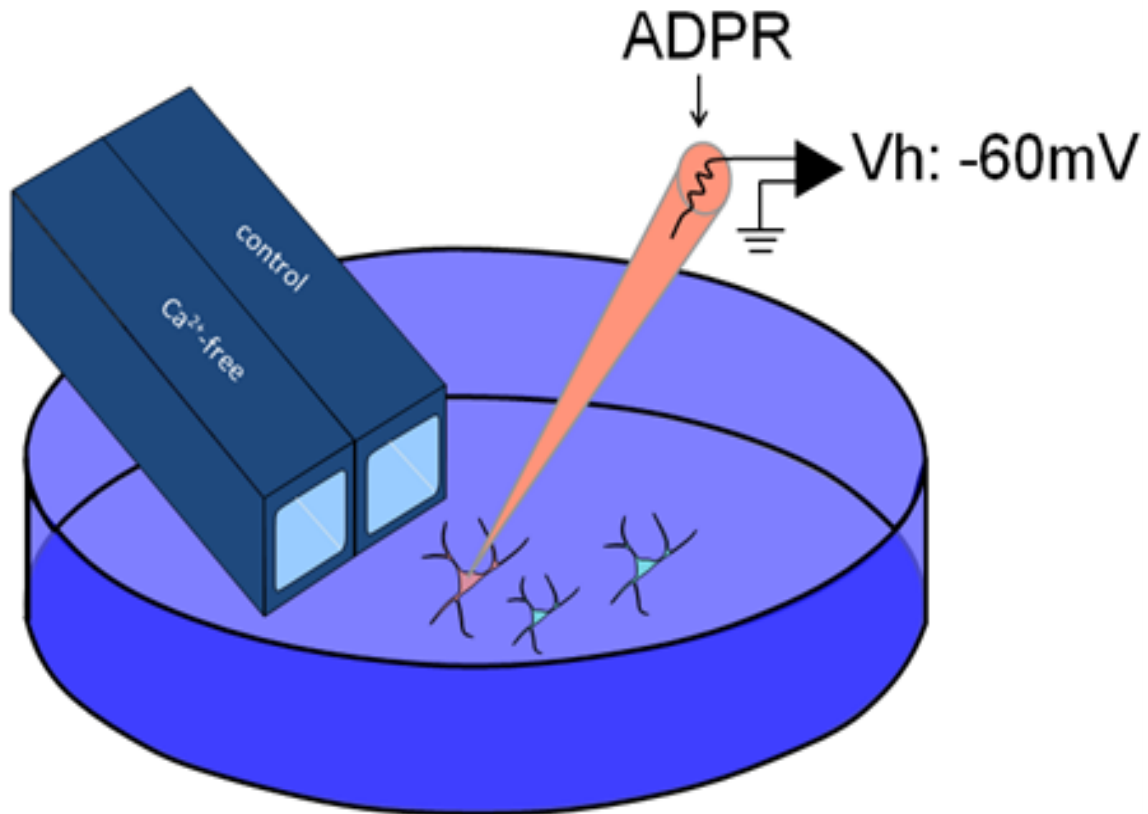


Figure 2.1 – Whole-cell patch-clamp recording setup from HEK293 cells stably expressing inducible TRPM2 channels. 0.3mM ADPR is added to the patch pipette solution to activate the channel. Cells are exposed to Ca^{2+} free ECF or ECF with variable concentrations of Ca^{2+} using a multi-barreled fast perfusion system. Cells are voltage clamped and maintained at -60mV unless noted. (Michael Jackson)

2.3 Generation of TRPM2 Intracellular Truncations

Forward and reverse primers were generated from pIRES-puro-flag-mTRPM2 template using Vector NTI software (Invitrogen). Primers included an *Asc*I and *Not*I enzymatic regions used for sub-cloning. TRPM2 truncations (figure 2.1) were designed to overlap candidate CaM consensus sites identified using *in silico* screening. Truncations were sub cloned into a pTNT-GST vector containing the required promoter region for the TNT Quick-Coupled Reticulocyte system (Promega) and were GST tagged to increased molecular weight and ensure sufficient lysine incorporation during experiments. The following constructs were generated for this project:

Construct	Forward Primer (5'→3')	Reverse Primer (3'→5')
pTNT-GST-CT1(1047-1163)	AGAGGCGCGCCAACTACA CCTT	AATATGCGGCCGCTAGTCCATG TCCAGCAGATCCA
pTNT-GST-CT2(1163-1278)	AATTAGGCGCGCCAATGGA CCAGGTGAAGAGGTCAG	TAATGCGGCCGCTACTTCTCAG CGGTGTAAAAGGG
pTNT-GST-CT3(1278-1395)	AATAGGCGCGCCAGAGAAG GATGTGGCTCTCACAGAC	TAATTAGCGGCCGCTATGGTA GCATCTCCCCTGGCT
pTNT-GST-CT4(1395-1507)	zTATTAGGCGCGCCACTAC CACGGAAGCTGAAACGGGT	AATATGCGGCCGCTACTTGAGC TGCTTATGCCTCT
pTNT-GST-CT5(1047-1082)	AGAGGCGCGCCAACTACA CCTT	AATATGCGGCCGCTACTTGAGC TGCTTATGCCTCT

pTNT-GST- CT6(1108-1163)	AGGCGCGCCAAAGAACAAG CTGGAGAAGAACGAGGA	AATATGCGGCCGCTAGTCCATG TCCAGCAGATCCA
pTNT-GST- CT7(1047-1082)	AGAGGCGCGCCAAACTACA CCTT	TAATTAGCGGCCGCTAAAACC AGCTGAGGCTCCCAC
pTNT-GST- CT8(1082-1163)	TTAATTAAGGCGCGCCACC ACTCATCCTCCTCAGCCA	AATATGCGGCCGCTAGTCCATG TCCAGCAGATCCA
pTNT-GST- CT10(1277-1339)	AATAGGCGCGCCAGAGAAG GATGTGGCTCTCACAGAC	TAATTAGCGGCCGCTAAAACC AGCTGAGGCTCCCAC
pTNT-GST- CT11(1339-1396)	AATAGGCGCGCCATTTGGT CCCAACCACACTCTGCA	TAATTAGCGGCCGCTATGGTA GCATCTCCCCTGGCT
pTNT-GST- CT12(1277-1374)	AATAGGCGCGCCAGAGAAG GATGTGGCTCTCACAGAC	AATTAGCGGCCGCTACATCACT AGCACCTCCAGCA
pTNT-GST- CT13(1374-1396)	AATTAGGCGCGCCAATGAA GCTGCCTCGCTCTGAGCA	TAATTAGCGGCCGCTATGGTA GCATCTCCCCTGGCT
pTNT-GST-NT1(1- 256)	TAGGCGCGCCAATGGAGTC CTT	ATTATGCGGCCGCTACATGGG ATGGATCAGTCCCT
pTNT-GST-NT2(250- 505)	ATTATAGGCGCGCCAGAGG GACTGATCCATCCCATG	AATGCGGCCGCTAATTCTCCAG AAAGAGCCTCACG
pTNT-GST-NT3(499- 750)	ATTAGGCGCGCCAGTGAGG CTCTTTCTGGAGAATGG	ATTAATGCGGCCGCTAGCCATT GTCCACACAGAGC
pTNT-GST-NT4(1- 150)	TAGGCGCGCCAATGGAGTC CTT	AATTAATTAATTGCGGCCGCT AGGAGGGCGTGTCTGGGAGA

pTNT-GST-NT5(150-250)	TAGGCGCGCCATCCAGTGT CATCTACCAGCTCATGA	ATTATGCGGCCGCCTACATGGG ATGGATCAGTCCCT
pTNT-GST-NT6(1-201)	TAGGCGCGCCAATGGAGTC CTT	TTAATTGCGGCCGCCTATCCAGT GATGATCCAGGCCC
pTNT-GST-NT7(201-250)	TTAATTAAGGCGCGCCAGG AGGATCCCACACAGGCGT	ATTATGCGGCCGCCTACATGGG ATGGATCAGTCCCT
pTNT-GST-NT15(395-423)	AAGGCGCGCCAGAAAACCA GATTGTGGAATGGACCA	TTAAGCGGCCGCCTAATCCTTGC CTTCCCGGAAGAT
pTNT-GST-MutCT5(1047-1082)	AGAGGCGCGCCAAACTACA CCTT	AATATGCGGCCGCCTACTTGAGC TGCTTATGCCTCT
pTNT-GST-MutCT11(1339-1396)	AATAGGCGCGCCATTTGGT CCCAACCACACTCTGCA	TAATTAGCGGCCGCCTATGGTA GCATCTCCCCTGGCT
pTNT-GST-MutNT5(150-250)	TAGGCGCGCCATCCAGTGT CATCTACCAGCTCATGA	ATTATGCGGCCGCCTACATGGG ATGGATCAGTCCCT
pTNT-GST-MutNT15(395-423)	AAGGCGCGCCAGAAAACCA GATTGTGGAATGGACCA	TTAAGCGGCCGCCTAATCCTTGC CTTCCCGGAAGAT

Table 1 - Summary of TRPM2 truncation constructs generated and primers utilized for PCR. Note: Constructs marked *Mut contain the substitution mutations outlined in figure 2.2, all other constructs were generated from an mTRPM2 cDNA template.

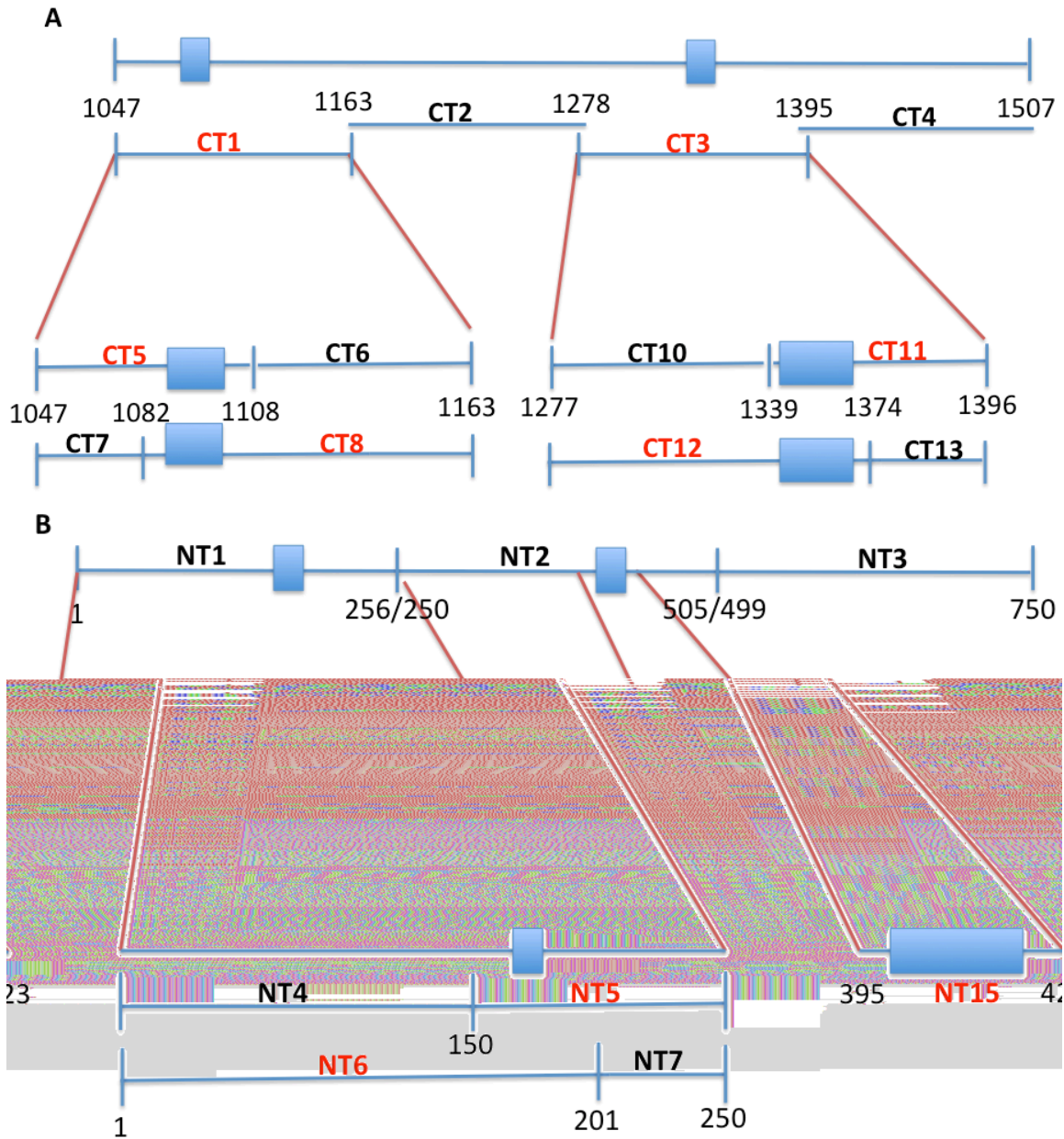


Figure 2.2 – Schematic of TRPM2 truncations generated for CaM-Sepharose binding experiments. A series of overlapping truncations were generated strategically based on results from *in silico* screening of TRPM2 for CaM consensus sites. Truncations were expressed in a GST-tagged vector with promoter regions required for the TNT Reticulocyte Quick-Coupled Kit (Promega). Candidate CaM binding sites identified by *in silico* screening are indicated by blue rectangles.

DNA fragments were generated utilizing KOD polymerase (EMDMillipore) touch down PCR. Samples were run on a 1.5% Agarose gel (1µl Ethidium Bromide per 20ml gel) to visualize products under UV exposure. Bands containing the DNA fragments were excised from the gel and purified with Gene Elute gel extraction kit (Sigma Aldrich). Extraction followed manufacturers guidelines, centrifugation occurred at 16000RCF for 1min and 50µl of elution solution was used for each column. Digestions were prepared for the eluted fragments consisting of 2µl 10000U/ml Ascl, 1µl 20000U/ml NotI, 10µl digestion Buffer #4, 10µl 10X BSA, and 100µl H₂O. Digestions were incubated at 37°C for 1 hour. Samples were run on a 1.5% Agarose gel (1µl Ethidium Bromide per 20ml gel) to visualize products under UV exposure. Bands containing the DNA fragments were excised from the gel and purified with GeneElute™ Gel Extraction Kit (Sigma-Aldrich). Extraction followed manufacturers guidelines; 35µl of elution solution was used for each column.

pTNT-GST Ascl, NotI, cip vector was prepared including a Kozak region and Poly-A tail required for the TNT quick-coupled transcription/translation system (Promega). Ligation reaction mixture was prepared with a 3:1 fragment to vector (50ng) ratio, DNA ligase and DNA ligase buffer for 1 hour at room temperature. DNA was transformed into 50µl JM109 bacteria (Promega) following manufacturers guidelines (40 second heat shock at 42°C, 1 hour incubation at 37°C 275 Rev/min). Bacteria was grown overnight on LB-Amp agar plates incubated at 37°C. Several colonies were identified per plate and grown overnight in 5ml LB-Amp incubated at 37°C 275 Rev/min. Plasmid DNA was extracted using a GenElute™ Plasmid Miniprep Kit (Sigma-Aldrich) following manufacturers guidelines; 100µl of elution

solution was used for each column. Plasmid DNA was analyzed using a restriction enzyme digestion for sites *AscI* and *NotI* and visualized on a 1.5% Agarose (1 μ l Ethidium Bromide per 20ml) gel. Positive candidates were confirmed with sequencing.

2.4 TNT Quick-Coupled Transcription/Translation System (Promega)

Plasmid DNA was transcribed and translated using the TNT Quick-Coupled Transcription/Translation System (Promega) according to manufacturers protocol. Plasmid DNA was maximized to 7 μ l based on the least concentrated sample. 2 μ l FluoroTect™ Green_{Lys} (Promega) was supplanted into the mixture to fluorescently label finished protein products. The reaction mixture was incubated in a thermal cycler for 60 minutes at 30 °C.

2.5 Calmodulin-Sepharose pull-down of TRPM2 truncations

30 μ l of well-packed CaM-Sepharose were prepared and washed using a 2mM Ca²⁺ or 5mM EGTA pH 8.0, 150mM NaCl and 50mM Tris-HCl pH 7.4 solution. Solution was lightly mixed and centrifuged for 1 min at 500RCF and wash solution extracted from the beads using a 27G needle. Beads were washed three times and 4 μ l of protein generated from each TNT reaction (section 2.4) were added to a final volume of 500 μ l from wash solution. Incubated overnight at 4°C on a nutating rotator, samples were wash 5 times in the method previously described. Washed beads were made to a final volume of 60 μ l with SDS-BM loading buffer. Samples including 1 μ l of input (section 2.4) and SDS-BM loading buffer were heated at 60°C

for three minutes. A 10-12% SDS-page was performed to visualize samples (20µl of bead solution, total volume of input) and was imaged using a fluorescent filtered VersaDoc™ MP system (Biorad).

2.6 TRPM2-CaM Candidate Site-Directed Mutagenesis

Substitution mutagenesis was outsourced and performed by TopGeneTechnologies (Montreal, QC). Single-point substitution mutations to several amino acids within CaM candidate sites of TRPM2 were performed. Utilizing mTRPM2 as a template two overlapping fragments of TRPM2 were generated using PCR and primers incorporating designated substitution mutations. The resulting PCR products were run on an Agarose gel and purified with GenElute™ Gel-Extraction Kit (Sigma-Aldrich) following manufacturers guidelines. The fragments were digested with either *AscI* or *NotI* as previously described (section 2.3) and ligated to pIRESpuro-flag plasmid. Ligated plasmid DNA was transformed to JM109 bacteria, grown overnight on LB-Amp Agar plates (37°C), and several colonies grown in 5ml of LB-Amp (37°C 275Rev/min) as previously described (section 2.3). Plasmid DNA was purified from bacteria using GenElute™ Plasmid Miniprep Kit (Sigma-Aldrich), and verified by an *AscI* and *NotI* digestion and the mTRPM2-coding region sequenced as previously described (section 2.3). I performed additional sequencing analysis for the full-length of all mutants generated to ensure correct mutants were generated.

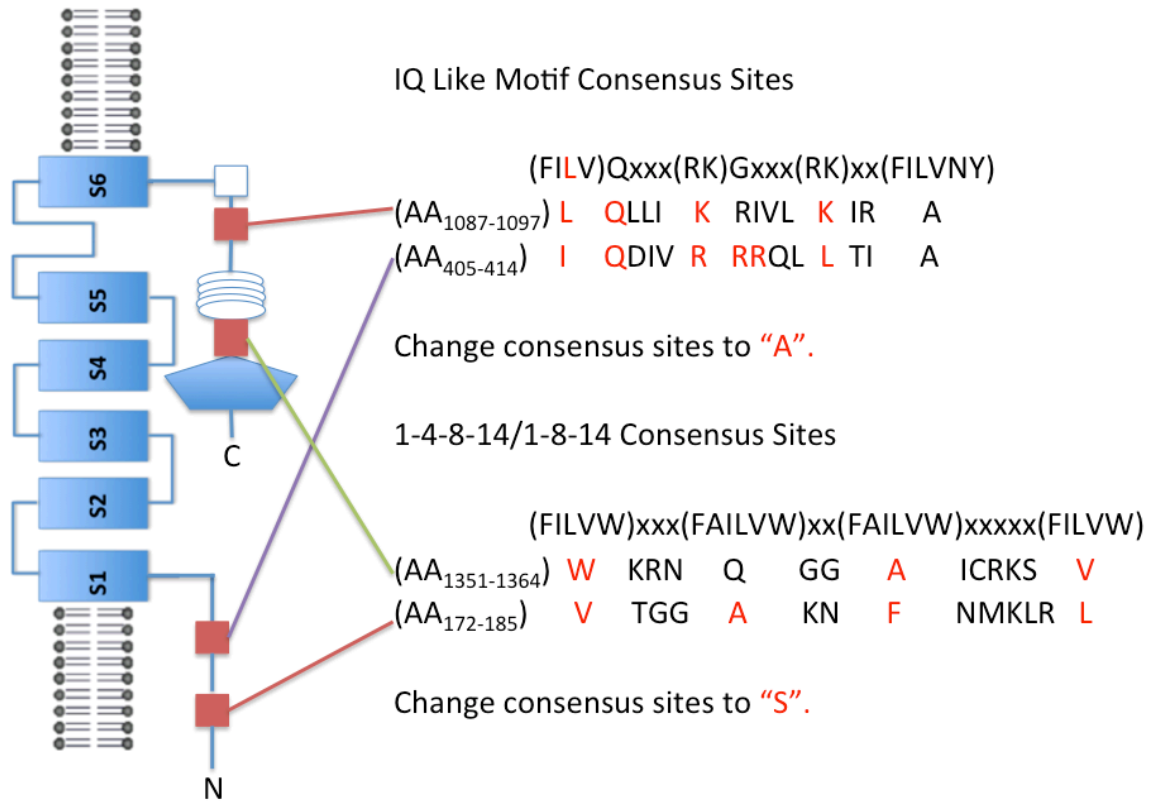


Figure 2.3 – Schematic of site directed substitution mutagenesis at four CaM consensus-binding sites located on the intracellular terminals of TRPM2. IQ-like motifs received Alanine substitutions at key amino acids while the 1-14 consensus sites had Serine substitutions at key amino acids. The mutations and consensus maps are summarized above for each construct. In total four separate constructs, one for each CaM candidate site was generated.

2.7 Western Blotting

HEK293 cells transfected with mTRPM2-CaM_{Mut} outlined in figure 2.3 were grown for 48 hours to confluency as previously described (section 2.2). Western blot analysis was also performed on Trex293-stable C-term and N-term TRPM2 cells. Lysis buffer was generated using 150mM NaCl, 0.1% NP-40, 2mM CaCl₂, 50mM Tris-HCL (pH 7.5) and 1 Mini-complete protease inhibitor cocktail tablet (Roche). Each 6cm dish was treated with 200μl of lysis solution and collected in a microtube. Lysates were incubated at 4°C for 30 minutes on a nutating platform, centrifuged at 16000RCF at 4°C for 30 minutes and the supernatant collected. A BCA protein assay (Thermo) was performed to determine protein concentrations. 40μg of protein was made to a final volume of 18μl with SDS-BM loading buffer and H₂O and incubated at 37°C for 10 minutes. An SDS-page was performed using a 10% protein gel to 10ml (4.0ml H₂O, 3.3ml 30% acrylamide mix, 2.5ml 1.5M Tris (pH 8.8), 0.1ml 10% SDS, 0.1ml 10% APS, and 0.004ml TEMED), a 5% stacking gel was generated in the same manner substituting 1.0M Tris (pH 6.8). The protein was transferred to a nitrocellulose membrane and verified with Ponceau S stain (Sigma-Aldrich). The membrane was washed with TBS-T and blocked for 1 hour with 5% milk/TBS-T on a belly-dance shaker. The membrane was incubated with 1:10000 anti-flag HRP for 2 hours then washed 3 times with TBS-T for 10 minutes. Finally the membrane was exposed to ECL reagent (0.5ml Supersignal West Pico Stable Peroxide Solution [Thermo] and 0.5ml Supersignal West Pico Luminal/Enhancer [Thermo]). Finally the blot was imaged using chemiluminescence on a VersaDoc™ MP system (Biorad).

2.8 Drugs and Peptides

The sources of drugs and materials for this study are as follows: NaCl, Glucose, CaCl₂, MgCl₂, BaCl₂, Gluconic acid, CsOH, ADPR, Mg(ATP)₂, EGTA, Ponceau S Stain, GenElute™ Plasmid Miniprep Kit, GenElute™ Plasmid Midiprep Kit, GenElute™ Gel-Extraction Kit, BSA, Dulbecco's Modified Eagle Medium (Sigma-Aldrich), Supersignal West Pico Stable Peroxide Solution, Supersignal West Pico Luminal/Enhancer, BCA Protein Assay kit (Thermo), Hepes (Bioshop), Mini-complete protease inhibitor cocktail tablet (Roche), TNT Quick-Coupled Transcription/Translation System, JM109 bacteria, FluoroTect™ Green_{Lys} (Promega), KOD polymerase (EMDMillipore), Doxycycline (Pfizer), JetPrime (Polyplus), Ascl, NotI, cip (New England Biolab) CaM1-Sepharose (GE Healthcare).

2.9 Statistical Analysis

All population data are expressed as mean ± SEM. Two-way ANOVA were used to compare between two groups, as well as student's t-test. Student's t-test was performed on the average of Inactivation (Iss/Ip) % between two groups. Paired t-test was used to compare within groups; Inactivation (Iss/Ip) % between 0.5mM and 2mM Ca²⁺. The significance level was held constant at p<0.05.

Section 3

RESULTS

3.1 Extracellular Ca²⁺ modulation of TRPM2 CDI

A whole-cell patch-clamp recording protocol (section 2.1) was designed to measure TRPM2 currents. TRPM2 was stably transfected into T-REX293 cells with a tetracycline-inducible promoter region. T-REX293 cells were induced with doxycycline 24-48 hours prior to recordings. TRPM2 was activated with ICS containing 0.3mM ADPR. Currents were initially allowed to develop to 1nA in the presence of Ca²⁺ because ADPR diffusion into the cytoplasm limits initial current onset. Extracellular solution containing varying concentrations of Ca²⁺ was administered via a multi-barreled fast perfusion system. Administration of 0mM Ca²⁺ ECS rapidly inhibits TRPM2 current. The recording protocol consists of 3min applications of 0.5mM or 2mM Ca²⁺ ECS followed by 5 minutes of Ca²⁺-free solution. During Ca²⁺ administration (figure 1.2) I observed a slow increase in current reaching peak amplitude (I_p). This is followed by a marked current inactivation over several minutes, reaching a maintained steady state (I_{ss}). When measuring and referring to CDI we define it as the ratio between the I_{ss}/I_p. 3-minute application of Ca²⁺-containing ECS was sufficient to fully resolve TRPM2 CDI. Previous unpublished findings from our laboratory (Figure A1) indicate full recovery from TRPM2 CDI may be achieved with Ca²⁺-free ECS administration. 5-minute applications of 0mM Ca²⁺ ECS ensured full recovery between Ca²⁺-containing ECS administration.

An experimental protocol was designed to test the extracellular Ca²⁺ relationship of TRPM2 CDI. Depolarizing the cellular membrane, which reduces the driving force of Ca²⁺ through TRPM2 channels, can further modulate TRPM2 CDI.

During Ca^{2+} -free applications, holding voltage was varied in 20mV increments. By varying holding voltage between -100mV to -20mV, I extrapolated the current-voltage relationship (IV-curve) of TRPM2 CDI. An I/V curve relationship of TRPM2 CDI was determined for 0.5mM, 2mM and 5mM Ca^{2+} ECS applications. Two extracellular Ca^{2+} concentrations are shown, 2mM (Figure 3.1A) or 0.5mM (Figure 3.1B). CDI of TRPM2 channels are relatively large with 2mM applications of Ca^{2+} (Figure 3.1A) and CDI is reduced in a linear fashion with changes in voltage. The extrapolation of the linear IV relationship roughly mimics the Ca^{2+} ionic driving forces and the reversal potential of Ca^{2+} (Figure 3.1C).

Preliminary evidence from our laboratory has indicated reduced TRPM2 CDI when Ca^{2+} administration in the ECS was lowered to 0.5mM. The voltage-current relationship was determined for 0.5mM Ca^{2+} (Figure 3.1B). The significantly reduced CDI observed from lower $[\text{Ca}^{2+}]$ decreased in a linear fashion, but was rarely observed above -60mV. If $[\text{Ca}^{2+}]$ increased to 5mM resulted in no significant changes to TRPM2 CDI observed versus 2mM extracellular Ca^{2+} (not shown). This would suggest maximal TRPM2 CDI has reached a plateau at 2mM Ca^{2+} ECS. Increasing Ca^{2+} beyond this concentration is not sufficient to alter activation and subsequently inactivation. Both processes are all tightly regulated by intracellular $[\text{Ca}^{2+}]$, but maintained by Ca^{2+} influx from the ECS.

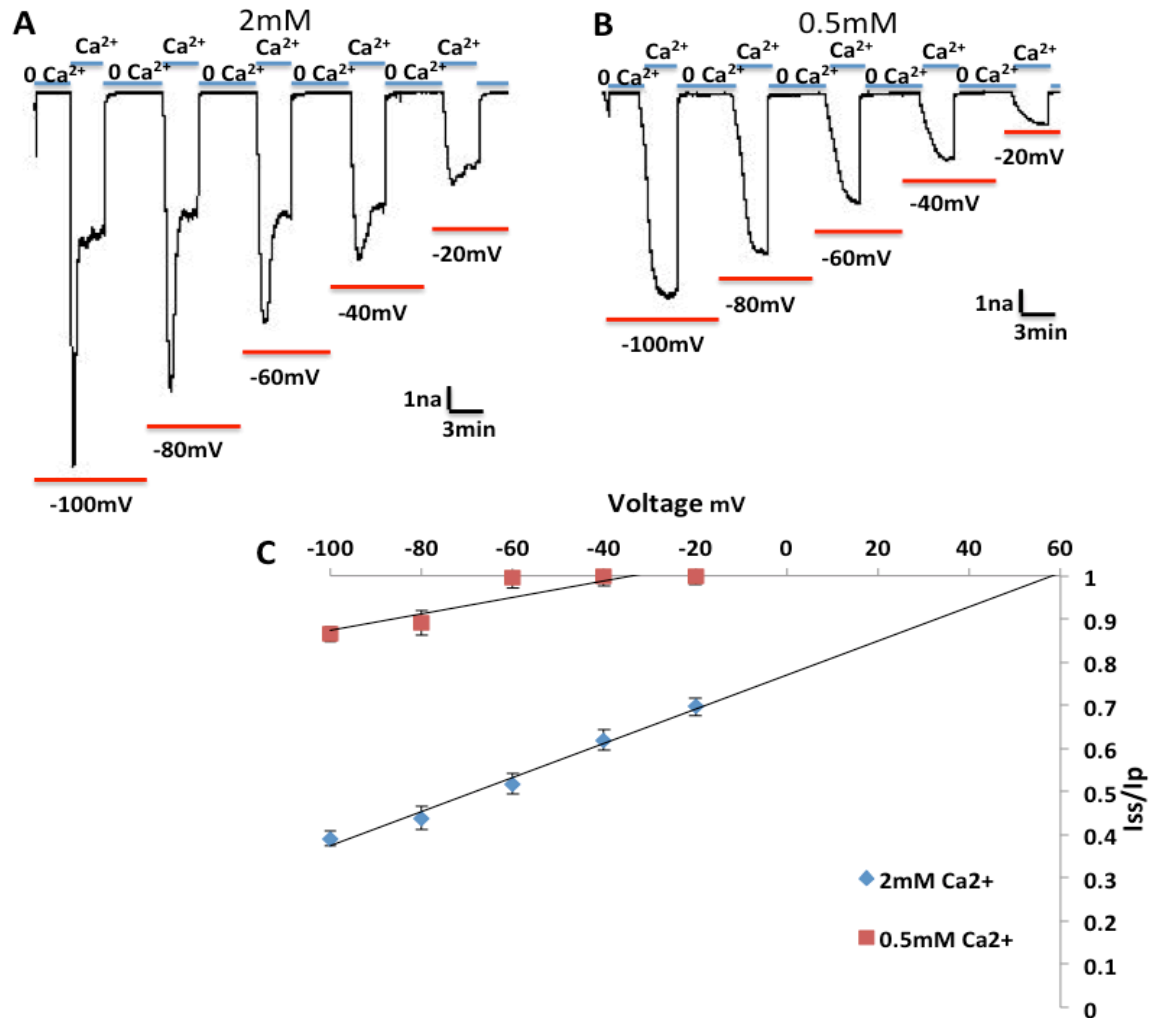


Figure 3.1 – Effect of varying the membrane holding potential on TRPM2 CDI. Representative traces of recordings from TRPM2 expressing HEK293 cells evoked in the presence of either **A.** 2mM Ca²⁺ ECS or **B.** 0.5mM Ca²⁺. CDI (steady-state to peak ratio) is markedly reduced when using lower [Ca²⁺] ECS. 5 min applications of Ca²⁺-free ECS abolish TRPM2 currents and allow full recovery from TRPM2 CDI. Membrane voltage was varied between -100mV to -20mV in 20mV steps and was raised at the halfway mark during the 0mM Ca²⁺ recovery period. **C.** Analysis of CDI between [Ca²⁺] treatments and voltage steps was plotted and analyzed. Both concentrations resulted in a linear decrease in TRPM2 CDI as voltage was raised. Notably CDI reverses around the Ca²⁺ reversal potential of Ca²⁺ in the 2mM [Ca²⁺] treatment (n=6).

3.2 CaM-Sepharose pull-down of TRPM2 C-terminal truncation

Electrophysiological recordings from T-Rex293 cells stably expressing TRPM2 indicate CDI of TRPM2 currents. Furthermore TRPM2 currents are activated and inactivated with different sensitivity to Ca^{2+} . We have evidence that CaM binding, which is unique from the site of activation (NT_{10}), might mediate CDI. Previous findings by Tong et al., 2006 only pursued the interaction of CaM with TRPM2 within the N-terminal of TRPM2. However Tong et al., 2006 still identified modest binding within the C-terminal that was not pursued further. To examine the potential interaction of CaM with the C-term of TRPM2, we generated a truncation mutant of mTRPM2 (Figure 3.2A) consisting of only its C-term domain. The C-term of TRPM2 was generated by PCR from full-length mTRPM2 and flag-tagged for detection by Western blotting. HEK293 cells stably expressing flag tagged mTRPM2 or mTRPM2 C-term truncation were induced with doxycycline 48 hours followed by cell lysis and protein extraction. CaM-Sepharose pull-down was performed with both full length and C-term truncation fragments and CaM binding assessed. The binding solution contained 2mM Ca^{2+} . C-term mTRPM2 truncations were successfully pulled down (Figure 3.2B) with CaM-Sepharose. This provides evidence for additional CaM binding sites on the TRPM2 intracellular tail not previously analyzed in the literature (n=3).

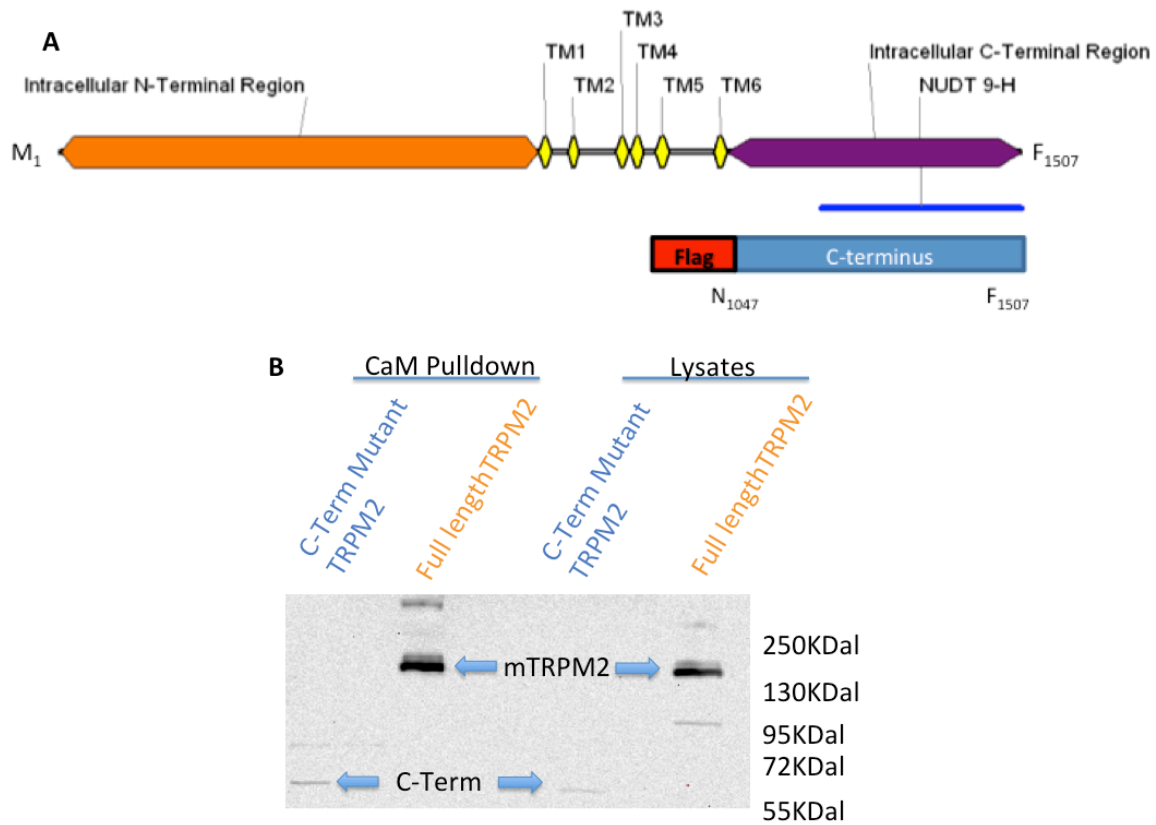


Figure 3.2 – CaM-Sepharose pulldown of mTRPM2 C-terminal fragment. **A.** Schematic of the C-term mTRPM2 fragment generated by PCR and tagged with flag for Western blotting resolution (Natalie Lavine). **B.** Western blot of full length and C-terminal truncated mTRPM2 lysates pulled down with CaM-Sepharose in a 2mM Ca²⁺ binding solution. The C-term was found to associate with CaM beads, suggesting the existence of previously unrecognized CaM -binding sites within this portion of TRPM2 channels.

3.3 – A systematic analysis of TRPM2 C-term CaM candidate sites

Previous findings have identified an IQ-like CaM consensus region located on the intracellular N-terminal of TRPM2 channels located at region 406-414AA (Tong et al., 2006). Endogenous CaM binding to this N-term IQ-like motif is essential for the Ca²⁺-CaM activation of TRPM2 channels (Tong et al., 2006). TRPM2 current can no longer be elicited from a TRPM2 mutant with substitution mutations at this site, regardless of [ADPR] or [Ca²⁺] utilized (Csandy and Torocsik, 2009). Tong et al., identified weak binding of CaM within the C-terminal of TRPM2 channels and hinted at additional CaM binding sites that were not abolished by an NT_{IQ} mutation. We postulated that additional, previously unrecognized sites that mediate CDI could be identified within TRPM2.

CaM binding sites are loosely defined by a consensus amino acid sequence, several of which have been identified including an IQ-like and 1-8-14 sites (Jurado et al., 1999). Using the Calmodulin Target Database resource (© 2002 Ikura Lab, Ontario Cancer Institute), the two terminal chains of TRPM2 were individually analyzed for CaM consensus binding sites. The *in silico* screening for the TRPM2 intracellular N-terminal successfully identified the known IQ-like motif. The successful identification of the CaM site responsible for TRPM2 activation provides validation of the approach. In total three additional candidate CaM consensus sites have been identified, and their relative locations to other important structural components of TRPM2 summarized on the TRPM2 protein schematic outlined in Figure 3.2. An IQ-like site was found at 1084-1105AA C-terminal roughly overlapping the coiled-coil region (Figure 3.3). 1-8-14 consensus sites located at the

N-terminal and C-terminal of TRPM2 were also identified at 161-197AA, which is within a conserved portion of the N-terminal chain, and at 1344-1373AA of the C-terminal within the initial N-distal portion of the NUDIX domain (Perraud et al. 2003; Montell, 2005).

Using the TRPM2 CaM binding domains, identified from *in silico* screening, a series of mTRPM2 truncations were developed. The fragments were generated in order to determine whether CaM associates with the consensus sites we identified through *in silico* screening. Truncations were generated using PCR and sub-cloned into a vector with the promoter region for the TNT reticulocyte kit. The TNT Quick-Coupled Transcription/Translation kit consists of a master mix of cellular machinery and amino acids. Truncated TRPM2 fragments sub cloned into vector are transcribed and translated into protein, which is subsequently used for CaM-Sepharose pulldown. The second feature of the protocol is a fluorescent lysine that is supplanted into the master mix and produces fluorescent proteins. Truncations ranged from 30-250 amino acids in length. The variability in truncation size would create problems resolving bands run on a gel and would not ensure sufficient lysine incorporation. We therefore tagged with GST to both increase size and ensure fluorescent lysine uptake.

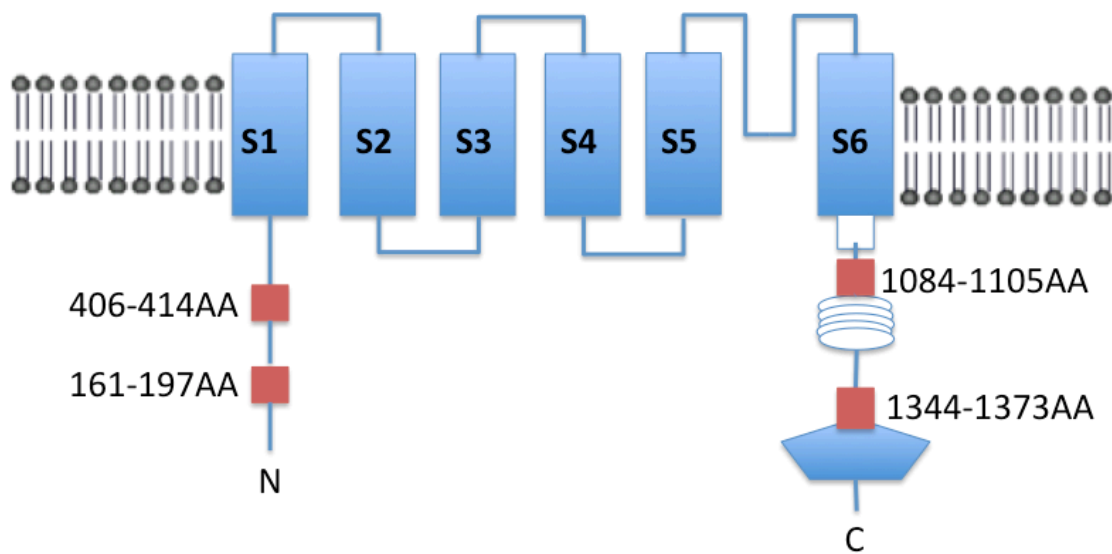


Figure 3.3 – Schematic of TRPM2 candidate CaM sites identified with *in silico* screening. IQ-like sites are located at 406-414AA and 1084-1105AA. The first of which is responsible for Ca²⁺-CaM activation of TRPM2 channels (Tong et al., 2006) and the second overlaps with the CCR located within the C-term of TRPM2. Two additional candidate CaM sites are located at 161-197AA and 1344-1373AA, they are both consistent with the 1-8-14-type consensus motif. 161-197AA is associated with a conserved N-term region and 1344-1373AA with the NUDIX region located on the C-term.

mTRPM2 truncated into four roughly equivalent parts, was incubated with CaM-Sepharose beads. Ca²⁺ sensitivity of binding was determined using either 2mM Ca²⁺ or Ca²⁺-free (5mM EGTA containing) binding solutions. Figure 3.4 summarizes these results. Three C-term fragments (CT1, CT3 and CT4) were found to associate with CaM. In contrast, pulldown of a GST-only negative control by CaM-Sepharose was minimal. Furthermore, an assessment of the Ca²⁺ dependence revealed that CaM association was reduced, but not completely abolished when binding was carried out in the absence of Ca²⁺. Figure 3.4D provides a numerical index of the binding results by performing a quantitative analysis comparing relative signal of input and pulldown gels. Fragment CT4 was inconsistent with predicted binding sites from the *in silico* screening. An additional unknown binding site may exist within this fragment, but it was not pursued at this time.

To confirm the specific association of CaM to target sequences identified by *in silico* screening, a second round of deletion constructs were generated in order to resolve the minimum binding domains within fragments CT1 and CT3. Figure 3.5 identifies a binding pattern consistent with the predicted IQ-like CaM binding site identified between 1084-1105AA. Consistent with previous findings, CaM binding was reduced but not completely abolished with 5mM EGTA; this is consistent with the previously reported association of ApoCaM with IQ-like motifs (Jurado et al., 1999). Figure 3.5D provides a numerical index of the binding results by performing a semi-quantitative relative analysis comparing input and binding fragments relative to CT8.

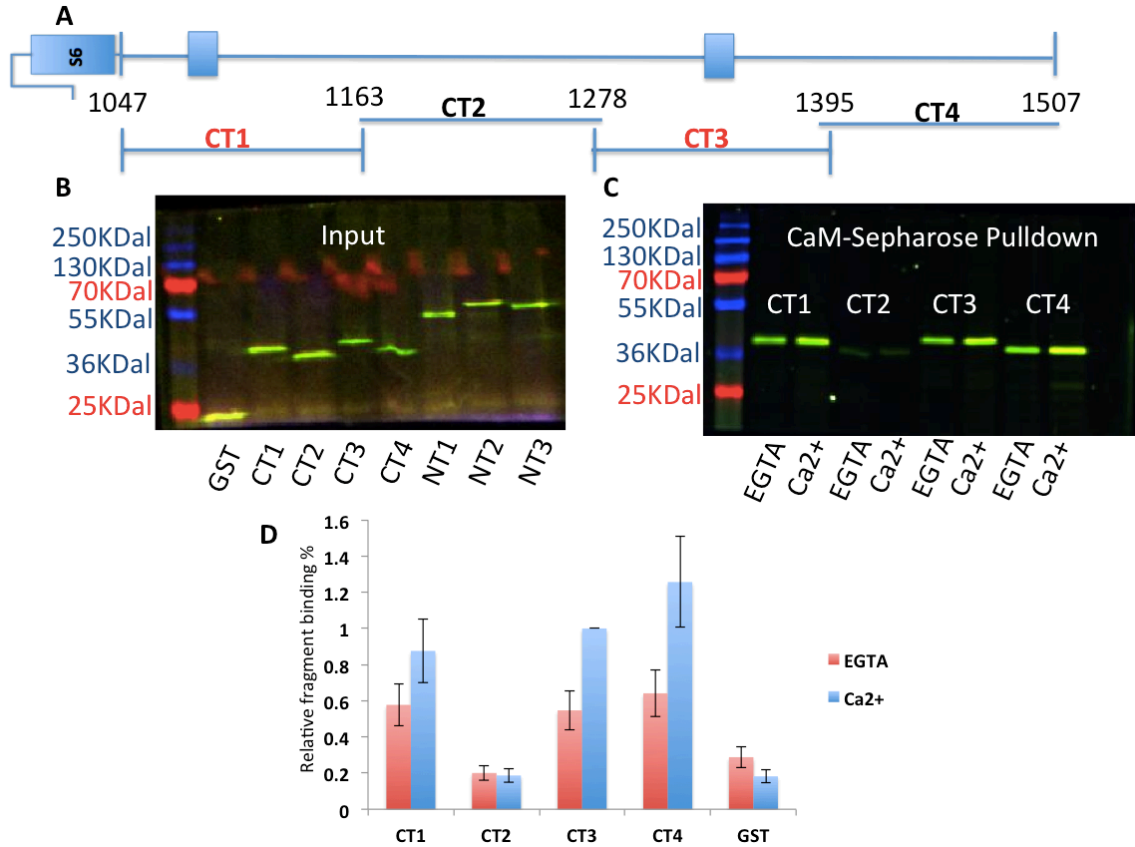


Figure 3.4 – CaM-Sepharose pulldown of mTRPM2 C-terminal truncations. **A.** TRPM2 C-terminal fragment design. Blue boxes represent *in silico* CaM binding sites. Four fragments were generated and tagged with GST to test for CaM binding. **B.** Input of protein fragments generated using TNT Quick Coupled translation system incorporating fluorescent lysine and resolved directly from an SDS-page gel. **C.** CaM-1 Sepharose beads incubated overnight with fragments. Beads were washed with a buffer containing either 5mM EGTA, or 2mM Ca²⁺. CT1 and CT3 bound as expected, CT2 was not capable of binding. However, CT4 displayed unexpected CaM binding, hinting at an undefined CaM consensus site in this region (n=3) **D.** Relative binding strength of fragments versus relative signal strength of inputs (n=3).

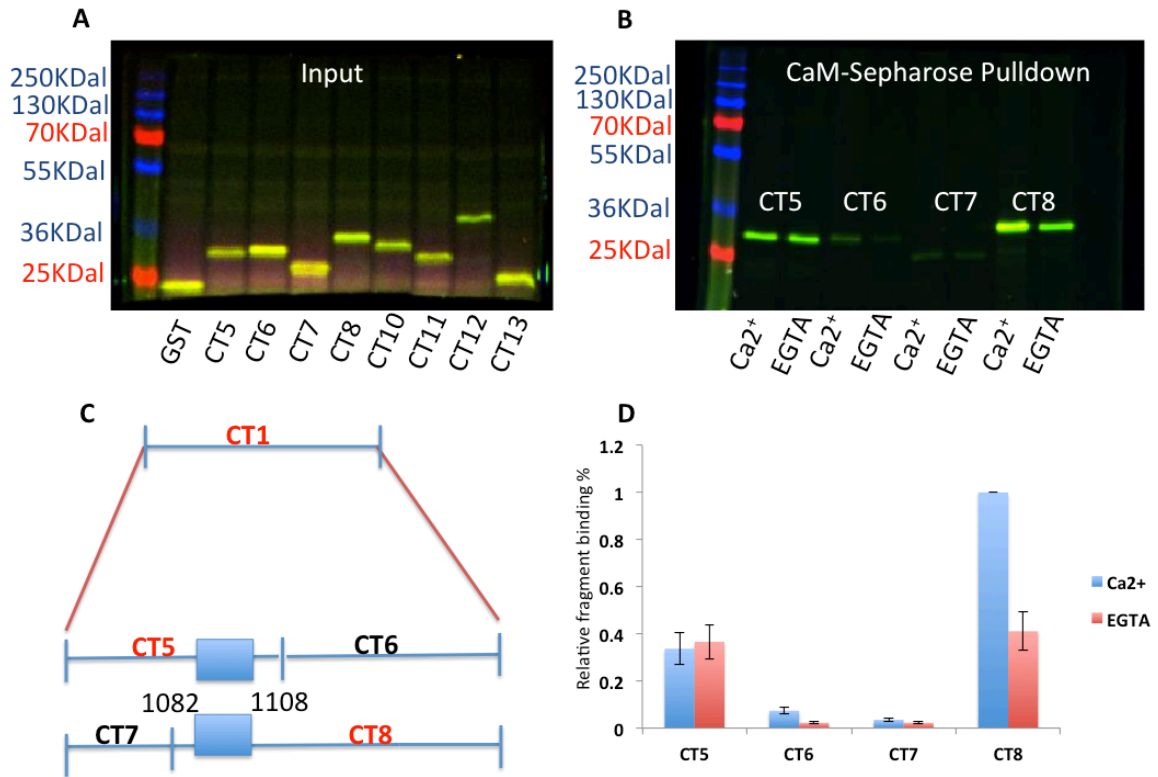


Figure 3.5 – CaM-Sepharose pulldown of mTRPM2 CT1 truncations containing a consensus IQ-like site at 1084-1105AA. **A.** Input of protein fragments generated using TNT Quick Coupled translation system incorporating fluorescent lysine and resolved directly from an SDS-page gel. **B.** CaM-1 Sepharose beads incubated overnight with fragments. Beads were washed with a buffer containing either 5mM EGTA, or 2mM Ca²⁺. All binding patterns are consistent with sites identified by *in silico* screening. (n=3) **C.** TRPM2 CT1-terminal fragment design. Blue boxes represent *in silico* CaM binding sites. Four fragments were generated and tagged with GST to test for CaM binding. **D.** Relative binding strength of fragments versus relative signal strength of inputs (n=3).

We next examined the CT3 fragment harbouring a predicted 1-8-14 CaM consensus site associated with the region 1344-1373AA. Four further truncations outlined in Figure 3.5C were incubated with CaM-Sepharose with both 2mM and 5mM EGTA binding solutions. The predicted fragments CT11 and CT12 bound successfully to CaM-Sepharose beads, however unexpected binding was identified in fragment CT10. Whether this non-specific binding translates to full-length TRPM2 remains to be determined. Similar to previous findings, CaM binding was not completely abolished in a Ca²⁺-free 5mM EGTA binding solution. Figure 3.6D provides a numerical index of the binding results by performing a semi-quantitative relative analysis comparing input and binding fragments relative to CT11.

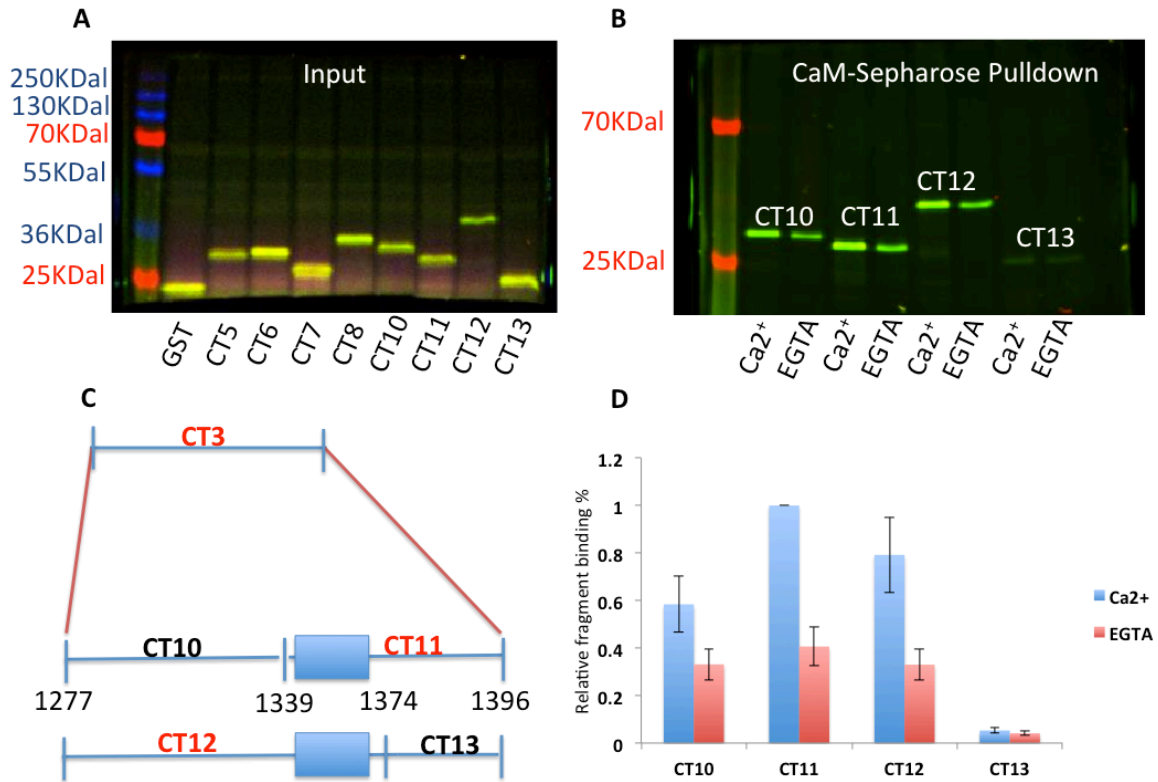


Figure 3.6 - CaM-Sepharose pulldown of mTRPM2 CT3 truncations containing theoretical 1-8-14-consensus site at 1344-1373AA. **A.** Input of protein fragments generated using TNT Quick Coupled translation system incorporating fluorescent lysine and resolved directly from an SDS-page gel. **B.** CaM-1 Sepharose beads incubated overnight with fragments. Beads were washed with a buffer containing either 5mM EGTA, or 2mM Ca²⁺. CT10 showed unexpected CaM binding not characteristic with any theoretical CaM sites. (n=3) **C.** TRPM2 CT3-terminal fragment design. Blue boxes represent *in silico* CaM binding sites. Four fragments were generated and tagged with GST to test for CaM binding. **D.** Relative binding strength of fragments versus relative signal strength of inputs on a representative gel (n=3).

3.5 – A systematic analysis of TRPM2 N-term CaM candidate sites

The N-terminal of TRPM2 was divided into three overlapping fragments of roughly equivalent sizes. The candidate 1-8-14 site lies within fragment NT1 while the IQ-like CaM site, responsible for activation (Tong et al., 2006), falls within fragment NT2 (Figure 3.7A). All three fragments demonstrated strong association with CaM-Sepharose, which was only partially reduced with 5mM EGTA binding solutions. Figure 3.7D provides a numerical index of the binding results by performing a semi-quantitative analysis comparing input and binding fragments relative to NT1. Literature exists concerning two IQ-like CaM sites falling on NT3 believed to be responsible for the abolished current observed in TRPM2-ΔN (missing 537-556AA); however, mutation to either site resulted in no significant alterations to full-length TRPM2 function compared to wild-type (Kuhn et al., 2009). The CaM sites on NT3 are not believed to be responsible for CaM regulation of TRPM2 (Kuhn et al., 2009) and, accordingly, were not pursued any further in this thesis.

Truncations to NT1 containing 1-8-14-consensus CaM candidate site 161-197AA were carried out in a similar fashion to those previously outlined (Figure 3.8C). Only those truncations overlapping the predicted consensus site strongly bound to CaM-Sepharose, confirming that this consensus-binding site is the sole site responsible for CaM binding in this region (Figure 3.8). Figure 3.8D provides a numerical index of the binding results by performing a semi-quantitative analysis comparing input and binding fragments relative to NT5.

3.5 The effects of substitution mutagenesis at TRPM2 candidate CaM sites

Substitution mutagenesis was carried out at the four-candidate CaM binding sites as summarized in Figure 2.3. Four truncations were selected (Figure 3.9A) including one newly generated fragment overlapping the IQ-like site responsible for TRPM2 activation (named NT15). These truncations contained a minimal amount of extraneous amino acids and the CaM candidate site and have been previously tested in sections 3.4 and 3.5. Truncations mimicking those selected but incorporating the outlined substitution mutations were created to compare CaM binding change from WT to mutated CaM candidate sites. As implicated by Tong et al., 2006, substitution mutations to the NT_{IQ} site did not fully abolish CaM-Sepharose pulldown. I found consistent binding patterns for truncation NT_{IQ}; binding at this site was significantly reduced but not completely abolished relative to a GST control. A reduction in binding was observed (Figure 3.9) in fragments NT15 and CT11, but no significant reduction occurred for fragments NT5 and CT5 (n=3). Relative binding analysis is summarized in future sub-sections relating to each specific fragment.

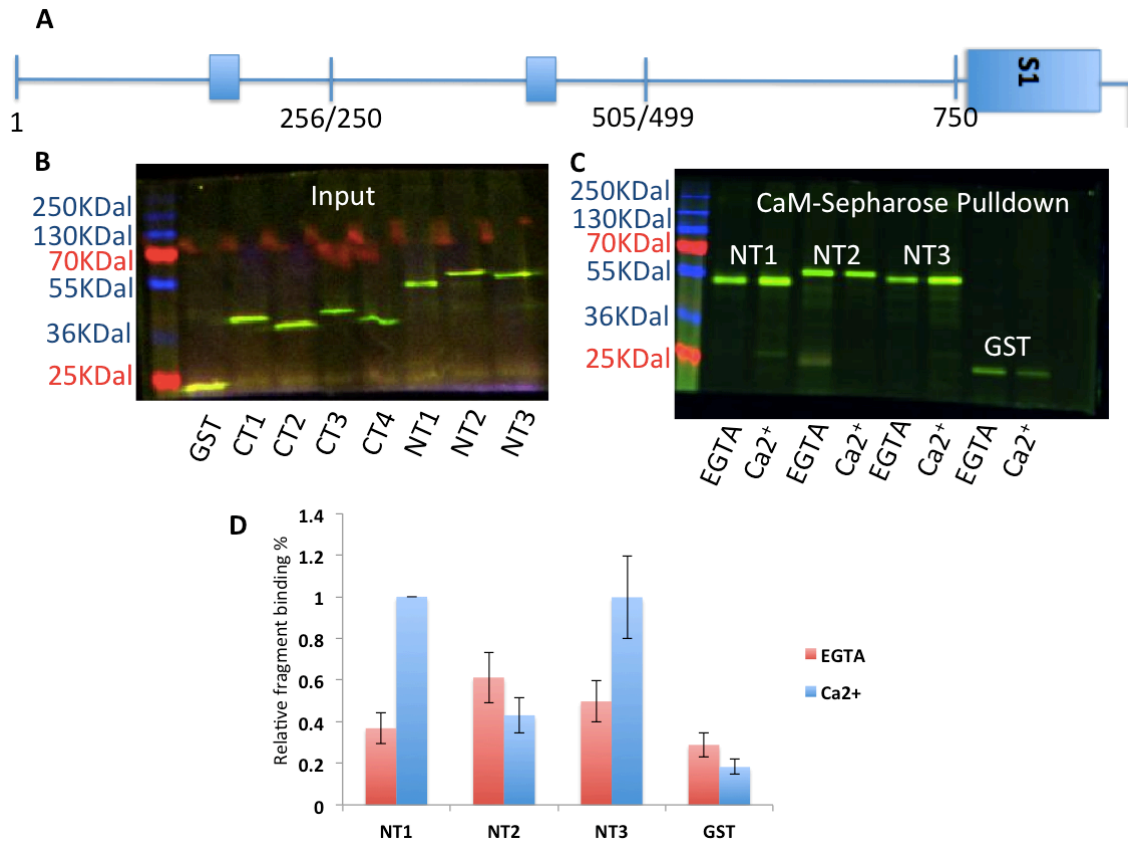


Figure 3.7 - CaM-Sepharose pulldown of mTRPM2 N-terminal truncations. **A.** TRPM2 N-terminal fragment design. Blue boxes represent *in silico* CaM binding sites. Three fragments were generated and tagged with GST to test for CaM binding. **B.** Input of protein fragments generated using TNT Quick Coupled translation system incorporating fluorescent lysine and resolved directly from an SDS-page gel. **C.** CaM-1 Sepharose beads incubated overnight with fragments. Beads were washed with a buffer containing either 5mM EGTA, or 2mM Ca²⁺. NT1 and NT2 bound as expected. However NT3 displayed unexpected CaM binding. (n=3) **D.** Relative binding strength of fragments versus relative signal strength of inputs on a representative gel (n=3).

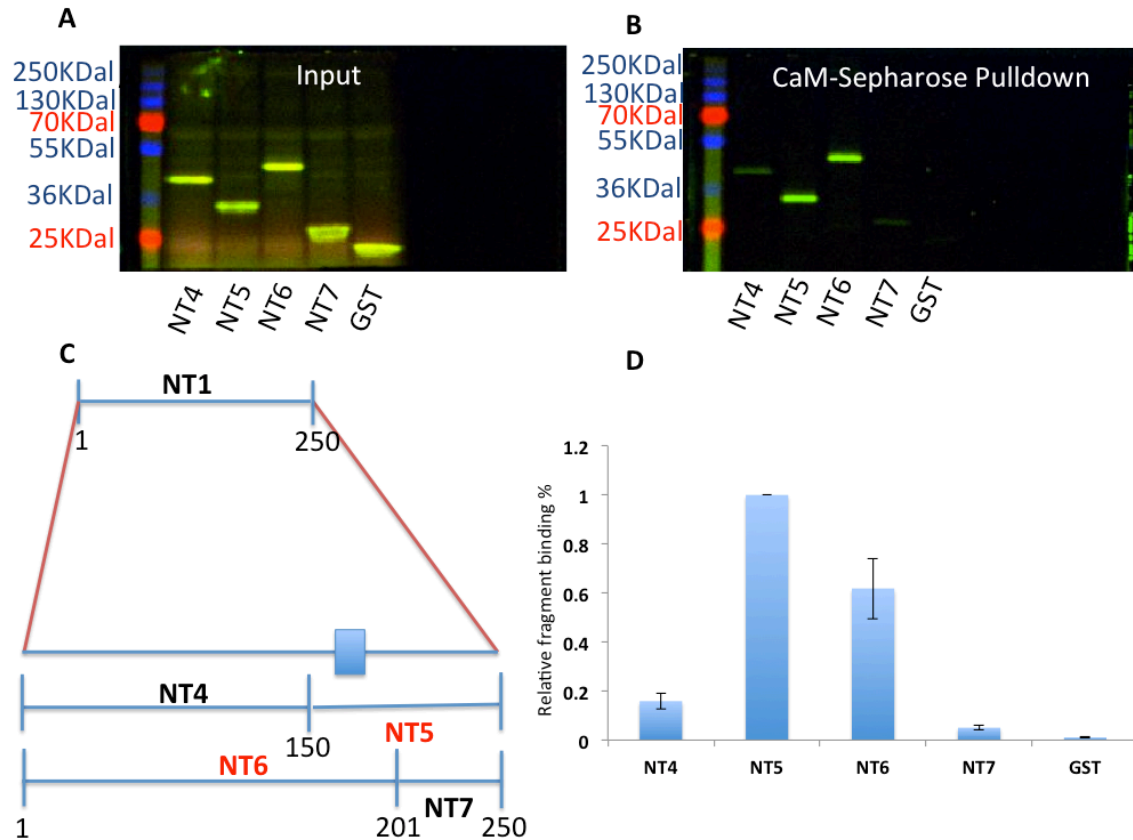


Figure 3.8 - CaM-Sepharose binding of mTRPM2 CT1 truncations containing theoretical 1-8-14-consensus site at 161-197AA. **A.** Input of protein fragments generated using TNT Quick Coupled translation system incorporating fluorescent lysine and resolved directly from an SDS-page gel. **B.** CaM-1 Sepharose beads incubated overnight with fragments. Beads were washed with a buffer containing 2mM Ca²⁺. All binding patterns are consistent with sites identified by *in silico* screening. (n=3) **C.** TRPM2 NT1-terminal fragment design. Blue boxes represent *in silico* CaM binding sites. Four fragments were generated and tagged with GST to test for CaM binding. **D.** Relative binding strength of fragments versus relative signal strength of inputs on a representative gel (n=3).

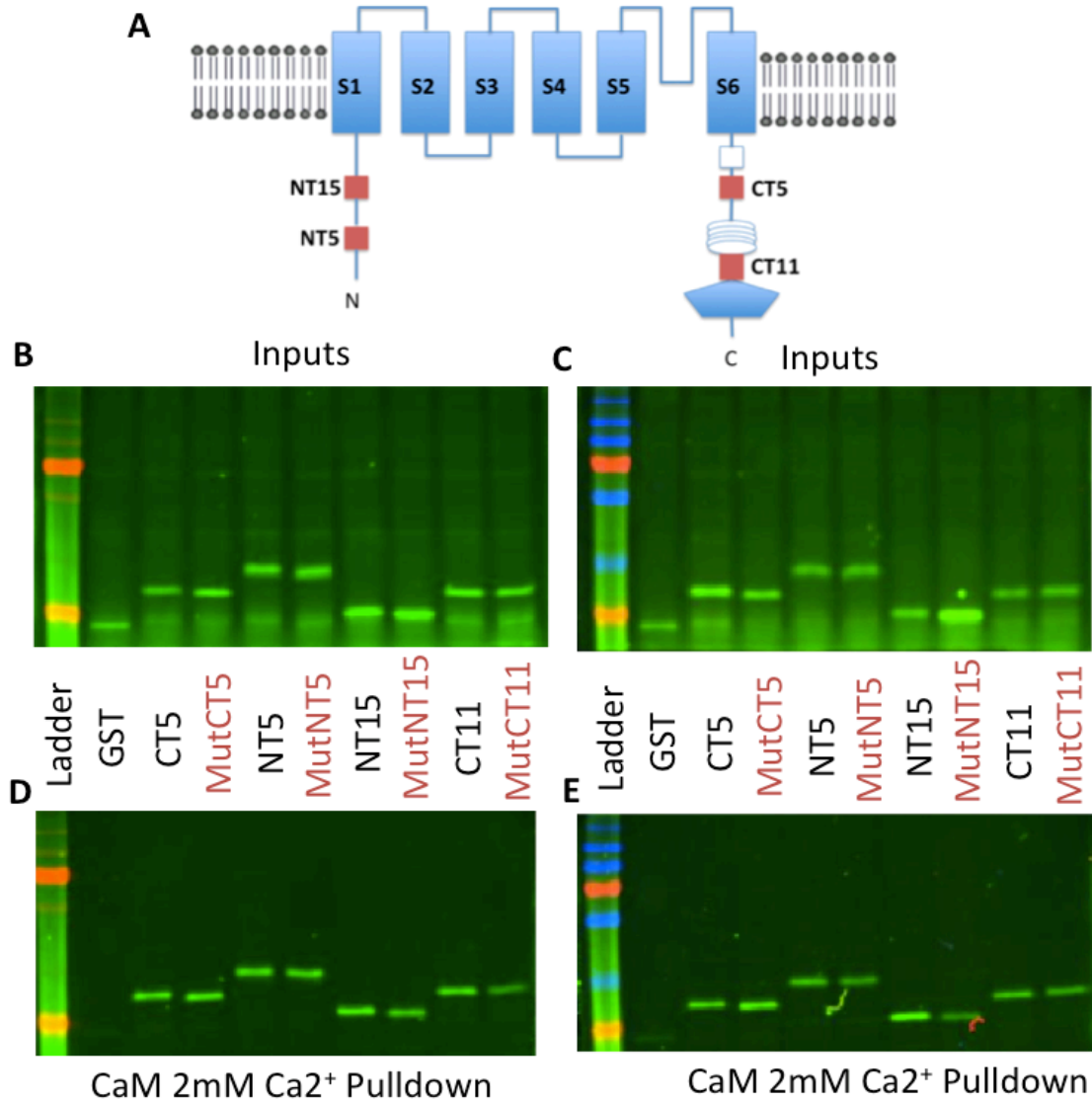


Figure 3.9 - CaM-Sepharose pulldown of mTRPM2 CaM candidate site mutated fragments. **A.** TRPM2 schematic of approximate truncation fragments locations overlapping candidate CaM sites. Four new fragments were generated with substituted amino acids (Figure 2.3) and tagged with GST to test for CaM binding. **B/C.** 2 representative gels of input protein fragments generated using TNT Quick Coupled translation system incorporating fluorescent lysine and resolved directly from an SDS-page gel. **D/E.** 2 representative gels CaM-1 Sepharose beads incubated overnight with fragments. Beads were washed with a buffer containing 2mM Ca²⁺. Fragment binding to CaM was reduced (NT15, CT11) or unchanged (CT10, NT10) but in all cases was not completely abolished by any of the mutations. (n=3).

3.6 Assessment of CaM site NT_{1Q} and flag-mTRPM2-CaM_{Mut}(NT_{1Q})

Tong et al., 2006 identified a CaM binding site located on the N-term (Figure 3.10A) of TRPM2 responsible for Ca²⁺-CaM mediated activation. My first objective was to reproduce the CaM binding mutant previously generated by Tong et al., 2006. Furthermore the regulatory changes of flag-mTRPM2-CaM_{Mut}(NT_{1Q}) would be assessed using our novel and distinct electrophysiological recording protocol as a reference for future mutants. I successfully reproduced results produced by Tong et al., 2006. Protein expression of flag-mTRPM2-CaM_{Mut}(NT_{1Q}) was confirmed from HEK293 cell lysates on a Western blot tested with anti-flag. CaM binding analysis was assessed for truncated fragment NT15 containing the normal NT_{1Q} site versus -_{Mut}NT15 using flag-mTRPM2-CaM_{Mut}(NT_{1Q}) as a PCR template (Figure 3.9). Substitution mutations at the NT_{1Q} site resulted in a significant decrease ($p=0.009$, NT15=1.0, _{Mut}NT15=0.57±0.157, n=3) to CaM-Sepharose binding to the truncated mTRPM2 fragment versus wild type (Figure 3.10C). Finally, TRPM2 transfected into HEK293 cells was assessed (n=6) using whole-cell patch-clamp recordings with 0.3mM ADPR in the patch pipette and 0.5mM or 2mM Ca²⁺ ECS applications (Figure 3.10D). Flag-mTRPM2-CaM_{Mut}(NT_{1Q}) resulted in a complete abolishment (n=6) of current to either Ca²⁺ ECS applications (3.10E). Furthermore, when ADPR was increased to 5mM (n=6) to test for a potential shift in ADPR responsiveness, TRPM2 currents were still not produced (Figure 3.10E). These results are consistent with the produced by Tong et al., 2006 that the role of the NT_{1Q} CaM site is to regulate TRPM2 Ca²⁺-CaM mediated channel activation.

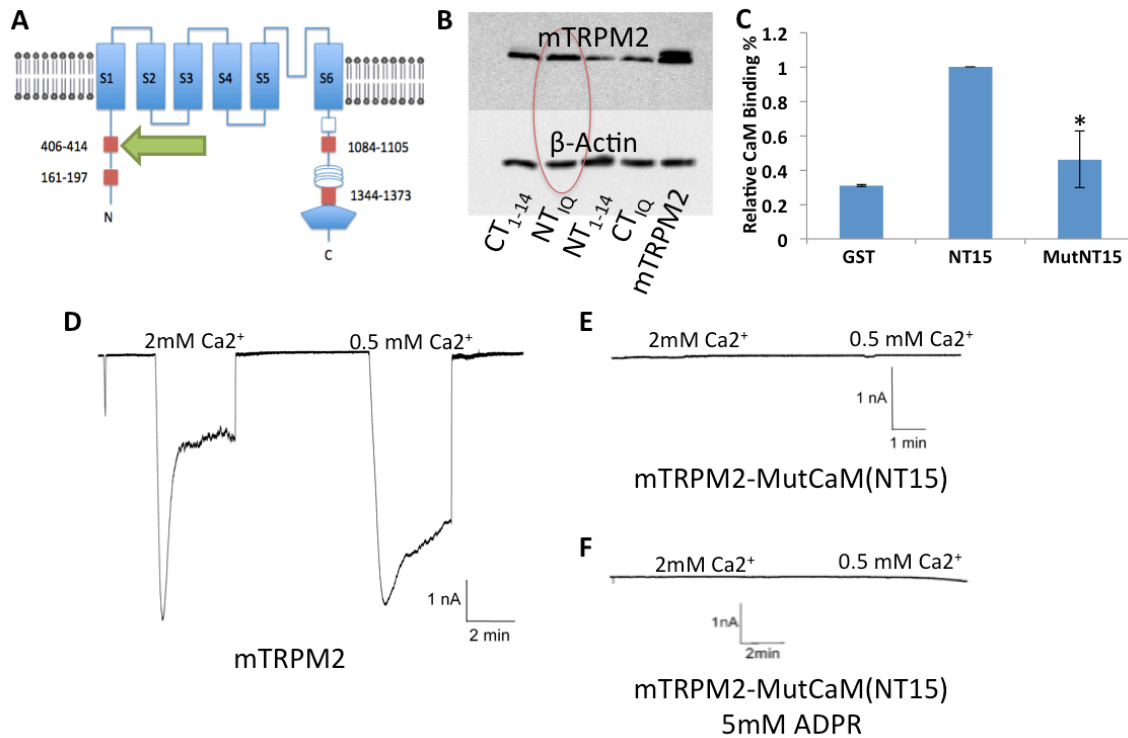


Figure 3.10 – Analysis of flag-mTRPM2-CaM_{Mut}(NT_{1Q}) **A.** TRPM2 schematic highlighting the mutation's location on the N-terminal. **B.** Protein lysates of flag-mTRPM2-CaM_{Mut}(NT_{1Q}) from transfected HEK293 cells confirm expression when probed for anti-flag on a Western blot (n=3). **C.** A truncated NT15 fragment generated from a flag-mTRPM2-CaM_{Mut}(NT_{1Q}) template (MutNT15) resulted in a significant decrease in CaM-Sepharose binding (p=0.009, NT15=1.0, MutNT15=0.57±0.157, n=3). **D.** Sample trace whole-cell patch-clamp recording of Hek293 transfected with mTRPM2 exposed to ECF with 0.5mM or 2mM Ca²⁺ treatments. **E.** Sample trace whole-cell patch-clamp recording of Hek293 transfected with flag-mTRPM2-CaM_{Mut}(NT_{1Q}) exposed to ECS with 0.5mM or 2mM Ca²⁺ treatments (n=6). **F.** Sample trace using 5mM ADPR.

3.7 Assessment of CaM site CT₁₋₁₄ and flag-mTRPM2-CaM_{Mut}(CT₁₋₁₄)

The next mutant to be tested, flag-mTRPM2-CaM_{Mut}(CT₁₋₁₄), overlaps with the NUDIX domain of TRPM2, responsible for ADPR activation of the channel (Perraud et al., 2003). Protein expression of Flag-mTRPM2-CaM_{Mut}(CT₁₋₁₄) was confirmed from HEK293 cell lysates on a Western blot tested with anti-flag (Figure 3.11B). CaM binding analysis was assessed for truncated fragment CT11 containing the normal CT₁₋₁₄ site versus MutCT11 (Figure 3.9). Substitution mutations at the CT₁₋₁₄ site resulted in a significant decrease ($p=0.002$, CT11=1.0, MutCT11=0.61±0.09, n=3) to CaM-Sepharose binding to the truncated mTRPM2 fragment versus wild type (Figure 3.11C). Finally, TRPM2 transfected into HEK293 cells was assessed (n=6) using whole-cell patch-clamp recordings with 0.3mM ADPR in the patch pipette and 0.5mM or 2mM Ca²⁺ ECS applications (Figure 3.11D). Flag-mTRPM2-CaM_{Mut}(CT₁₋₁₄) resulted in no significant change of CDI to either 0.5mM (Figure 3.11F) ($p=0.760$, mTRPM2=0.933±0.0503, mTRPM2-CaM_{Mut}(CT₁₋₁₄)=0.825±0.0675, n=6) or 2mM (Figure 3.11G) ($p=0.115$, mTRPM2=0.284±0.0169, mTRPM2-CaM_{Mut}(CT₁₋₁₄)=0.318±0.0107, n=6) Ca²⁺ ECS application. These results suggest the CT₁₋₁₄ CaM binding site has no regulatory role for either TRPM2 activation or inactivation, because reduction in CaM binding as a result of substitution mutagenesis caused no change in current amplitude or CDI.

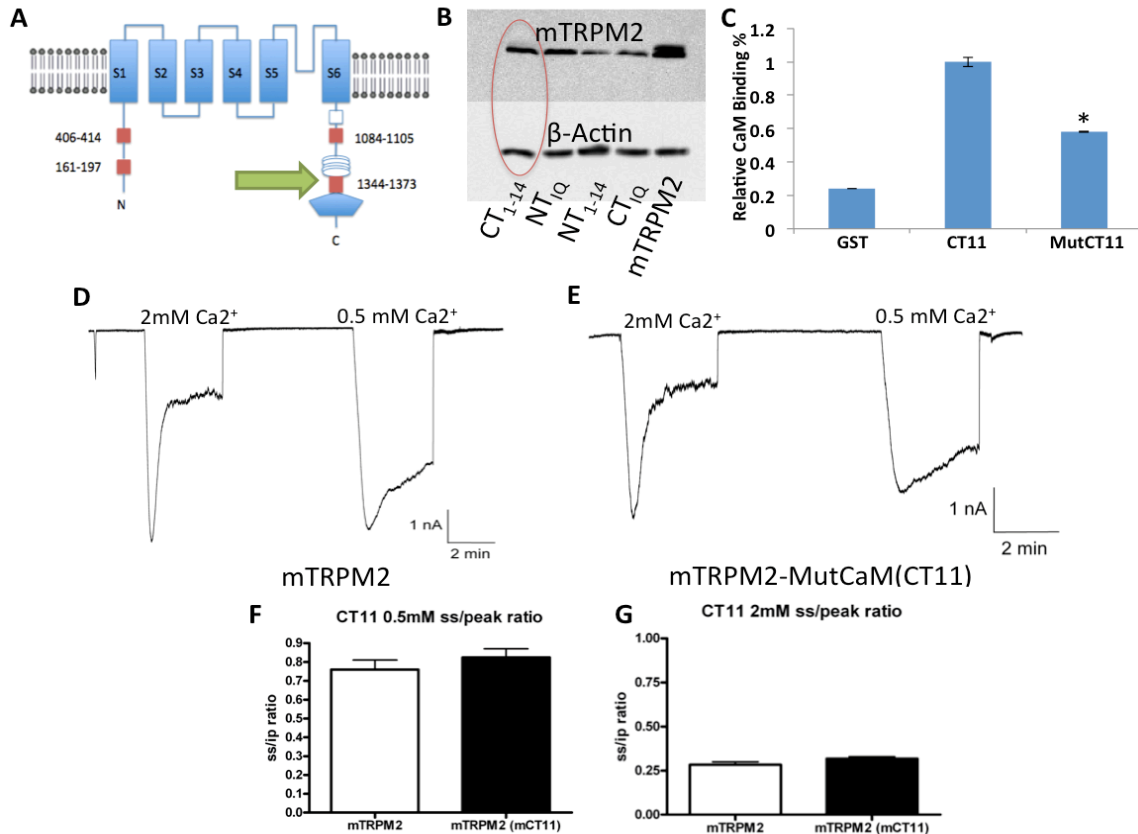


Figure 3.11 – Analysis of flag-mTRPM2-CaM_{Mut}(CT₁₋₁₄) **A.** TRPM2 schematic highlighting the mutation's location on the N-terminus. **B.** Protein lysates of flag-mTRPM2-CaM_{Mut}(CT₁₋₁₄) from transfected HEK293 cells confirmed expression when probed for anti-flag on a Western blot (n=3). **C.** A truncated CT11 fragment generated from a flag-mTRPM2-CaM_{Mut}(CT₁₋₁₄) template (MutCT11) resulted in a significant decrease (p<0.05) in CaM-Sepharose binding (p=0.002, CT11=1.0, MutCT11=0.61±0.09, n=3) **D.** Sample trace whole-cell patch-clamp recording of Hek293 transfected with mTRPM2 exposed to ECS with 0.5mM or 2mM Ca²⁺ treatments. **E.** Sample trace whole-cell patch-clamp recording of Hek293 transfected with flag-mTRPM2-CaM_{Mut}(CT₁₋₁₄) exposed to ECS with 0.5mM or 2mM Ca²⁺ treatments (n=6). **F.** No significant change to CDI of TRPM2 was found at 0.5mM Ca²⁺ or **(G.)** 2mM Ca²⁺ ECS applications for the mutant versus control (p<0.05) (n=6)

3.8 Assessment of CaM site CT_{IQ} and flag-mTRPM2-CaM_{Mut}(CT_{IQ})

The flag-mTRPM2-CaM_{Mut}(CT_{IQ}) mutant overlaps with the CCR region of TRPM2, thought to be responsible for unknown protein-protein interaction and the formation of the TRPM2 tetramer through subunit formation (Perraud et al., 2003). Flag-mTRPM2-CaM_{Mut}(CT_{IQ}) was transfected into HEK293 cells, reduced protein expression (n=3) was found in cell lysates versus wild type TRPM2 on a Western blot tested with anti-flag (Figure 3.12B). CaM binding analysis was assessed for truncated fragment CT5 containing the normal CT_{IQ} site versus MutCT5 (Figure 3.9). Substitution mutations at the CT_{IQ} site resulted in no significant change (p=0.158, CT5=1.0, MutCT5=1.48±0.48, n=3) to CaM-Sepharose binding to the truncated mTRPM2 fragment versus wild type (Figure 3.12C). Finally, TRPM2 transfected into HEK293 cells was assessed (n=6) using a whole-cell patch-clamp recording with 0.3mM ADPR in the patch pipette and 0.5mM or 2mM Ca²⁺ ECS applications (Figure 3.12E). Flag-mTRPM2-CaM_{Mut}(CT_{IQ}) resulted in a greatly reduced TRPM2 current response (n=6) to either Ca²⁺ ECS applications versus wild type TRPM2 (3.12F). Furthermore, when ADPR was increased to 5mM (n=6) to test for a potential shift in ADPR responsiveness, TRPM2 currents were still reduced (Figure 3.12G).

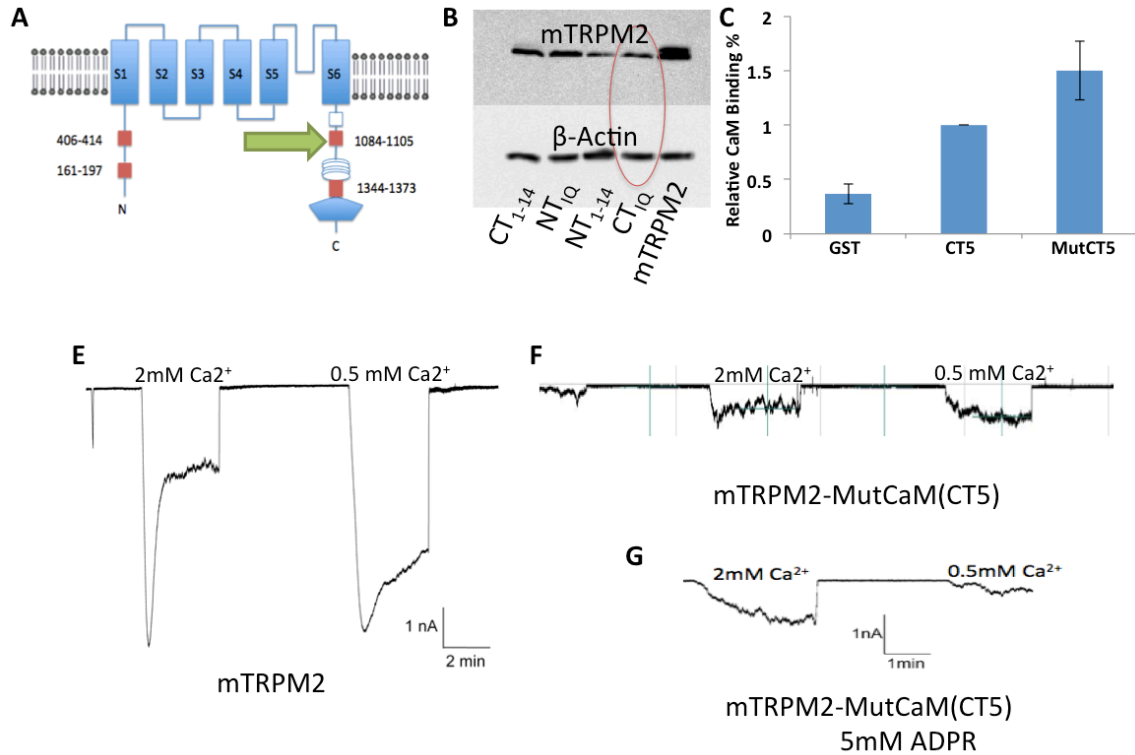


Figure 3.12 – Analysis of flag-mTRPM2-CaM_{Mut}(CT_{1Q}) **A.** TRPM2 schematic highlighting the mutation's location on the C-terminal. **B.** Protein lysates of flag-mTRPM2-CaM_{Mut}(CT_{1Q}) from transfected HEK293 cells show reduced expression when probed for anti-flag on a Western blot (n=3). **C.** A truncated CT5 fragment generated from a flag-mTRPM2-CaM_{Mut}(CT_{1Q}) template (MutCT5) resulted in no significant change (p=0.158, CT5=1.0, MutCT5=1.48±0.48, n=3) in CaM-Sepharose binding. **E.** Sample trace whole-cell patch-clamp recording of Hek293 transfected with mTRPM2 exposed to ECS with 0.5mM or 2mM Ca²⁺ treatments. **F.** Sample trace whole-cell patch-clamp recording of Hek293 transfected with flag-mTRPM2-CaM_{Mut}(CT_{1Q}) exposed to ECS with 0.5mM or 2mM Ca²⁺ treatments (n=6). **G.** Sample trace using 5mM ADPR.

3.9 Assessment of CaM site NT_{1-14} flag-mTRPM2-CaM_{Mut}(NT_{1-14})

The flag-mTRPM2-CaM_{Mut}(NT_{1-14}) mutant is found in a highly conserved NT region thought to be responsible for protein trafficking and expression (Perraud et al., 2003). Flag-mTRPM2-CaM_{Mut}(NT_{1-14}) was transfected into HEK293 cells, reduced protein expression (n=3) was found in cell lysates versus wild type TRPM2 on a Western blot tested with anti-flag (Figure 3.13B). CaM binding analysis was assessed for truncated fragment NT5 containing the normal NT_{1-14} site versus -_{Mut}NT5 (Figure 3.9). Substitution mutations at the NT_{1-14} site resulted in no significant change ($p=0.161$, $NT5=1.0$, $_{Mut}NT5=1.17\pm 0.175$, n=3) to CaM-Sepharose binding to the truncated mTRPM2 fragment versus wild type (Figure 3.13C). Finally, TRPM2 transfected into HEK293 cells was assessed (n=6) using a whole-cell patch-clamp recording with 0.3mM ADPR in the patch pipette and 0.5mM or 2mM Ca^{2+} ECS applications (Figure 3.13D). Flag-mTRPM2-CaM_{Mut}(NT_{1-14}) resulted in a complete abolishment of TRPM2 current response (n=6) to either Ca^{2+} ECS applications versus wild type TRPM2 (3.13E). Furthermore, when ADPR was increased to 5mM (n=6) to test for a potential shift in ADPR responsiveness, TRPM2-like currents were still completely abolished (Figure 3.13F).

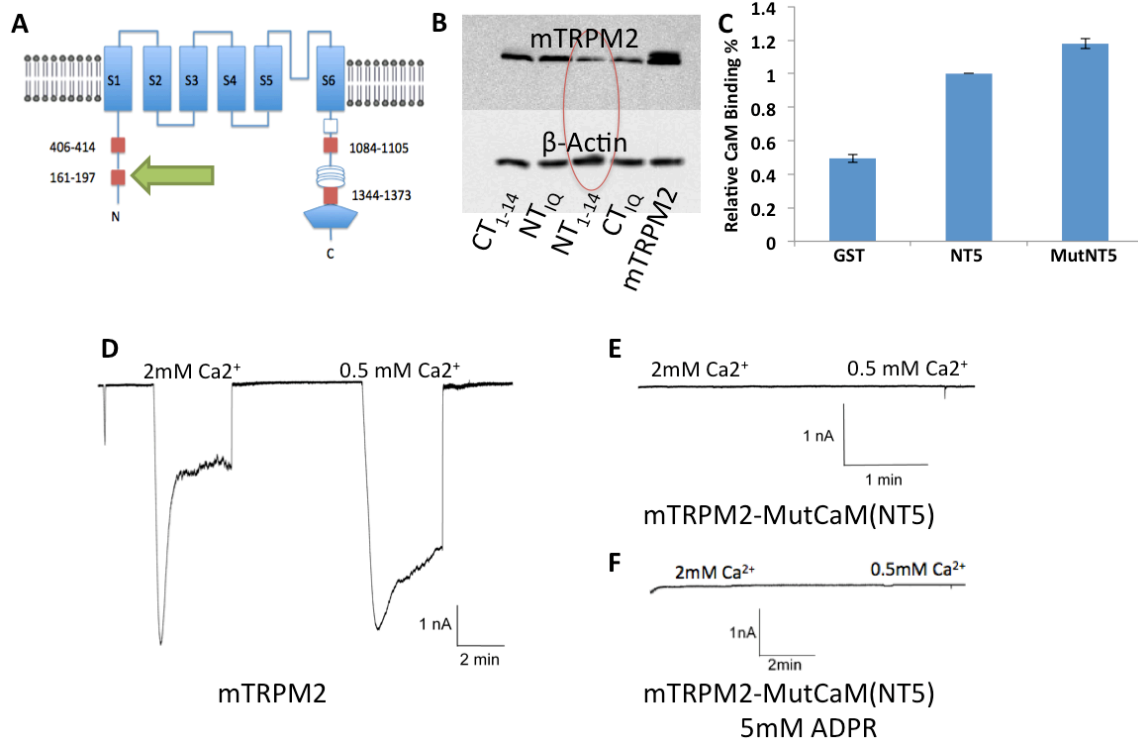


Figure 3.13 – Analysis of flag-mTRPM2-CaM_{Mut}(NT₁₋₁₄) **A.** TRPM2 schematic highlighting the mutation's location on the C-terminal. **B.** Protein lysates of flag-mTRPM2-CaM_{Mut}(NT₁₋₁₄) from transfected HEK293 cells show reduced expression when probed for anti-flag on a Western blot (n=3). **C.** A truncated CT5 fragment generated from a flag-mTRPM2-CaM_{Mut}(NT₁₋₁₄) template (_{Mut}NT5) resulted in no significant change ($p>0.05$) in CaM-Sepharose binding ($p=0.161$, NT5=1.0, _{Mut}NT5=1.17±0.175, n=3). **D.** Sample trace whole-cell patch-clamp recording of Hek293 transfected with mTRPM2 exposed to ECF with 0.5mM or 2mM Ca²⁺ treatments. **E.** Sample trace whole-cell patch-clamp recording of Hek293 transfected with flag-mTRPM2-CaM_{Mut}(NT₁₋₁₄) exposed to ECS with 0.5mM or 2mM Ca²⁺ treatments (n=6). **F.** Sample trace using 5mM ADPR failed to produce a TRPM2-like current.

3.10 Analysis of the hTRPM2 P1018L substitution

Findings by Hermosura et al., 2008 implicated a TRPM2 rundown in response to Ca^{2+} treatments when expressing a TRPM2 P1018L substitution common in a Guamian population. We were interested to test whether this rundown was similar to our novel CDI requiring CaM. Using my whole-cell patch-clamp protocol, which includes 0.3mM ADPR in the patch pipette, and alternating treatments of 0.5mM and 2mM Ca^{2+} , recordings were carried out from transfected HEK293 cells for hTRPM2 (Figure 3.14A/C) and hTRPM2 P1018L (Figure 3.14B/D). Contrary to those previously reported observations made using a different protocol, I did not observe a significant change to CDI under either 0.5mM (Figure 3.14E) ($p=0.933$, hTRPM2= 0.933 ± 0.459 , P1018L= 0.957 ± 0.217 , $n=6$) or 2mM (Figure 3.14F) ($p=0.922$, hTRPM2= 0.594 ± 0.0585 , P1018L= 0.601 ± 0.0432 , $n=6$) Ca^{2+} ECS applications versus wild type hTRPM2. However an interesting observation arose when comparing peak amplitudes between the wild type and mutant forms of hTRPM2. The peak amplitude ratio of the 0.5mM versus 2mM Ca^{2+} was significantly (Figure 3.14G) lower for the hTRPM2 P1018L mutant than that of wild type TRPM2 ($p=0.001$, hTRPM2= 1.75 ± 0.192 , P1018L= 0.880 ± 0.0476 , $n=6$). In other words the substitution mutation at P1018L appears to result in a higher TRPM2 current than normal for low Ca^{2+} ECS treatments, the implications of this finding will be discussed.

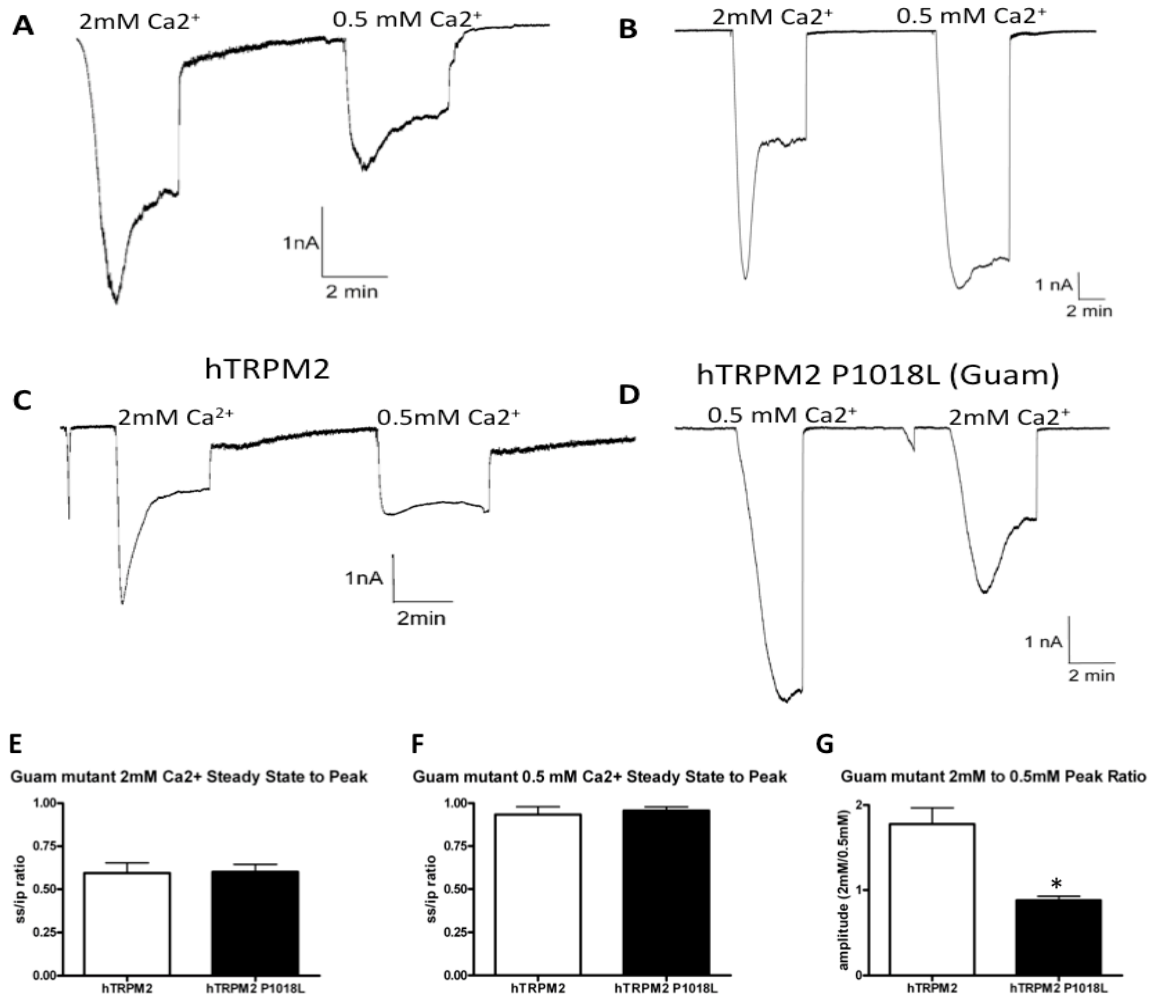


Figure 3.14 – Analysis of CDI for the hTRPM2 P1018L mutant. **A/C.** Sample whole-cell patch-clamp trace recording of hTRPM2 transfected into HEK293 cells with 0.3mM ADPR and 2mM or 0.5mM Ca²⁺ ECS applications. **B/D.** Sample trace recording of hTRPM2 P1018L. **E.** No significant difference in CDI was observed for hTRPM2 versus hTRPM2 P1018L with 2mM Ca²⁺ ECS applications ($p > 0.05$, $n = 6$). **F.** No significant difference in CDI was observed for hTRPM2 versus hTRPM2 P1018L with 0.5mM Ca²⁺ ECS applications ($p > 0.05$, $n = 6$). **G.** A significant difference between the ratio of 0.5mM and 2mM Ca²⁺ ECS applications was found for hTRPM2 versus hTRPM2 P1018L ($p < 0.05$, $n = 6$).

3.11 - TRPM2 CDI in hTRPM2 versus mTRPM2

I made an interesting but unexpected observation worth noting during the course of this thesis. HEK293 cells were transfected with either mTRPM2 (Figure 3.15B) or hTRPM2 (Figure 3.15A) used as control recordings for the CaM mutant or the Guam mutant portions of this project. Intriguingly a significant difference was observed for TRPM2 CDI, with mTRPM2 undergoing a significantly higher (Figure 3.15C/D) amount of inactivation in response to 2mM ($p < 0.001$, hTRPM2=0.594±0.0585, mTRPM2=0.284±0.0169, n=6) or 0.5mM ($p = 0.0291$, hTRPM2=0.933±0.0459, mTRPM2=0.760±0.0503, n=6) Ca²⁺. Several explanations for this phenomenon will be discussed further.

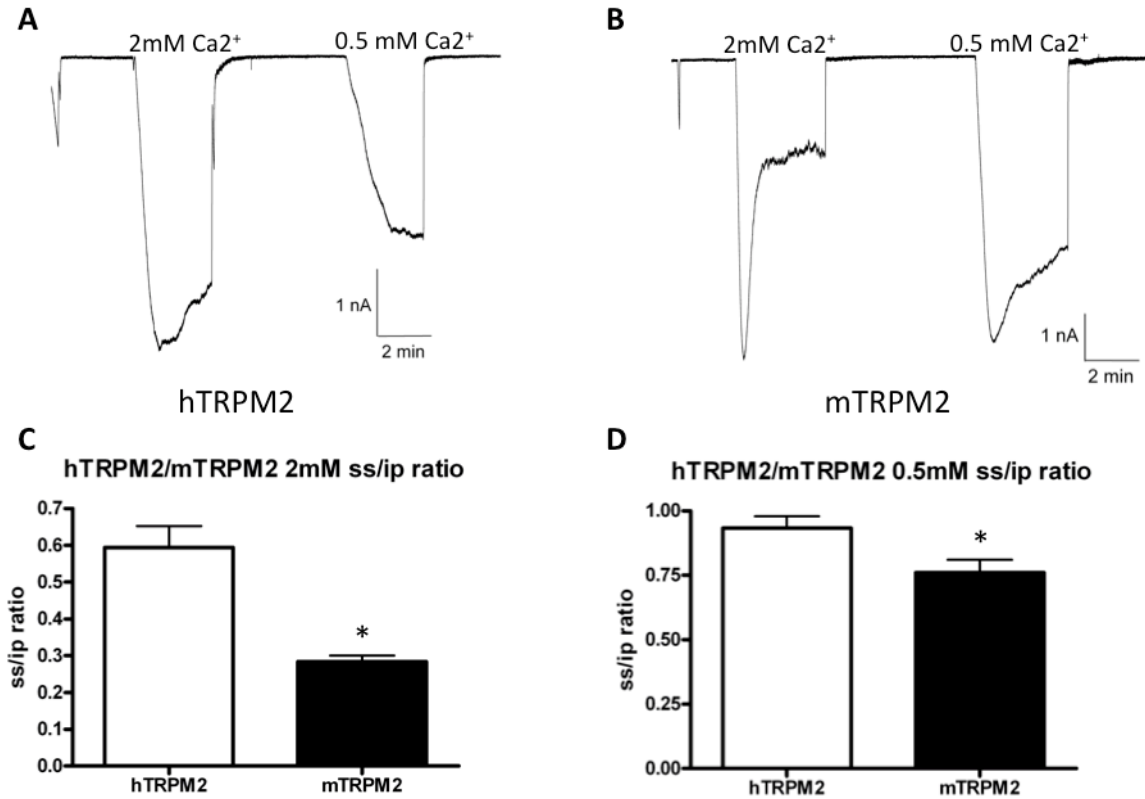


Figure 3.15 – Analysis of CDI for mTRPM2 versus hTRPM2. **A.** Sample whole-cell patch-clamp trace recording of hTRPM2 transfected into HEK293 cells with 0.3mM ADPR and 2mM or 0.5mM Ca²⁺ ECS applications. **B.** Sample whole-cell patch-clamp trace recording of mTRPM2 transfected into HEK293 cells with 0.3mM ADPR and 2mM or 0.5mM Ca²⁺ ECS applications. **C.** A significant difference between TRPM2 CDI was observed between hTRPM2 and mTRPM2 under 2mM Ca²⁺ applications ($p < 0.001$, hTRPM2 = 0.594 ± 0.0585 , mTRPM2 = 0.284 ± 0.0169 , $n = 6$). **D.** A significant difference between TRPM2 CDI was observed between hTRPM2 and mTRPM2 under 0.5mM Ca²⁺ applications ($p = 0.0291$, hTRPM2 = 0.933 ± 0.0459 , mTRPM2 = 0.760 ± 0.0503 , $n = 6$).

Section 4

DISCUSSION

4.1 Summary of Key Findings

The primary goal of this thesis was to uncover the mechanism through which CDI of TRPM2 occurs. We based our approach on a previous study by Tong et al., 2006 that hinted at unknown CaM binding sites on TRPM2. We choose a strategy of creating truncation mutations to produce minimum CaM binding domains (Zhulke and Reuter, 1998) and a substitution mutation strategy at those minimum-binding domains (Zuhlke et al., 1999; Tong et al., 2006). The novel findings from this project are summarized below:

- 1) TRPM2 undergoes CDI that is increased with larger applications of extracellular Ca^{2+} . CDI of TRPM2 has a linear voltage relationship that mimics the Ca^{2+} ionic reversal potential (Figure 3.1).
- 2) *In silico* screening of TRPM2 terminals reveals 3 novel candidate CaM consensus site sites. Additionally a truncated C-terminal of TRPM2 stably expressed in HEK293 cells binds with CaM-Sepharose in the presence of Ca^{2+} .
- 3) A systematic analysis of truncated TRPM2 domains confirms 3 new binding sites (CT_{IQ}, CT₁₋₁₄ and NT_{IQ}). Binding is not completely abolished in absence of Ca^{2+} .
- 4) An assessment of substitution mutations to four different CaM sites were preformed:
 - NT_{IQ}: confirmed expression, reduced CaM binding, abolished current.
 - CT₁₋₁₄: confirmed expression, reduced CaM binding, no CDI change.
 - CT_{IQ}: reduced expression, regular CaM binding, reduced current.
 - NT₁₋₁₄: reduced expression, regular CaM binding, abolished current.

5) The Guam mutant hTRPM2 P1018L shows normal CDI but increased current amplitude under 0.5mM Ca²⁺ applications.

6) There is a significantly higher CDI for mTRPM2 versus hTRPM2.

4.2 TRPM2 CDI is mediated by extracellular Ca²⁺

Our laboratory having previously identified TRPM2 CDI were interested in defining the mechanism. Previous unpublished work has established TRPM2 CDI is dependent on intracellular [Ca²⁺] and can be fully recovered from after a period of 0 Ca²⁺ exposure. I next wanted to establish how the extracellular [Ca²⁺] mediates TRPM2 CDI and whether this process is affected by membrane voltage. TRPM2 conductance is not directly influenced by membrane voltage. However, current is still indirectly affected by the electrical gradient of cations. By raising membrane holding voltage the peak amplitude of TRPM2 current is decreased and therefore our measurement of CDI (I_{ss}/I_p).

An experimental protocol was designed with 3 min exposures of either 2mM or 0.5mM Ca²⁺. Between Ca²⁺ sweeps a 5 minute 0mM Ca²⁺ exposure allowed complete recovery from CDI and furthermore voltage was raised in 20mV steps. Figure 3.1 outlines the finding from this experiment. TRPM2 CDI was highly evident with 2mM Ca²⁺; however, CDI was only apparent for 0.5mM Ca²⁺ treatments when holding voltage was below -60mV. The reason for this is likely twofold: under higher concentrations of Ca²⁺ influx is larger and this translates to higher intracellular [Ca²⁺] and therefore greater TRPM2 CDI. Secondly as voltage is hyperpolarized the

electrical force driving Ca^{2+} entry is greater thus increasing intracellular $[\text{Ca}^{2+}]$ and thereby TRPM2 CDI.

Also of note TRPM2 CDI at the 2mM Ca^{2+} treatment decreased in a linear fashion as membrane voltage was depolarized. The most likely explanation is that voltage is not directly mediating TRPM2 CDI. Instead the Ca^{2+} electrical gradient is altered, lowering influx into the intracellular environment and slowing CDI. This is further evidenced by the extrapolation of the 2mM Ca^{2+} CDI trend, which approximates the reversal potential of Ca^{2+} cations under this conditions.

4.3 Ca^{2+} -CaM binding, Ca^{2+} specificity and ApoCaM

With a basic understanding of the mechanisms that regulate TRPM2, I next wanted to establish if the CaM complex is interacting with TRPM2 to evoke CDI. Evidence from Tong et al., 2006 implicated additional uncharacterized CaM binding sites with unknown function. Previous studies have been conducted where proteins have been modulated by Ca^{2+} -CaM at more than one binding site (Scott et al., 1997; Wang et al., 1989; Buschmeier et al., 1987). Success has been achieved by generating a series of protein truncations and carrying out substitution mutagenesis at this target site to resolve the physiological function (Zhulke and Reuter, 1998; Zuhlke et al., 1999). Using a similar strategy I first performed an *in silico* screening of TRPM2 which successfully identified three additional CaM sites on the intracellular N- and C-terminal not discussed in the literature (Figure 3.3). A truncation strategy was initially developed with stable expression of flag-tagged truncated fragments. A C-term TRPM2 truncation incubated with CaM-Sepharose was initially resolved with a

Western blot (Figure 3.3), further confirming my suspicion that previously undiscovered CaM binding sites exist in the terminal ends of TRPM2.

A new protocol was adopted that allows for a much more rapid screening of truncated fragments and determination of the minimum binding domain. The TNT quick-coupled reticulocyte system allows for transcription and translation of a plasmid into a fluorescent protein. The second feature of this system is direct in-gel imaging of a protein, greatly reducing the time required to perform the binding experiments of this thesis and a more rapid confirmation of minimum binding sites. All truncated fragments were tagged with GST in both an effort to increase molecular weight for small-truncated fragments and to ensure sufficient lysine incorporation into every fragment. GST also acted as a negative binding control for which truncated fragments binding to CaM-Sepharose could be compared. Great success was achieved with this approach, I experimentally confirmed three new candidate sites which were able to interact with CaM-Sepharose in consensus with the *in silico* screening. Figure 3.5 confirmed a CT_{IQ} site located at 1084-1105AA, Figure 3.6 a CT₁₋₁₄ located at 1344-1373AA and finally Figure 3.8 a NT_{IQ} site at 161-197AA.

We developed our truncation strategy around the TNT Quick-Coupled Transcription/Translation kit, which allowed for more rapid CaM-binding analysis versus traditional use of cell lysates. This method has been used previously to identify CaM interaction with channels, particularly using radiolabeled serine (Fanger et al., 1999). For my purposes fluorescent lysine reduced many of the hurdles when dealing with radiolabeled amino acids. A limitation with the kit

however prevented complete analysis of truncated fragments. The protein concentration of the truncated fragments cannot be determined from the protein-rich reaction solution. Due to this fact inputs were only controlled by volume, but protein concentration of each sample was variable. Signal strength is also variable from fragment to fragment depending on the number of fluorescent lysine. This limited experimental analysis to semi-quantitative only and was achieved by standardizing volume between the fragment input and pull-down. While it was efficient for quick confirmation of binding domains, the true strength of the interaction needs to be determined using cellular lysates of truncated fragments and standardized using a BSA assay and Western blotting. It was our hope to rapidly identify and characterize sites and return to further analyze candidate sites that demonstrated a physiological function. The protocol rapidly achieved this goal and worked successfully for our purposes.

A Ca^{2+} -free 5mM EGTA solution reduced, but did not completely abolish, CaM-Sepharose binding to any of the truncated TRPM2 fragments. A secondary explanation may account for some ApoCaM interaction at these sites, especially prominent amongst IQ-like sites (Jurado et al., 1999). Future analysis will need to elucidate the true Ca^{2+} -specificity at these binding sites. This would be achieved through repeating experiments with lysates of HEK293 cells transfected with truncated TRPM2 fragments. We decided to then pursue electrophysiological recordings from mutated TRPM2 at candidate sites. This would provide a more accurate analysis of the physiological relevance of these sites for mediation of TRPM2 CDI.

4.4 *NT_{1Q}* and *TRPM2* activation

Tong et al., 2006 originally characterized a NT_{1Q} site responsible for TRPM2 Ca²⁺-CaM activation. I replicated the substitution mutations performed by their group and first examined the effects of those substitution mutations within our unique experimental recording protocol. Similar to findings by Tong et al., 2006 I discovered a reduction in CaM-Sepharose binding (Figure 3.10C), but not a complete abolishment as a result of the substitution mutation. CaM-Sepharose pulldown was still greater than GST alone; therefore the residual binding cannot be completely attributed to GST. As predicted, TRPM2 current could not be recorded in HEK293 cells transfected with flag-mTRPM2-CaM_{Mut}(NT_{1Q}). When intracellular ADPR was increased to 5mM no Ca²⁺ mediated current was observed, which is expected from a site that is necessary for TRPM2 activation. The analysis of the Tong et al., 2006 mutant acts as a validation for the experimental design carried out in this thesis.

4.5 *CT₁₋₁₄* and the *TRPM2* NUDIX domain

The second mutant I examined was at the CT₁₋₁₄ site overlapping with the NUDIX domain, responsible for ADPR binding and activation of TRPM2 (Perraud et al., 2003). It is possible that high intracellular [Ca²⁺] create an active CaM that indirectly competes with ADPR and prevents activation of TRPM2. Substitution mutations to the CT₁₋₁₄ site successfully reduced, but did not completely eliminate, CaM binding (Figure 3.11C) similar to what I observed with the NT_{1Q} mutant. Furthermore the full length flag-mTRPM2-CaM_{Mut}(CT₁₋₁₄) successfully expressed in HEK293 cells (Figure 3.11B). Despite these findings flag-mTRPM2-CaM_{Mut}(CT₁₋₁₄)

current and CDI appear to be completely normal (Figure 3.11) compared to WT mTRPM2 recordings.

The findings from this mutant are important for two reasons. First it acts as a strong validation that the process of substitution mutagenesis itself does not alter channel gating properties. Secondly it would appear that Ca^{2+} -CaM does not appear to be competing with ADPR binding in order to evoke CDI, at least at this CaM candidate site. Based on these findings it would appear the CT₁₋₁₄ candidate site has no critical physiological role in TRPM2 function or regulation.

4.6 CT_{1Q} and the TRPM2 CCR

A substitution mutation to the CT_{1Q} candidate CaM binding site produced some unexpected but exciting results. The CT_{1Q} site overlaps with the CCR, originally predicted to play some unknown role in the TRPM2 channel structure, expression or gating (Perraud et al., 2003). In fact a CCR is often involved in protein-protein interactions, a Ca^{2+} -CaM complex may play a functional role by changing the channel gating very close to the pore region. Substitution mutations to site CT_{1Q} resulted in no significant change to CaM-Sepharose binding in a truncated fragment compared to WT (Figure 3.12C). Despite this, a significant reduction in TRPM2 current was apparent from HEK293 cells transfected with flag-mTRPM2-CaM_{Mut}(CT_{1Q}) (Figure 3.12). The mutant TRPM2 still displayed some Ca^{2+} responsiveness, but the reduced current could not be recovered with increased 5mM ADPR. The current observed from flag-mTRPM2-CaM_{Mut}(CT_{1Q}) is different than that obtained from flag-mTRPM2-

CaM_{Mut}(NT_{IQ}), the site responsible for TRPM2 activation, as that mutant completely abolished all current regardless of Ca²⁺ application.

Several reasons for the reduced current may be likely: a reduced expression was found in Western blotting from cell lysates compared to the previous mutant examined (Figure 3.12B). Secondly surface expression remains to be determined, reduced flag-mTRPM2-CaM_{Mut}(CT_{IQ}) at the membrane may result in a reduced current. The CCR has also been implicated in formation of the tetrameric structure of TRPM2, if the substrate formation is altered by the mutations near the CCR region a malformed tetramer may result in reduced TRPM2 current seen from flag-mTRPM2-CaM_{Mut}(CT_{IQ}). Finally the Ca²⁺-CaM site may be altering activation or inactivation kinetics, once again facing a common problem with separating overlapping kinetics both driven by the Ca²⁺-CaM complex. While the CT_{IQ} sites specific role in TRPM2 CDI is still unknown, evidence from flag-mTRPM2-CaM_{Mut}(CT_{IQ}) recordings suggests a novel site critical for proper TRPM2 function that has not been thoroughly discussed in the literature.

4.7 NT₁₋₁₄ and conserved NT regions

The final CaM candidate site to be discussed is a second NT site with a 1-14 CaM consensus map. Similar to site CT_{IQ} some unexpected but interesting results were produced by a substitution mutation to this region. Comparing the NT_{IQ} mutated site and wild type, no significant change to CaM-Sepharose binding was found (Figure 3.13C). Despite this finding, a complete abolishment of current was found from HEK293 cells transfected with flag-mTRPM2-CaM_{Mut}(NT₁₋₁₄) (Figure

3.13). The response to Ca^{2+} treatments, which completely mimics the mutant NT_{10} site responsible for Ca^{2+} -CaM activation of the TRPM2 channel (Tong et al., 2006). Despite an increase to 5mM ADPR, currents were still unable to be elicited from flag-mTRPM2-CaM_{Mut}(NT_{1-14}).

Future work remains to determine if this substitution mutant is preventing proper trafficking and expression at the membrane. Relatively little is known about the role of the highly conserved NT region, but it is believed to be primarily responsible for channel expression (Perraud et al., 2003). Similar to the CT_{10} mutant reduced expression was observed from lysates of transfected HEK293 with flag-mTRPM2-CaM_{Mut}(CT_{10}) (Figure 3.13B). Several explanations may exist for the abolished TRPM2 current, but only abolished expression at the membrane would account for the complete absence of current. Alternatively multiple sites responsible to Ca^{2+} -CaM activation may exist. The precise reason the mutations performed to NT_{1-14} alter TRPM2 current remain to be established, but this second CaM site holds a strong potential for playing an important physiological role in proper TRPM2 protein function.

4.8 hTRPM2 P1018L CDI and peak amplitude

Very little has been discussed in the literature concerning TRPM2 CDI, in fact our novel recording protocol seems to have revealed a major physiological feature of the channel that has been largely overlooked. A study by Hermosura et al., 2008 examined a genetic mutant hTRPM2 with a proline to leucine substitution at site 1018 occurring near the pore-forming region of TRPM2. Their results implicate the

substitution creating an increase in inactivation over time not observed for wild-type TRPM2. We believed this increased inactivation may be the same as our own CDI observed from TRPM2 transfected HEK293 cells. The P1018L hTRPM2 mutant it was transfected into HEK293 cells and whole-cell patch-clamp recordings performed with 2mM Ca²⁺ or 0.5mM Ca²⁺ applications.

Several key differences exist between the recording protocols I utilized and the Hermosura et al., 2008 paper. Primarily cells were held at -80mV compared to -60mV for my recordings. Additionally I prime cells with 2mM Ca²⁺ to both ensure sufficient activation and diffusion of ADPR and EGTA into the intracellular environment. The Hermosura group maintains cells in 1.5mM Ca²⁺ solution throughout compared to my use of Ca²⁺-free solution to prevent current while the intracellular solution diffuses. These differences may result in different activation and inactivation kinetics, which may not reveal strong TRPM2 CDI I normally observe from WT TRPM2 channels. I discovered that the P1018L hTRPM2 mutant did not have a significant change to CDI for either 2mM or 0.5mM Ca²⁺ applications (Figure 3.14). The suggestion by Hermosura et al., 2008 that hTRPM2 P1018L has an increased form of inactivation was not apparent within our recording protocol. However an interesting result was found by comparing peak amplitude between 0.5mM and 2mM Ca²⁺ applications, where an increased TRPM2 current was observed under low Ca²⁺ for the mutant form versus wild type. The results from Hermosura et al., 2007 suggested loss of TRPM2 P1018L function causes neurodegeneration, which is counterintuitive to what we know about TRPM2 function. In contrast my findings of increased Ca²⁺ influx is more intuitive. The

implications of this finding are intriguing and should be followed up with future studies with the P1018L hTRPM2 mutant. In addition to a substitution mutation, low environmental concentration of Mg^{2+} and Ca^{2+} have been implicated in Guam ALS and PD (Hermosura et al., 2007). Whether these environmental factors act synergistically with an increased TRPM2 current under low Ca^{2+} remains to be determined. Furthermore whether these findings translate to a physiological outcome of these diseases cannot yet be claimed, but nevertheless offer an exciting avenue to explore.

4.9 Implications of increased mTRPM2 CDI

One additional finding has lead to more questions about the process of TRPM2 CDI and the site(s) through which this CaM regulated process occurs. All experiments apart from hTRPM2 P1018L used mTRPM2 as a control and template for mutations. As such I noticed a significant difference between the two forms of TRPM2 (Figure 3.15) whereby mTRPM2 had significant higher CDI under both 0.5mM and 2mM Ca^{2+} applications versus hTRPM2. I will postulate on the reasoning behind these differences, but until further experimentation occurs the mechanism is unknown.

I performed blast sequencing between mTRPM2 and hTRPM2, which revealed an 85% sequence homology between mTRPM2 and hTRPM2. Structures implicated in TRPM2 function are highly conserved between both mTRPM2 and hTRPM2. Intriguingly only one of the candidate CaM sites CT_{IQ} has three substitutions in the IQ region to non-critical binding residues; the effect this has on

CaM binding to this site may be further pursued. Targeted substitution mutations to the CT_{1Q} site could replicate the differences in sequence homology from either form of TRPM2 and electrophysiological recordings performed. Further work still is required to determine the exact means NT₁₋₁₄ or CT_{1Q} regulate TRPM2, but if CT_{1Q} alters CDI the differences between mouse and human may result from these AA substitutions.

4.10 Significance of Work

Many diseases involve aberrant cellular behavior or cell death. The involvement of TRPM2 with Ca²⁺ influx and oxidative mediated stress has led to a focus on the channels role in disease throughout the body. TRPM2 has been linked to genetic diseases, is activated by reactive oxygen species and is a mechanism for delayed cell death (Perraud et al., 2005). TRPM2 is a self-regulating channel controlled by the Ca²⁺-CaM complex. Inactivation may prevent Ca²⁺ intracellular overload during high Ca²⁺ influx and subsequent damage to cells. A specific antagonist for the TRPM2 channel has also yet to be identified. For this reason a more thorough understanding of the CDI of the channel may lead to further breakthroughs leading to therapeutic treatments.

Many diseases have been implicated to be a result of TRPM2 dysfunction; here I will highlight the current literature and the ways through which a more thorough understanding of TRPM2 regulation may be beneficial. Recent evidence suggests TRPM2 KO mice have higher insulin secretion and blood glucose levels (Uchida et al., 2011). Interestingly knockouts may be protected from diet-induced

obesity and insulin resistance (Zhang et al., 2012). KO mice had higher energy expenditure, even though insulin secretion was inhibited. TRPM2 KO mice avoid hyper insulinemia, which prevents obesity through development of insulin resistance (Zhang et al., 2012; Uchida et al., 2011). Overall, the lowered insulin secretion under high fat diets creates a better metabolic state (Zhang et al., 2012). A case-control study to assess TRPM2 correlation with type-2 diabetes found no evidence for SNP's or TRPM2 mutations (Romero et al., 2010). TRPM2 may be targeted to promote insulin release or therapeutically treat pre-diabetic patients albeit with the risk of malignancy from damaged Beta cells (Uchinda et al., 2011; Scharenberg, 2009).

The role of melastatin in tumor proliferation in aberrant melanoma cells has generated interest for other TRP family members. Hypomethylation of the genome often leads to transcriptional noise and antisense transcripts generated in cancerous cells (Orfanelli et al., 2008). Two TRPM2 antisense transcripts caused by a promoter in intron 24 were identified named TRPM2-AS and TRPM2-TE (Orfanelli et al., 2008). Quantitative RT-PCR has discovered TRPM2-AS in 80% of melanoma cell lines and TRPM2-TE expression was also correlated. These transcripts may reduce TRPM2 current by interrupting the tetrameric structure as subunit members (Orfanelli et al., 2008). Knocking down the aberrant transcripts or overexpressing TRPM2 increased melanoma cell apoptosis and necrosis (Orfanelli et al., 2008). Additionally TRPM2 knockdown in prostate cancer cells inhibits cell proliferation, but knocking down in non-cancerous cells had no effect (Zeng et al., 2010). The knockdown was independent of the PARP pathway (Zeng et al., 2010). Interestingly

TRPM2 was also highly expressed and clustered around the cell nuclei in the cancerous cells (Zeng et al., 2010).

A correlation between SNP in exon 11 of TRPM2 and early onset bi-polar disorder (BD) was identified (Xu et al., 2009). Also a linkage analysis was performed with 600 bipolar research subjects and control subjects (McQuillin et al., 2006). A base pair change from aspartic acid to glutamic acid at amino acid 543 was significantly associated with the disorder (McQuillin et al., 2006). Another study compared oxidative stress induced TRPM2 currents from lymphoblast cells of bipolar and non-afflicted control individuals (Roedding et al., 2012). Interestingly rotenone an oxidative stressor increased Ca^{2+} in BD patient B lymphoblast cells, whereas TRPM2 currents were decreased from normal patients (Roedding et al., 2012).

A mutation to EFCH1 has been associated with Juvenile myoclonic epilepsy and inhibits Ca^{2+} currents (Kanata et al., 2012). EFCH1 enhances TRPM2 currents contributing to cell death (Kanata et al., 2012). EFCH1 is believed to associate with TRPM2 to mediate processes other than cell death such function and development of the central nervous system in normal physiology (Kanata et al., 2012).

TRPM2 has been implicated directly in several neurodegenerative diseases resulting from Ca^{2+} neuronal cell death and apoptosis. Several groups have examined experimental stroke models and their subsequent effect on TRPM2 regulation (Jia et al., 2011; Fonfria et al., 2006). TRPM2 mRNA expression was increased at 1 and 4 weeks following a middle cerebral artery occlusion in rats (Fonfria et al., 2006). High TRPM2 expression was seen in human C13 microglia,

which are activated and involved in neuroprotection during phagocytosis and mediate neurotoxic damage (Fonfria et al., 2006). Knockdowns of TRPM indicated ADPR mediated activation and Ca^{2+} influx may promote neural cell death around the area of injury following ischemia (Fonfria et al., 2006). Sex specific effects of oxygen-glucose deprivation were observed in mice with knocked-down TRPM2 using shRNA and pharmacological inhibitor clotrimazole (Jia et al., 2011). Infarct volume was significantly reduced with both treatments in males, but no reduction was observed for female mice (Jia et al., 2011).

The same group examined TRPM2's role in Alzheimer's' Disease (AD) by examining $\text{A}\beta_{1-42}$ toxicity on striatal rat cultures at 2-7 days (Fonfria et al., 2005). Three methods of reducing functional TRPM2 were utilized: PARP blocker (SB-750139), siRNA and TRPM2-S splice variant transfections (Fonfria et al., 2005). All three strategies significantly reduced cell death from oxidative stress (Fonfria et al., 2005). The study was inherently limited in its use of non-physiological levels of non-oligomeric forms of $\text{A}\beta_{1-42}$, striatal cultures where AD does not occur and poor TRPM2 antibodies. TRPM2 currents have since been isolated in hippocampal cultures (Olah et al., 2009) and additional work from our own laboratory is following up on the association between AD and TRPM2 (unpublished).

Finally dysfunction of TRPM2 has been linked to an hTRPM2 P1018L variant. I have developed a more thorough understanding through which the P1018L variant alters TRPM2 function and the possible implications it has for normal physiological function. The increased hTRPM2 currents for the P1018L Guam variant under 0.5mM Ca^{2+} provide new evidence towards the neurodegeneration seen in Guam

patients. Previous studies by Hermosura et al., 2009 only identified increased TRPM2 inactivation within their recording protocol. This finding seemingly disagrees with a correlation of increased neurodegeneration; a reduction in TRPM2 current and therefore Ca^{2+} -influx would more likely cause neuroprotection. It remains to be determined whether the association between low environmental Ca^{2+} , increased hTRPM2 P1018L current with low extracellular $[\text{Ca}^{2+}]$ and neurodegenerative disorders amongst the Guam population is significant. However, these preliminary findings are exciting and should be pursued in the future.

While the exact mechanism behind CDI has yet to be conclusively identified, two strong candidate sites at NT_{1-14} and CT_{IQ} exist that appear to play critical physiological functions in TRPM2 regulation. Whether CaM has a regulatory function in TRPM2 CDI remains to be determined. However, the evidence of multiple CaM sites required for proper TRPM2 function hint at a tight regulation of TRPM2 CDI by CaM. Whether one or more of these sites is directly responsible for CDI should be followed by future studies. The mutants tell us that TRPM2 regulation by Ca^{2+} -CaM may be more complicated than previously envisioned, with two sites (NT_{1-14} and CT_{IQ}) being required for proper TRPM2 function.

4.11 Future Directions

Many interesting findings about TRPM2 have been discovered throughout this thesis, but the story behind TRPM2 CDI remains illusive. Two strong candidate sites CT_{IQ} and NT_{1-14} cannot conclusively be implicated for TRPM2 CDI, but appear to have a critical role in channel function or regulation. Future work with these sites

needs to confirm proper expression of the protein before the alterations in current can be completely attributed to substitution mutations at these target sites. Furthermore, an interesting observation between mTRPM2 and hTRPM2 has revealed a significant difference between CDI at both 0.5mM and 2mM Ca^{2+} . The AA sequence of the CT_{10} site may provide a novel mutation strategy for which CDI may be altered without interrupting the protein expression or trafficking. Mutations at the CT_{10} site may be negatively impacting substrate interaction of the tetramer, but a less aggressive mutation using hTRPM2 as a guideline may provide a functional mTRPM2 channel with altered CDI.

Future experiments with truncated fragments should be pursued using transfected HEK293 cells and cellular lysates. Fragments generated using cellular machinery will be more representative of physiological folding, a limitation of the protocol I used for the binding experiments. Ca^{2+} -dependence of CaM-Sepharose binding with truncated fragments from cell lysates may reveal a more representative understanding of how the CaM candidate sites interact with CaM.

4.12 Overall Conclusions

Several important conclusions have been drawn from the course of this thesis. Very little was known about TRPM2 CDI, I successfully defined the inactivation as being tightly regulated by extracellular $[\text{Ca}^{2+}]$. The literature behind CaM interaction at the TRPM2 N- and C-terminal was incomplete. A systematic analysis of the TRPM2 terminals revealed three novel sites named CT_{10} , CT_{1-14} and NT_{1-14} . While we cannot conclude the exact regulatory nature behind two of these

mutations, it would appear that CT_{IQ} and NT₁₋₁₄ have a critical role in TRPM2 function; current was greatly reduced and completely abolished respectively by substitution mutations at these sites. Using our novel recording protocol we discovered CDI is not altered for hTRPM2 P1018L. However an interesting finding showcases an increased current under low Ca²⁺. Future studies may reveal a tight link between low environmental Mg²⁺ and Ca²⁺ and this phenomenon, further implicating Guam ALS and PD correlated with this mutant hTRPM2 population. One final finding reveals a significant higher amount of CDI for mTRPM2 versus hTRPM2. The exact mechanism or physiological relevance behind this altered CDI remains to be determined but stands as another exciting avenue for the future of this story.

My results will advance the current understanding of TRPM2 regulation, CaM interaction and CDI as well as providing novel insight into a human genetic mutation implicated in neurodegenerative disease.

Section 5

REFERENCES

- Apel, E. D., Byford, M. D., Au, D., Walsh, K. A., and Storm, D. R. Identification of protein kinase C phosphorylation site in neuromodulin. *Biochemistry*, 29, 2330-2335.
- Babu, Y., Sack, J. S., Greenhough, T. J., Bugg, C. E., Means, A. R., Cook, W. J. (1985). Three-dimensional structure of calmodulin. *Nature*, 315(6014), 37-40.
- Beck, A., Kolisek, M., Bagley, L. A., Fleig, A., and Penner, R. (2006). Nicotinic acid adenine dinucleotide phosphate and cyclic ADP-ribose regulate TRPM2 channels in T lymphocytes. *The FASEB Journal*, 20, 962-964.
- Belrose, J. C., Xie, Y. F., Gierszewski, L. J., MacDonald, J. F., and Jackson, M. F. (2012). Loss of glutathione homeostasis associated with neuronal senescence facilitates TRPM2 channel activation in cultured hippocampal pyramidal neurons. *Molecular Brain*, 5(11), 1-11.
- Buelow, B., Song, Y., and Scharenberg, A. M. (2008). The Poly(ADP-ribose) Polymerase PARP-1 is required for the oxidative stress-induced TRPM2 activation in lymphocytes. *Journal of Biological Chemistry*, 283 (36), 24571-24583.
- Buschmeier, B., Meyer, H. E., and Mayr, G. W. (1987). *J Biol Chem*, 262, 9454-9462.
- Chung, K. K. H., Freestone, P. S., and Lipski, J. (2011) Expression and functional properties of TRPM2 channels in dopaminergic neurons of the substantia nigra of the rat. *J Neurophysiol.* 106, 2865-2875.
- Clapham, D. E. (2003). TRP channels as cellular sensors. *Nature*. 426, 517-524.
- Crivici, A., and Ikura, M. (1995). Molecular and structural basis of target recognition by calmodulin. *Annu. Rev. Biophys. Biomol. Struct.* 24, 85-116.
- Csanady, L. (2010). Permeating proton found guilty in compromising TRPM2 channel activity. *J Physiol.* 588(10), 1661-1662.
- Csanady, L., and Torocsik, B. (2009). Four Ca²⁺ ions activate TRPM2 channels by binding in deep crevices near the pore but intracellularly of the gate. *Journal of General Physiology*, 133(2), 189-203.
- Dargent, B., Paillart, C., Carlier, E., Alcaraz, G., Martin-Eauclaire, M. F., and Couraud, F. (1994). Sodium channel internalization in developin neurons. *Neuron*, 13(3), 683-690.
- Davidovic, L., Vodenicharov, M., Affar, E. B., and Poriere, G. G. (2001). Importance of Poly(ADP-Ribose) glycohydrolase in the control of Poly(ADP-Ribose) metabolism. *Experimental Cell Research*. 268, 7-13.

- Di, A., Gao, X., Qian, F., Kawamura, T., Han, J., Hecquet, C., Ye, R. D., Vogel, S. M., and Malik, A. B. (2012). The redox-sensitive cation channel TRPM2 modulates phagocyte ROS production and inflammation. *Nature Immunology*, 13(1), 29-36.
- Dietrich, A., and Gudermann, T. Another TRP to endothelial dysfunction: TRPM2 and endothelial permeability. *Circulation Research*. 102, 275-277.
- Du J, Xie J, Yue L. (2009a). Intracellular calcium activates TRPM2 and its alternative spliced isoforms. *Proc Natl Acad Sci USA*, 106, 7239-7244.
- Du, J., Xie, J., and Yue, L. (2009b). Modulation of TRPM2 by acidic pH and the underlying mechanisms for pH sensitivity. *Journal of General Physiology*, 134(6), 461-488.
- Duncan, L. M., Deeds, J., Hunter, J., Shao, J., Holmgren, L. M., Woolf, E.A., Tepper, R. I., and Shyjan A. W. (1998). Down-regulation of the novel gene melastating correlates with potential for melanoma metastasis. *Cancer Research*. 58(7): 1515-1520.
- Fleig, A., and Penner, R. (2004). The TRPM ion channel subfamily: molecular, biophysical and functional features. *Trends Pharmacol. Sci.* 25, 633-639.
- Fonfria, E., Marshall, I. C., Benham, C. D., Boyfield, I., Brown, J. D., Hill, K., Hughes, J. P., Skaper, S. D., and McNulty, S. (2004). TRPM2 channel opening in response to oxidative stress is dependent on activation of poly(ADP-ribose) polymerase. *Br. J. Pharmacol.* 143, 186-192.
- Fonfria, E., Marshall, I. C. B., Boyfield, I., Skaper, S. D., Huges, J. P., Owen, D. E., Zhang, W., Miller, B., A., Benham, C. D., and McNulty, S. (2005). Amyloid β -peptide(1-42) and hydrogen peroxide-induced toxicity are mediated by TRPM2 in rat primary striatal cultures. *Journal of Neurochemistry*. 95, 715-723.
- Fonfria, E., Mattei, C., Hill, K., Brown, J. T., Randall, A., Benham, C. D., Skaper, S. D., Campbell, C. A., Crook, B., Murdock, P. R., Wilson, J. M., Maurio, F. P., Owen, D. E., Tilling, P. L., and McNulty, S. (2006) TRPM2 is elevated in the tMCAO stroke model, transcriptionally regulated, and functionally expressed in C13 microglia. *Journal of Receptors and Signal Transduction*. 26, 179-198.
- Friedberg, F. (1990). Species comparison of calmodulin sequences. *Protein Se Data Anal*, 3(4), 335-337.
- Grubisha, O., Rafter, L. A., Takanishi, C. L., Xu, X., Tong, L., Perraud, A. L., Scharenberg, A. M., and Denu, J. M. (2006). Metabolite of SIR2 reaction modulates TRPM2 ion channel. *Journal of Biological Chemistry*, 281, 14057-14065.
- Hara, Y., Wakamori, M., Ishii, M., Maeno, E., Nishida, M., Yoshida, T., Yamada H.,

- Shimizu, S., Mori, E., Kudoh, J., Shimizu, N., Kurose, H., Okada, Y., Imoto, K., Mori, Y., (2002). LTRPC2 Ca²⁺-permeable channel activated by changes in redox status confers susceptibility to cell death. *Mol. Cell.* 9, 163–173.
- Haraguchi, K., Kawamoto, A., Isami, K., Maeda, S., Kusano, A., Asakura, K., Shirakawa, H., Mori, Y., Nakagawa, T., and Kaneko, S. TRPM2 contributes to inflammatory and neuropathic pain through the aggravation of pronociceptive inflammatory responses in mice. *Cellular/Molecular*, 32(11), 3931-3941.
- Harteneck, C., Plant, T. D., and Schultz, G. (2000). From worm to man: three subfamilies of TRPM channels. *Trends Neurosci.* 23, 159-166.
- Hecquet, C. M., Ahmmed, G. U., Vogel, S. M., and Malik, A. B. (2008) Role of TRPM2 channel in mediating H₂O₂-induced Ca²⁺ entry and endothelial hyperpermeability. *Circulating research*, 102, 347-355.
- Heiner, I., Eisfeld, J., and Luckhoff, A. (2003). Role and regulation of TRP channels in neutrophil granulocytes. *Cell Calcium*, 33, 533–540.
- Heiner, I., Eisfeld, J., Warnstedt, M., Radukina, N., Jungling, E., Luckhoff, A. (2006) Endogenous ADP-ribose enable calcium-regulated cation currents through TRPM2 channels in neutrophil granulocytes. *Biochem. J.* 398, 225-232.
- Hermosura, M. C., and Garruto, R. M. (2007). TRPM7 and TRPM2 – candidate susceptibility for western pacific ALS and PD? *Biochimica et Biophysica Acta.* 1772 822-835.
- Hermosura, M. C., Cui, A. M., Go, R. M. V., Davenport, B., Shelter, C. M., Heizer, J. W., Schmitz, C., Mocz, G., Garruto, R. M., and Perraud, A. L. (2008). Altered functional properties of a TRPM2 variant in Guamanian ALS and PD. *PNAS*, 105(46), 18029-18034.
- Hill, K., Benham, C. D., McNulty, S., and Randall, A. D. (2004a). Flufenamic acid is a pH-dependent antagonist of TRPM2 channels. *Neuropharmacology.* 47, 450-460.
- Hill, K., McNulty, S., and Randall, A. D., (2004b). Inhibition of TRPM2 channels by the antifungal agents clotrimazole and econazole. *Arch Pharmacol.* 370, 227-237.
- Hill, K., Tigue, N. J., Kellsell, R. E., Benham, C. D., McNulty, S., Schaefer, M., and Randall, A. D. (2006). Characterization of recombinant rat TRPM2 and a TRPM2-like conductance in cultured rat striatal neurons. *Neuropharmacology*, 50, 89-97.
- Hoeflich, K. P., and Ikura, M. (2002). Calmodulin in action: diversity in target recognition and activation mechanisms. *Cell*, 108, 739 –742.
- Inamura, K., Sano, Y., Mochizuki, S., Yokoi, H., Miyake, A., Nozawa, K., Kitada, C.,

- Matsushime, H., Furuichi and K. (2003). Response to ADP-Ribose by activation of TRPM2 in the CRI-G1 insulinoma cell line. *J Membrane Biol.* 191, 201-207.
- Jia, J., Verma, S., Nakayama, S., Quillinan, N., Grafe, M. R., Hurn, P. D., and Herson, P. S. (2011). Sex differences in neuroprotection provided by inhibition of TRPM2 channels following experimental stroke. *Journal of Cerebral Flow & Metabolism*, 31, 2160-2168.
- Jiang L. H. (2007). Subunit interaction in channel assembly and functional regulation of transient receptor potential melastatin (TRPM) channels. *Biochem Soc Trans.* 35:86-8
- Jiang, L. H., Yang, W., Zou, J., and Beech, D. J. (2010). TRPM2 channel properties, functions and therapeutic potentials. *Expert. Opin. Ther. Targets.* 14, 973-988.
- Jurado, L. A., Chockalingam, P. S., and Jarrett, H. W. (1999) Apocalmodulin. *Physiological Reviews.* 79(3), 661-677.
- Kanato, M., Numata, T., Aguan, K., Hara, Y., Kiyonaka, S., Yamamoto, S., Miki, T., Sawamura, S., Suzuki, T., Yamakawa, K, and Mori, Y. (2012). The juvenile myoclonic epilepsy-related protein EFHC1 interacts with redox-sensitive TRPM2 channel linked to cell death. *Cell Calcium*, 51,179-185.
- Kevit, R. E., Dalgarno, D. C., Levine, B. A., and Williams, R. J. (1984). H-NMR studies of calmodulin. The nature of the Ca²⁺-dependent conformational change. *Eur J Biochem*, 139, 109-114.
- Knowles, H., Heizer, J. W., Li, Y., Chapman, K., Ogden, C. A., Andreasen, K., Shapland, E., Kucera, G., Mogan, J., Humann, J., Lenz, L. L., Morrison, A. D., and Perraud, A. L. (2011). Transient receptor potential melastatin 2 (TRPM2) ion channel is required for innate immunity against *Listeria monocytogenes*. *PNAS*, 108(28), 11578-11583.
- Kolisek, M., Beck, A., Fleig, A., and Penner, R. (2005). Cyclic ADP-ribose and hydrogen peroxide synergize with ADP-ribose in the activation of TRPM2 channels. *Mol. Cell* 18, 61-69.
- Kraft, R., Grimm, C., Grosse, K., Hoffman, A., Sauerbruch, S., Kettenmann, H., Schultz, G., and Harteneck, C. (2004). Hydrogen peroxide and ADP-ribose induce TRPM2-mediated calcium influx and cation currents in microglia. *Am. J. Physiol. Cell Physiol.* 286, 129-137.
- Kraft, R., Grimm, C., Frenzel, H., and Harteneck, C. (2006). Inhibition of TRPM2 cation channels by N-(p-amycinnamoyl)anthranilic acid. *BR J. of Pharmacol.* 148, 264-273.

- Kuhn, F. J. P., and Luckhoff, A. (2004). Sites of the NUDT9-H domain critical for ADP-ribose activation of the cation channel TRPM2. *J. Biol. Chem.* 279(45), 46431-46437.
- Kuhn, F. J. P., Knop, G., and Luckhoff, A. (2007). The transmembrane segment S6 determines cation versus anion selectivity of TRPM2 and TRPM8. *Journal of Biological Chemistry*, 282(38), 27598-27609.
- Kuhn, F. J. P., Kuhn, C., Naziroglu, M., and Luckhoff, A. (2009). Role of an N-terminal splice segment in the activation of the cation channel TRPM2 by ADP-Ribose and hydrogen peroxide. *Neurochem. Res.* 34, 227-233.
- Lange, I., Penner, R., Fleig, A., and Beck, A. (2008) Synergistic regulation of endogenous TRPM2 channels by adenine dinucleotides in primary human neutrophils. *Cell Calcium*, 44, 604-615.
- Lange, I., Yamamoto, S., Partida-Sanchez, S., Mori, Y., Fleig, A., and Penner, R. (2009). TRPM2 functions as a lysosomal Ca²⁺-release channel in β cells. *Science Signalling*. 2(72), 1-11.
- Lupas, A., Van Dyke, M., and Stock, J., (1991). Predicting coiled coils from protein sequences. *Science*. 252(5010), 1162-1164
- Lynch, T. J., and Cheung, W. Y. (1979). Human erythrocyte Ca²⁺-Mg²⁺-ATPase: mechanism of stimulation by Ca²⁺. *Arch Biochem Biophys*, 194(1), 165-170.
- McHugh, D., Flemming, R., Xu, S. Z., Perraud, A. L., and Beech, D. J. (2003). Critical intracellular Ca²⁺ dependence of transient receptor potential melastatin 2 (TRPM2) cation channel activation. *J. Biol. Chem.* 278, 11002-11006.
- McQuillin, A., Bass, N. J., Kalsi, G., Lawrence, J., Puri, V., Choudhury, K., Detera-Wadleigh, S. D., Curtis, D., and Gurling, H. M. D. (2006). Fine mapping of a susceptibility locus for bipolar and genetically related unipolar affective disorders, to a region containing the C21ORF29 and TRPM2 genes on chromosome 21q22.3. *Molecular Psychiatry*, 11, 134-142.
- Mei, Z. Z., and Jiang, L. H. (2009). Requirement for the N-terminal coiled-coil domain for expression and function, but not subunit interaction of, the ADPR-activated TRPM2 channel. *Journal of Membrane Biology*. 230, 93-99.
- Mei, Z. Z., Mao, H. J., and Jiang, L. H. (2006a). Conserved cysteine residues in the pore region are obligatory for human TRPM2 channel function. *Am. J. Physiol. Cell Physiol.* 291, 1022-1028
- Mei, Z. Z., Xia, R., Beech, D. J., and Jiang, L. H. (2006b). Intracellular coiled-coil domain engaged in subunit interaction and assembly of melastatin-related transient

- receptor potential channel 2. *J. Biol. Chem.* 281, 38748–38756.
- Miller, B. A., (2004). Inhibition of TRPM2 function by PARP inhibitors protects cells from oxidative stress-induced death. *Br. J. Pharmacol.* 143, 515-516.
- Minke, B., and Cook, B. (2002). TRP channel proteins and signal transduction. *Physiol Rev.* 82, 429-472.
- Montell, C. (2005). The TRP superfamily of cation channels. *Science STKE* (272) re3, 1-24.
- Montell, C., and Rubin, G. M., (1989). Molecular characterization of the drosophila trp locus: a putative membrane protein required for phototransduction. *Neuron* 2. 1313-1323.
- Nadler, M. J., Hermosura, M. C., Inabe, K., Perraud, A. L., Zhu, Q., Stokes, A. J., Kurosaki, T., Kinet J. P., Penner, R., Scharenberg, A. M., and Fleig, A. (2001). LTRPC7 is a Mg²⁺-regulated divalent cation channel required for cell viability. *Nature*, 411, 590-595
- Nagamine, K., Kudoh, J., Minoshima, S., Kawasaki, K., Asakawa, S., Ito, F., and Shimizu, N. (1998). Molecular cloning of a novel putative Ca²⁺ channel protein (TRPC7) highly expressed in brain. *Genomics*. 54, 124-131.
- Naziroglu, M., Luckhoff, A., and Jungling, E. (2007). Antagonist effect of flufenamic acid on TRPM2 cation channels activated by hydrogen peroxide. *Cell Biochem Funct.* 25, 383-387.
- Olah, M. E., Jackson, M. F., Li, H., Perez, Y., Sun, H. S., Kiyonaka, S., Mori, Y., Tymianski, M., MacDonald, J. F. (2009). Ca²⁺-dependent induction of TRPM2 currents in hippocampal neurons. *J Physiol*, 587, 965-979.
- Orfanelli, U., Wnke, A. K., Doglioni, C., Russo, V., Bosserhoff, A. K., and Lavorgna, G. (2008). Identification of novel sense and antisense transcription at the TRPM2 locus in cancer. *Cell Research*, 18, 1128-1140.
- Perraud, A. L., Fleig, A., Dunn, C. A., Bagley, L. A., Launay, P., Schmitz, C., Stokes, A. J., Zhu, Q., Bessman, M. J., Penner, R., Kinet, J. P., and Scharenberg, A. M. (2001). ADP-ribose gating of the calcium-permeable LTRPC2 channel revealed by Nudix motif homology. *Nature*. 411, 595-599.
- Perraud, A. L., Schmitz, C., and Scharenberg, A. M. (2003). TRPM2 Ca²⁺ permeable cation channels: from gene to biological function. *Cell Calcium* 33, 519-531.
- Perraud, A. L., Takanishi, C. L., Shen, B., Kang, S., Smith, M. K., Schmitz, C., Knowles, H. M., Ferrais, D., Li, W., Zhang, J., Stoddard, B. L., and Scharenberg, A. M. (2005).

- Accumulation of free ADP-ribose from mitochondria mediates oxidative stress-induced gating of TRPM2 cation channels. *J Biol Chem* 280:6138-48
- Peterson, B. Z., DeMaria, C. D., and Yue, D. T. (1999). Calmodulin is the Ca²⁺ sensory for Ca²⁺-dependent inactivation of L-type calcium channels. *Neuron*, 22, 549-558.
- Phillips, A. M., Bull, A., Kelly, L. E. (1992). Identification of a drosophila gene encoding a calmodulin-binding protein with homology to the trp phototransduction gene. *Neuron* 8. 631-642.
- Roedding, A. S., Gao, A. F., Au-Yeung, W., Scarcelli, T., Li, P. P., Warsh, J. J. (2012). Effect of oxidative stress on TRPM2 and TRPC3 channels in B lymphoblast cells in bipolar disorder. *Bipolar Disorders*, 14, 151-161.
- Romero, J. R., Germer, S., Castonguay, A. J., Barton, N. S., Martin, M., and Zee, R. Y. L. (2010). Gene variation of the transient receptor potential cation channel, subfamily M, member 2 (TRPM2) and type 2 diabetes mellitus: a case-control study. *Clinica Chimica Acta*. 411, 1437-1440.
- Rowland, L. P. (2001). Amyotrophic lateral sclerosis, *New England Journal of Medicine*, 344, 1688-1700.
- Saimi, Y., and Kung C. (2002). Calmodulin as an ion channel subunit *Annu Rev Physiol*, 64, 289-311.
- Sano, Y., Inamura, K., Miyake, A., Mochizuki, S., Yokoi, H., Matsushime, H., and Furuichi, K. (2001). Immunocyte Ca²⁺ influx system mediated by LTRPC2. *Science* 293, 1327-1330.
- Scharenberg, A. M. (2005). TRPM2 and TRPM7: channel/enzyme fusions to generate novel intracellular sensors. *Eur J Physiol*. 451, 220-227.
- Scharenberg, A. M. (2009) TRPM2 and pancreatic β cell responses to oxidative stress. *Islets*. 1(2), 165-166.
- Scott, K., Sun, Y., Beckingham, K., and Zuker, C. S. (1997). Calmodulin regulation of drosophila light-activated channels and receptor function mediates termination of the light response in vivo. *Cell*, 91, 375-383.
- Shen, B. W., Lerraud, A. L., Scharenberg, A., and Stoddard, B. L. (2003). The crystal structure and mutational analysis of human NUDT9. *J. Mol. Biol*, 332, 385-398.
- Singh, B. B., Liu, X., Tang, J., Zhu, M. X., and Ambudkar, I. S. (2002). *Mol. Cell*, 9, 739 – 750
- Soldani, C., Lazze, M. C., Bottone, M. G., Tognon, G., Biggiogera, M., Pellicciari, C. E.,

- and Scovassi, A. I. (2001). Poly(ADP-ribose) polymerase cleavage during apoptosis: when and where? *Experimental Cell Research*. 269, 193-201
- Soldani, C., and Scovassi, A. I. (2002). Poly(ADP-ribose) polymerase-1 cleavage during apoptosis: an update. *Apoptosis*, 7, 321-328.
- Starkus J., Beck A., Fleig A., Penner R. (2007). Regulation of TRPM2 by extra- and intracellular calcium. *J Gen Physiol*, 130:427-40
- Starkus, J. G., Fleig, A., and Penner, R. (2010). The calcium-permeable non-selective cation channel TRPM2 is modulated by cellular acidification. *J Physiol*. 588, 1227-1240
- Takahashi, K., Sakamoto, K., and Kimura, J. (2012). Hypoxic stress induces transient receptor potential melastatin 2 (TRPM2) channel expression in adult rat cardiac fibroblasts. *J Pharmacol Sci*. 118(2), 186-197.
- Tang, J., Lin, Y., Zhang, Z., Tikunova, S., Birnbaumer, L., and Zhu, M. X. (2001). Identification of common binding sites for calmodulin and inositol 1,4,5-trisphosphate receptors on the carboxyl termini of trp channels. *J. Biol. Chem*, 276, 21303-21310.
- Togashi K., Hara, Y., Tominaga T., Higashi, T., Konishi, Y., Mori, Y., and Makoto T., (2006). TRPM2 activation by cyclic ADP-ribose at body temperature is involved in insulin secretion. *EMBO Journal*. 25:1804-1815.
- Togashi, K., Inada, H., and Tominaga, M. (2008). Inhibition of the transient receptor potential cation channel TRPM2 by 2-aminoethoxydiphenyl borate (2-APB). *BRJ of Pharmacol*, 153, 1324-1330.
- Toledo, S. A., Lange, I., Cortado, H., Bhagat, H., Mori, Y., Fleig, A. Penner, R., and Patrida-Sanchez, P. (2011). Dendritic cell maturation and chemotaxis is regulated by TRPM2-mediated lysosomal Ca²⁺ release. *FASEB Journal*, 25, 3529-3542.
- Tong, Q., Zhang, W., Conrad, K., Mostoller, K., Cheung, J. Y., Peterson, B. Z., and Miller, B. A. (2006). Regulation of the transient receptor potential channel TRPM2 by the Ca²⁺ sensor calmodulin. *Journal of Biological Chemistry* 281, 9076-9085.
- Uchida, K., Dezaki, K., Damdindorj, B., Inada, H., Shiuchi, T., Mori, Y., Yada, T., Minokoshi, Y., and Tominaga, M. (2011). Lack of TRPM2 impaired insulin secretion and glucose metabolisms in mice. *Diabetes*, 60, 119-126.
- Uemura, T., Kudoh, J., Noda, S., Kanba, S., and Shimizu, N. (2005). Characterization of human and mouse TRPM2 genes: identification of a novel N-terminal truncated protein specifically expressed in human striatum. *Biochemical and Biophysical Research Communications*, 328, 1232-1243.

- Virag, L., and Szabo, C. (2002). The therapeutic potential of Poly(ADP-Ribose) polymerase inhibitors. *Pharmacological Review*. 54, 375-429.
- Wang, C. L. A., Wang, L. W. C., and Lu R. C. (1989) *Biochem Biophys Res Commun*, 162, 746-752.
- Wehage, E., Eisfeld, J., Heiner, I., Jungling, E., Zitt, C., and Luckhoff, A. (2002). Activation of the cation channel long transient receptor potential channel 2 (LTRPC2) by hydrogen peroxide. A splice variant reveals a mode of activation independent of ADP-ribose. *J Biol Chem*. 277. 23150-6.
- Wilkinson, J. A., Scragg, J. L, Boyle, J. P., Nilius, B., and Peers, C. (2008) H₂O₂-stimulated Ca²⁺ influx via TRPM2 is not the sole determinant of subsequent cell death. *Eur J Physiol*. 455, 1141-1151.
- Yamamoto, S., Shimizu, S., Kiyonaka, S., Takahashi, N., Wajima, T., Hara, Y., Negoro, T., Hiroi, T., Kiuchi, Y., Okada, T., Kaneko, S., Lange, I., Felig, A., Penner, R., Nishi, M., Takeshima, H., and Mori, Y. (2009). TRPM2-mediated Ca²⁺ influx induces chemokine production in monocytes that aggravates inflammatory neutrophil infiltration. *Nat. Med*, 14(7), 738-747.
- Yang, K. T., Chang, W. L., Yang, P. C., Chien, C. L., Lai, M. S., Su, M. J., and Wu, M. L. (2006). Activation of the transient receptor potential M2 channel and poly(ADP-ribose) polymerase is involved in oxidant stress-induced cardiomyocyte death. *Cell Death Differ*, 13(10), 1815-1826.
- Yang, W., Zou, J., Xia, R., Vaal, M. L., Seymour, V. A., Luo, J., Beech, D. J. and Jiang, L. H. (2010). State-dependent inhibition of TRPM2 channel by acidic pH. *Journal of Biological Chemistry*. 285(40), 30411-30418.
- Yu, F.H., and Catterall, W. A. (2004). The VGL-chanome: a protein superfamily specialized for electrical signaling and ionic homeostasis. *Science STKE* 2004. (253)re15, 1-17.
- Xie, Y. Belrose, J. C., Lei, G., Tymianski, M., Mori, Y, MacDonald, J. F., and Jackson, M. F. (2011). Dependence of NMDA/GSK3 β mediated metaplasticity on TRPM2 channels at hippocampal CA3-CA1 synapses. *Molecular Brain*, 4(44), 1-9.
- Xu, C., Li, P. P., Cooke, R. G., Parikh, S. V., Wang, K. S., Kennedy, J. L., Warsh, J. J. (2009). TRPM2 variants and bipolar disorder risk: confirmation in a family-based association study. *Bipolar Disorders*, 11, 1-10.
- Zeng, X., Sikka, S. C., Huang, L., Sun, C., Xu, C., Jia, D., Abdel-Mageed, A. B., Pottle, J. E., Taylor, J. T., and Li, M. (2010). Novel role for the transient receptor potential

- channel TRPM2 in prostate cancer cell proliferation. *Prostate Cancer and Prostatic Diseases*. 13, 195-201.
- Zhang, S., Ehler, M. D., Bernhardt, J. P., Su, C., and Huganir, R. L. (1998) Calmodulin mediates calcium-dependent inactivation of N-methyl-aspartate receptors. *Neuron*, 21, 443-453.
- Zhang, W., Chu, X., Tong, Q., Cheung, J. Y., Conrad, K., Masker, K., Miller, B. A. (2003a). A novel TRPM2 isoform inhibits calcium influx and susceptibility to cell death. *J. Biol. Chem.* 278, 16222–16229.
- Zhang, W., Hirschler-Laszkiewicz, I., Tong, Q., Conrad, K., Sun, S., Penn, L., Barber, D. L., Stahl, R., Carey, D. J., Cheung, J. Y., and Miller, B. A. (2006). TRPM2 is an ion channel that modulates hematopoietic cell death through activation of caspases and PARP cleavage. *Am J Physiol Cell Physiol*, 290, 1146-1159.
- Zhang, W., Tong, Q., Conrad, K., Wozney, J., Cheung, J. Y., and Miller, B. A. (2007). Regulation of TRP channel TRPM2 by the tyrosine phosphatase PTPL1. *Am J Physiol Cell Physiol*, 292, 1746-1758.
- Zhang, Z., Okawa, H., Wang, Y., and Liman, E. R. (2005) Phosphatidylinositol 4,5-biphosphate rescues TRPM4 channels from desensitization, *The Journal of Biological Chemistry*, 280(47), 39185-39192.
- Zhang, Z., Zhang, W., Jung, D. Y., Ko, H. J., Lee, Y., Friedline, H., Lee, E., Jun, J., Ma, Z., Kim, F., Tsitsilianos, N., Chapman, K., Morrison, A., Cooper, M. P., Miller, B. A., Kim, J. K. (2012). TRPM2 Ca²⁺ channel regulates energy balance and glucose metabolism. *Am J Physiol Endocrinol Metab*, 302, 807-816.
- Zhang, Y. Hoon, M.A., Chandrashekar, J., Mueller, K. L., Book, B., Wu, D., Zuker, C. S., and Ryba, J.P. (2003b). Coding of sweet,bitter and umami tastes: different receptor cells sharing similar signaling pathways. *Cell*. 112, 293-301.
- Zuhlke, R. D., Pitt, G. S., Deisseroth, K., Tsien, R. W. and Reuter, H. (1999). Calmodulin supports both inactivation and facilitation of L-type calcium channel. *Nature*, 399, 159-162.
- Zhulke, R. D. and Reuter, H. (1998). Ca²⁺-sensitive inactivation of L-type Ca²⁺ channels depends on multiple cytoplasmic amino acid sequences of the α_{1C} subunit. *Proc Natl Acad Sci USA*, 95, 3287-3294.

Appendix

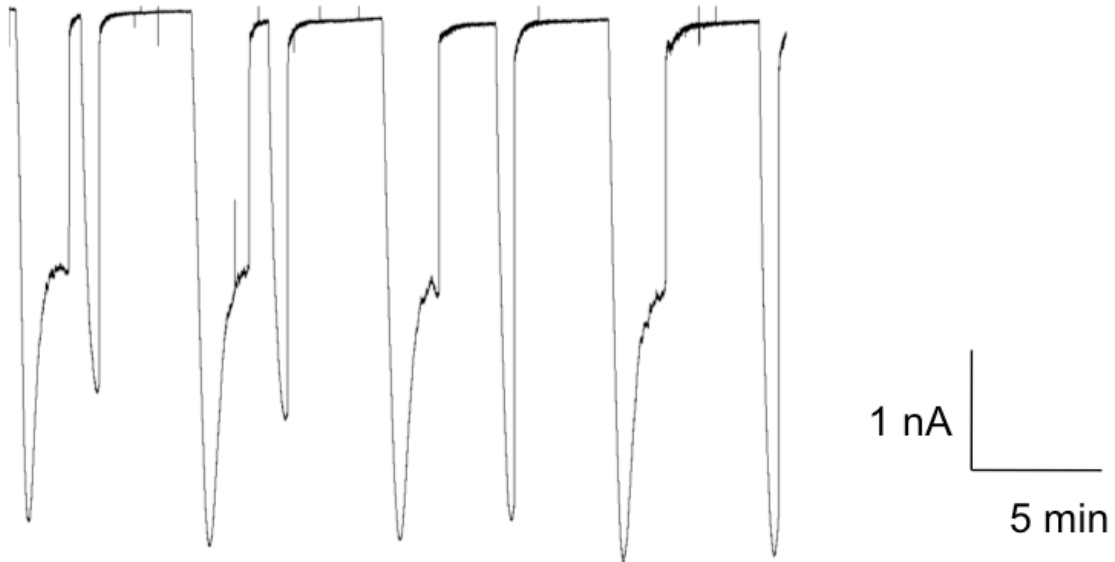


Figure A1 – (Oies Hussein, Unpublished) TRPM2 recovery from inactivation over time. 4 time intervals of 0mM Ca^{2+} treatments were utilized and peak amplitudes measures. Illustrating the recovery full recovery of TRPM2 from an inactivated steady state following a period of 3 minutes 0 Ca^{2+} .

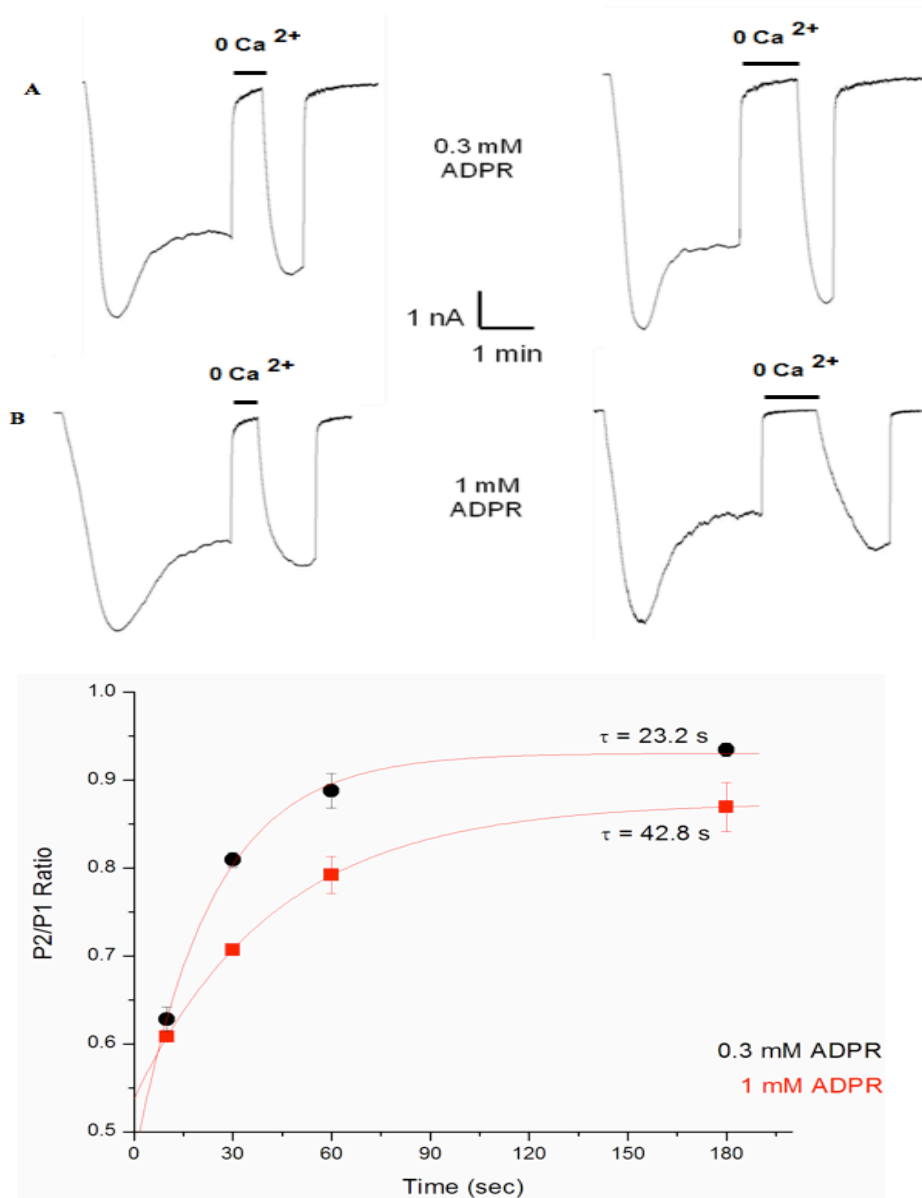


Figure A2 – (Oies Hussein, Unpublished). The role of ADPR on inactivation recovery. (A/B) Representative traces for HEK293 cells stably expressing doxycycline inducible TRPM2 channels. 0.3mM or 1mM ADPR was used in the patch pipette to activate TRPM2, and currents were elicited with 2mM treatments of Ca²⁺ ECF. Higher concentrations of ADPR slowed the recovery from inactivation in both 10sec and 30sec 0mM Ca²⁺ treatments. (C) Time course of recovery from inactivation was determined from the ratio of Peak 2/Peak 1. (n=4-9 and n=4-7)

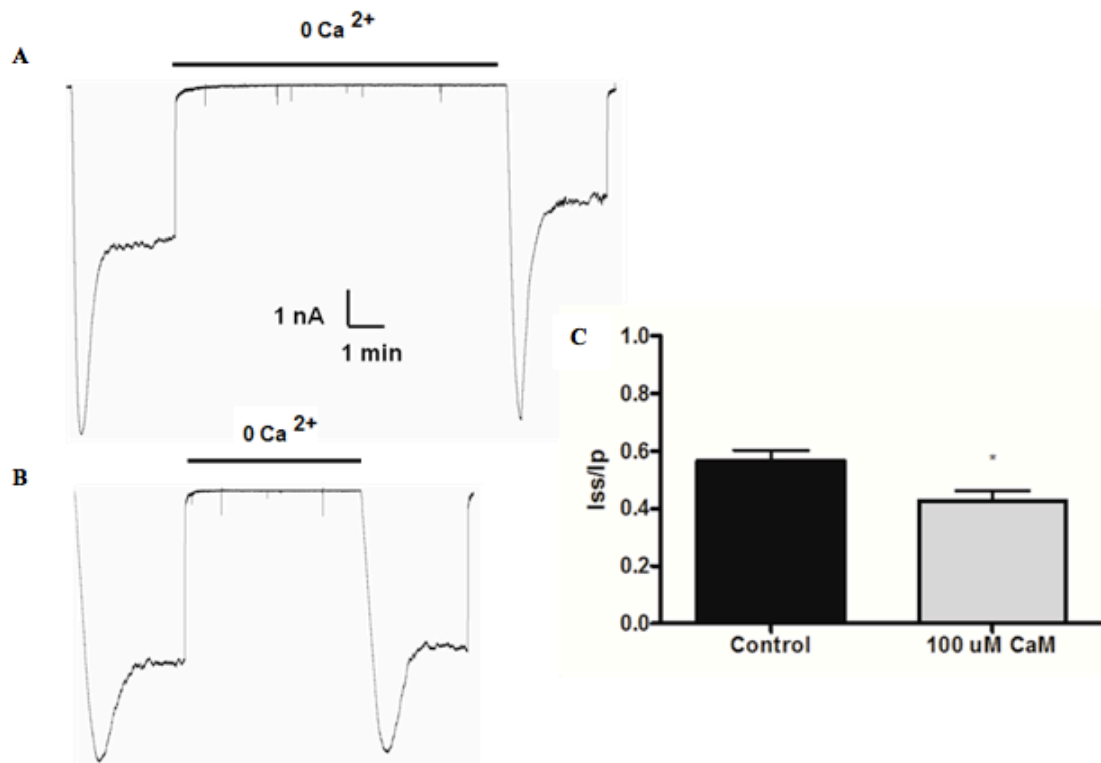


Figure A3 – (Oies Hussein, Unpublished). TRPM2 inactivation is dependent on intracellular CaM. (A/B) Trace recordings from HEK293 cells stably expressing doxycycline induced TRPM2 currents. (A) Characterization of TRPM2 current with 100uM Calmodulin in ICS (n=5) (B) Control recording, (C) Iss/Ip (% Inactivation) for control and 100uM CaM recordings, CaM significantly increased the inactivation of TRPM2 (p<0.05).

Curriculum Vitae

Education

QUEENS UNIVERSITY, Kingston, Ontario: 2012-2016

M.D. Candidate, Department of Medicine

WESTERN UNIVERSITY, London, Ontario: 2010-2012

M.Sc. Candidate, Neuroscience, Department of Anatomy and Cell Bio

UNIVERSITY OF WESTERN ONTARIO, London, Ontario: 2005-2010

Bachelor of Science, Honours Specialization Biology and Minor in Psychology

Honours and Awards

- Dean's Honour List 2010
- Laurene Paterson Scholarship 2010 (\$2100)
- Anne Sale Porte Scholarship 2010 (\$900)
- Western Graduate Research Scholarship 2010-2011 and 2011-2012 (\$7500)
- Canadian Association of Neuroscience Meeting Travel Bursary 2011 (\$500)

Publications and Presentations

Jillian C. Belrose, Fabiana A. Caetano, Kai Yang, **Brian M.W. Lockhart**, Michael F. Jackson, John F. MacDonald. 2012. Metal Ions in Stroke, *Mechanisms of calcium influx following stroke*. Springer

Lockhart, B.M.W., Hussein, O., MacDonald J.F., and Jackson, M.F.

Calcium-calmodulin dependent regulation of TRPM2

- Presented at Margaret Moffat Research Day 2011 in London, Ontario.
- Presented at Anatomy and Cell Biology Research Day 2011 in London, Ontario.
- Presented at the 6th Annual CAN Meeting 2011 in Quebec City, Quebec.
- Presented at the 7th Annual CAN Meeting 2012 in Vancouver, British Columbia.
- Presented at the London Health Science Research Day 2012 in London, Ontario.

Related Work Experience

ROBERTS RESEARCH INSTITUTE – UNIVERSITY OF WESTERN, London, Ontario: 2010-2012

M.Sc. Candidate, Graduate Student, Teaching Assistant